

AD-A243 734



December 11, 1991

Full Surface Testing of Grazing Incidence Mirrors

Principal Investigator: John L. Remo Ph.D.
E.R.G. Systems Inc.
Brackenwood Path
St. James, New York 11780
(516) 584-5540

DTIC
S
C
J
DEC 18 1991

Fifth Quarter Report: Introductory Outline

The goals of this project for the first year (first four quarters) have been achieved. These include:

1. Prototype design,
2. Procurement and testing of components,
3. Mathematics and algorithm development,
4. Interferogram data reduction algorithms,
5. Construction of first prototype, and
6. Automated operation software development.

The fifth quarter and sixth quarter goals are:

1. Construction and evaluation of a modified prototype,
2. Integration of automated hardware controls and software, and
3. Testing of the full surface interferometer on aspheric optical surfaces.

At the end of the fifth quarter, the above workplan objectives have been initiated and are expected to be completed by the end of the sixth quarter.

This report is divided into two parts; the first part is software/hardware sub-system controls which is graphically described in four figures. The data reduction software is displayed by twenty-one sets of interferograms and contour plots.

Research is supported by SDIO/IST and managed by ONR
Contract #N00014-90-C-0246

DISTRIBUTION STATEMENT A

Approved for public release;
Distribution Unlimited

91-18096



91 1216 050

FULL-SURFACE TESTING OF GRAZING INCIDENCE MIRROR

FIFTH QUARTERLY REPORT: 06/12 - 12/11, 1991

Accession For	
NTI	
BYAC TAC	
Unannounced	
Justification	
By Rec A240 356	
Distribution/	
Availability Codes	
Dist	Avail and/or Special
A-1	



1. SUMMARY

In this report we present the work done during the period from September 12 to December 11, 1991.

The tasks accomplished were:

- Implementation of the sub-system software/hardware control testing and integration into the interferometer system
- Acquisition of interferogram images and testing of the software data reduction programs
- Initial interferometer testing

2. SOFTWARE/HARDWARE SUB-SYSTEM CONTROLS

The automated operation system hardware design has been completed and tested. Individual sub-system controllers have been programmed and tested.

- The overall block diagram is shown in Diagram 1.
- The testing mirror positioning control block diagram is shown in Diagram 2.
- The future microstepper control block diagram is shown in Diagram 3.
- The video input/output control block diagram is shown in Diagram 4.

3. DATA REDUCTION SOFTWARE

The interferometer has been tested and twenty-one sets of interferograms have been acquired and processed with the new software programs. The initial results of the interferogram phase computation and display are included in this report. Further integration and automation of the control and processing will continue and be implemented during the next quarter.

The software packages that have been tested include the following.

A. Sub-system controller testing programs:

- Mirror positioning motor stage control programs
- Interferometer phase control programs
- Video camera and frame grabber/buffer control programs
- Video frame buffer and color video printer control programs
- Video frame buffer and laser printer continuous gray levels image printer mode control programs

B. Integration of system software packages:

- System control device programs
- Interferogram acquisition and storage programs
- Interferogram display programs
- Interferogram phase measurement programs
- Interferogram phase map display programs
 - . Phase map 3D plot with scale change, offset adjustable, title text input, hidden line removal display.
 - . Phase map thin line contour display, with contour level selection and color/black & white display option.
 - . Phase map thick contour display, with contour level selection and color/B&W display option.

C. Interferogram phase contour map reformatted into continuous gray level in the form of the video frame buffer data format and ready to display in the monitor as well as print out from the video printer.

D. Interferogram data reduction programs: Interferogram phase map with tilt removed (fitting and subtraction of best fit plane).

BLOCK DIAGRAM OF THE ELECTRICAL/DIGITAL SYSTEM

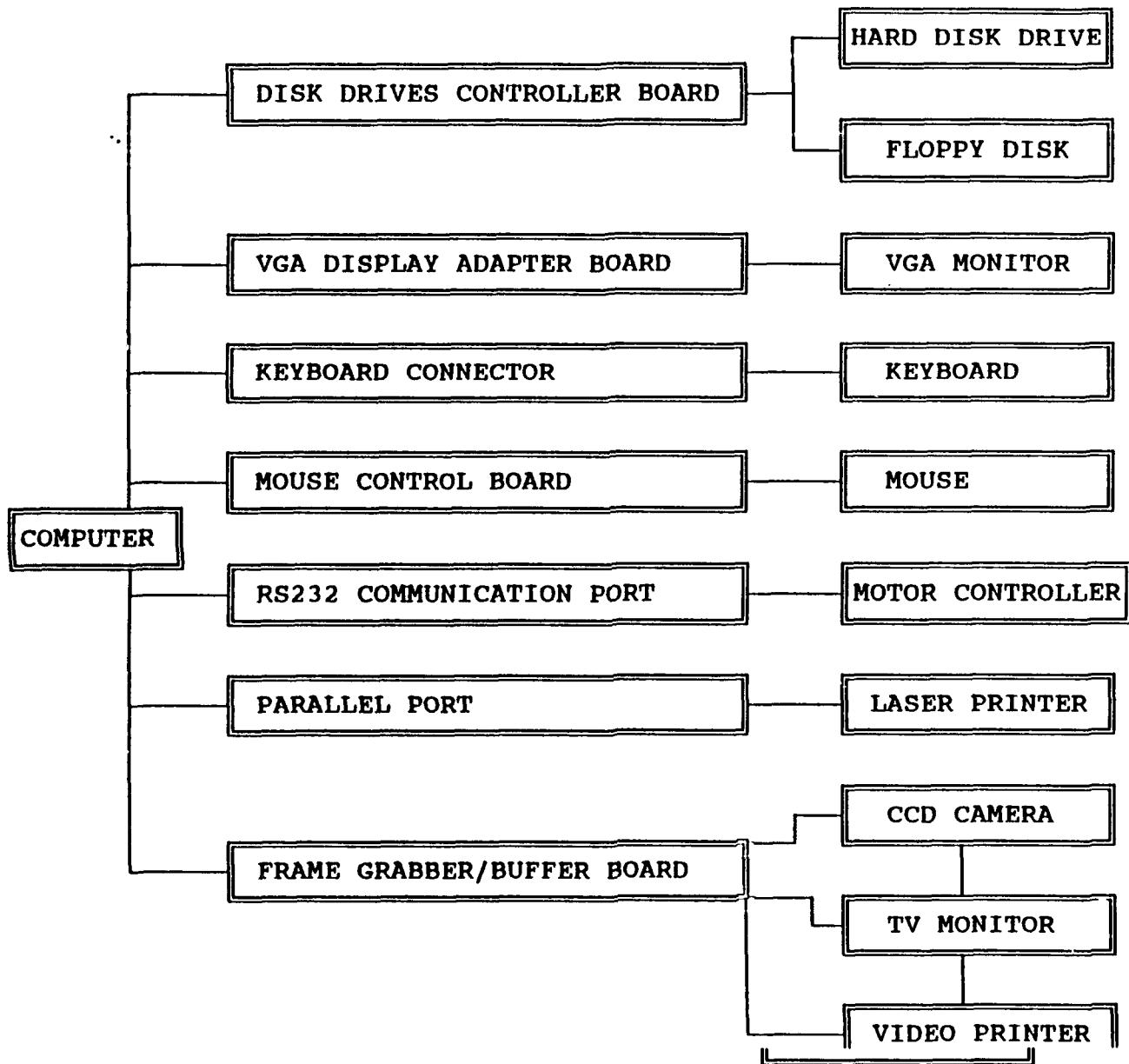


Diagram 1. Block Diagram of the Automated Operation Hardware System

BLOCK DIAGRAM OF THE POSITIONING CONTROL DEVICE

STEPPING MOTOR CONTROLLER SYSTEM

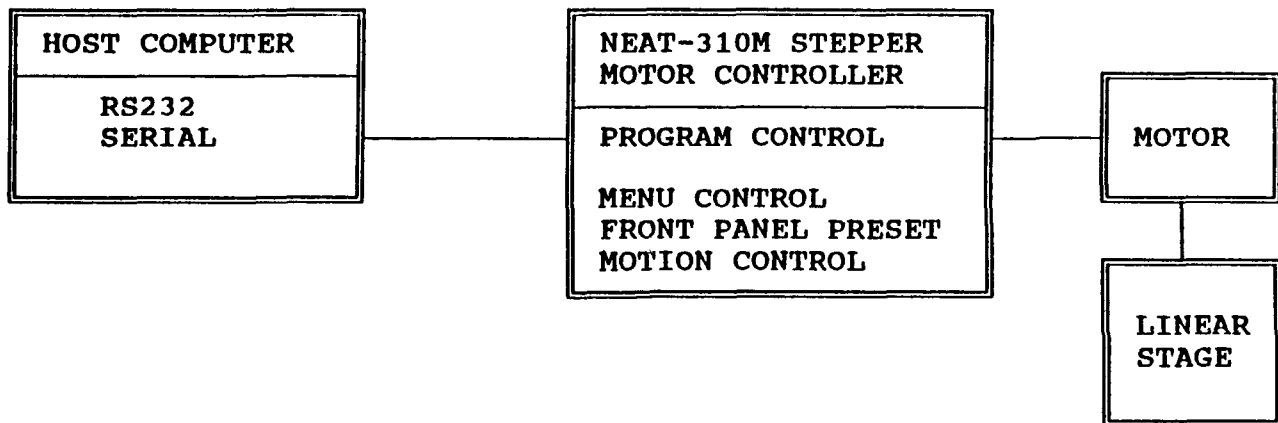


Diagram 2. Block Diagram of the Positioning Control Device

BLOCK DIAGRAM OF THE PHASE MODULATOR CONTROL DEVICE

STEPPING MOTOR CONTROLLER SYSTEM

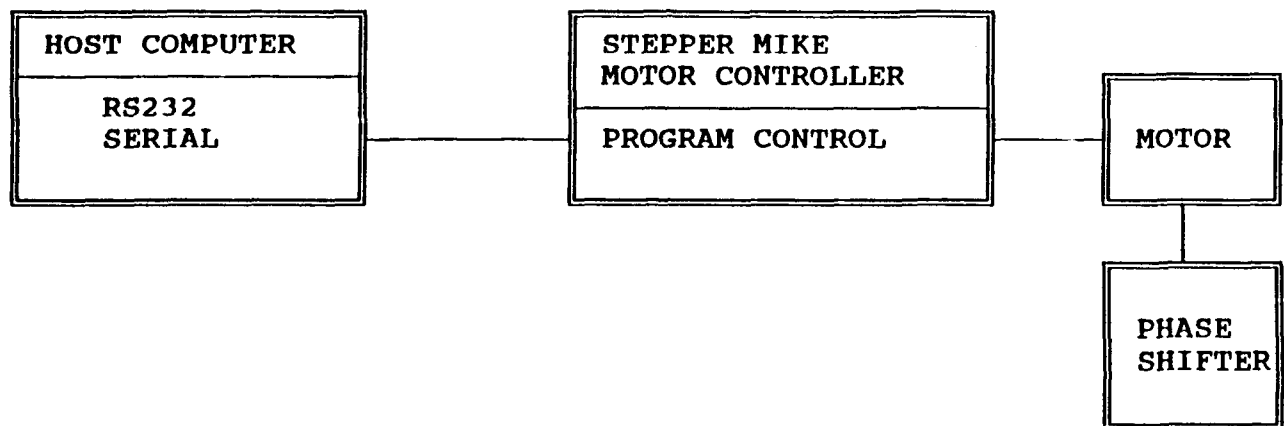


Diagram 3. Block Diagram of the Phase Modulation Control Device

CONNECTION DIAGRAM OF VIDEO INPUT/OUTPUT SYSTEM

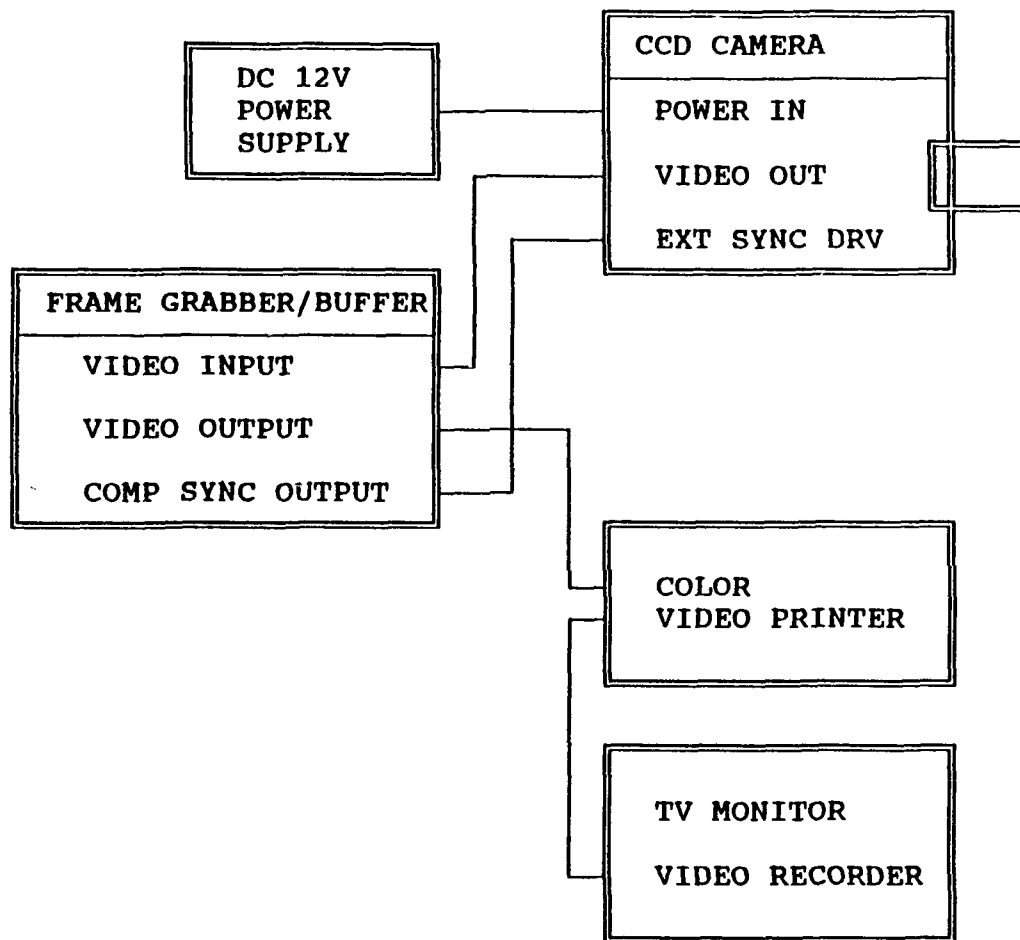


Diagram 4. Block diagram of the video input/output system

4. INTERFEROMETER PROTOTYPE TESTING

The interferometer system was further refined and made ready for initial testing of the software programs.

As the main purpose here was to test hardware and software, the interferometer was operated manually. The operation will be automated during the next quarter.

We acquired and computed a series of 21 interferograms that cover all possible alignment conditions. In every case, the wavefront slope was digitally computed and plotted in the form of isometric or contour maps.

The measurements are as follows for a subaperture of the cylindrical mirror under test:

Figure 1a: Photograph of X-shear interferogram, in focus and aligned in rotation

Figure 1b: 3-D isometric plot of wavefront slope function

Figure 1c, d: Contour maps of wavefront slope function

Figure 1e, f: Contour maps of wavefront slope with tilt removed

Figure 2a: Photograph of X-shear interferogram, in focus and with small misalignment (positive rotation)

Figure 2b: 3-D isometric plot of wavefront slope function

Figure 2c, d: Contour maps of wavefront slope function

Figure 2e, f: Contour maps of wavefront slope with tilt removed

Figure 3a: Photograph of X-shear interferogram, in focus and medium misalignment (positive rotation)

Figure 3b: 3-D isometric plot of wavefront slope function

Figure 3c, d: Contour maps of wavefront slope function

Figure 3e, f: Contour maps of wavefront slope function, with tilt removed

Figure 4a: Photograph of X-shear interferogram, in focus and large misalignment (positive rotation)

Figure 4b: 3-D isometric plot of wavefront slope function

Figure 4c, d: Contour maps of wavefront slope function

Figure 4e, f: Contour maps of wavefront slope function with tilt removed

Figure 5a: Photograph of X-shear interferogram, in focus and small misalignment (negative rotation)

Figure 5b: 3-D isometric plot of wavefront slope function

Figure 5c, d: Contour maps of wavefront slope function

Figure 5e, f: Contour maps of wavefront slope function with tilt removed

Figure 6a: Photograph of X-shear interferogram, in focus and medium misalignment (negative rotation)

Figure 6b: 3-D isometric plot of wavefront slope function

Figure 6c, d: Contour maps of wavefront slope function

Figure 6e, f: Contour maps of wavefront slope function with tilt removed

Figure 7a: Photograph of X-shear interferogram, in focus and large misalignment (large negative rotation)

Figure 7b: 3-D isometric plot of wavefront slope function

Figure 7c, d: Contour maps of wavefront slope function

Figure 7e, f: Contour maps of wavefront slope function with tilt removed

Figure 8a: Photograph of X-shear interferogram, out-of-focus and aligned

Figure 8b: 3-D isometric plot of wavefront slope function

Figure 8c, d: Contour maps of wavefront slope function

Figure 8e, f: Contour maps of wavefront slope function with tilt removed

- Figure 9a: Photograph of X-shear interferogram, out-of-focus and small misalignment (positive rotation)
- Figure 9b: 3-D isometric plot of wavefront slope function
- Figure 9c, d: Contour maps of wavefront slope function
- Figure 9e, f: Contour maps of wavefront slope function with tilt removed
-
- Figure 10a: Photograph of X-shear interferogram, out-of-focus and large misalignment (positive rotation)
- Figure 10b: 3-D isometric plot of wavefront slope function
- Figure 10c,d: Contour maps of wavefront slope function
- Figure 10e,f: Contour maps of wavefront slope function with tilt removed
-
- Figure 11a: Photograph of X-shear interferogram, out-of-focus and small misalignment (negative rotation)
- Figure 11b: 3-D isometric plot of wavefront slope function
- Figure 11c,d: Contour maps of wavefront slope function
- Figure 11e,f: Contour maps of wavefront slope function with tilt removed
-
- Figure 12a: Photograph of X-shear interferogram, out-of-focus and large misalignment (negative rotation)
- Figure 12b: 3-D isometric plot of wavefront slope function
- Figure 12c,d: Contour maps of wavefront slope function
- Figure 12e,f: Contour maps of wavefront slope function with tilt removed
-
- Figure 13a: Photograph of Y-shear interferogram, in focus and aligned in rotation
- Figure 13b: 3-D isometric plot of wavefront slope function
- Figure 13c,d: Contour maps of wavefront slope function
- Figure 13e,f: Contour maps of wavefront slope with tilt removed

- Figure 14a: Photograph of Y-shear interferogram, in focus and small misalignment in rotation
- Figure 14b: 3-D isometric plot of wavefront slope function
- Figure 14c,d: Contour maps of wavefront slope function
- Figure 14e,f: Contour maps of wavefront slope with tilt removed
-
- Figure 15a: Photograph of Y-shear interferogram, in focus and medium misalignment in rotation
- Figure 15b: 3-D isometric plot of wavefront slope function
- Figure 15c,d: Contour maps of wavefront slope function
- Figure 15e,f: Contour maps of wavefront slope with tilt removed
-
- Figure 16a: Photograph of Y-shear interferogram, in focus and large misalignment in rotation
- Figure 16b: 3-D isometric plot of wavefront slope function
- Figure 16c,d: Contour maps of wavefront slope function
- Figure 16e,f: Contour maps of wavefront slope with tilt removed
-
- Figure 17a: Photograph of Y-shear interferogram, out-of-focus and aligned in rotation
- Figure 17b: 3-D isometric plot of wavefront slope function
- Figure 17c,d: Contour maps of wavefront slope function
- Figure 17e,f: Contour maps of wavefront slope with tilt removed
-
- Figure 18a: Photograph of Y-shear interferogram, out-of-focus and small misalignment (positive rotation)
- Figure 18b: 3-D isometric plot of wavefront slope function
- Figure 18c,d: Contour maps of wavefront slope function
- Figure 18e,f: Contour maps of wavefront slope with tilt removed
-
- Figure 19a: Photograph of Y-shear interferogram, out-of-focus and large misalignment (positive rotation)

Figure 19b: 3-D isometric plot of wavefront slope function

Figure 19c,d: Contour maps of wavefront slope function

Figure 19e,f: Contour maps of wavefront slope with tilt removed

Figure 20a: Photograph of Y-shear interferogram, out-of-focus and small misalignment (negative rotation)

Figure 20b: 3-D isometric plot of wavefront slope function

Figure 20c,d: Contour maps of wavefront slope function

Figure 20e,f: Contour maps of wavefront slope with tilt removed

Figure 21a: Photograph of Y-shear interferogram, out-of-focus and large misalignment (negative rotation)

Figure 21b: 3-D isometric plot of wavefront slope function

Figure 21c,d: Contour maps of wavefront slope function

Figure 21e,f: Contour maps of wavefront slope with tilt removed

BLOCK DIAGRAM OF THE ELECTRICAL/DIGITAL SYSTEM

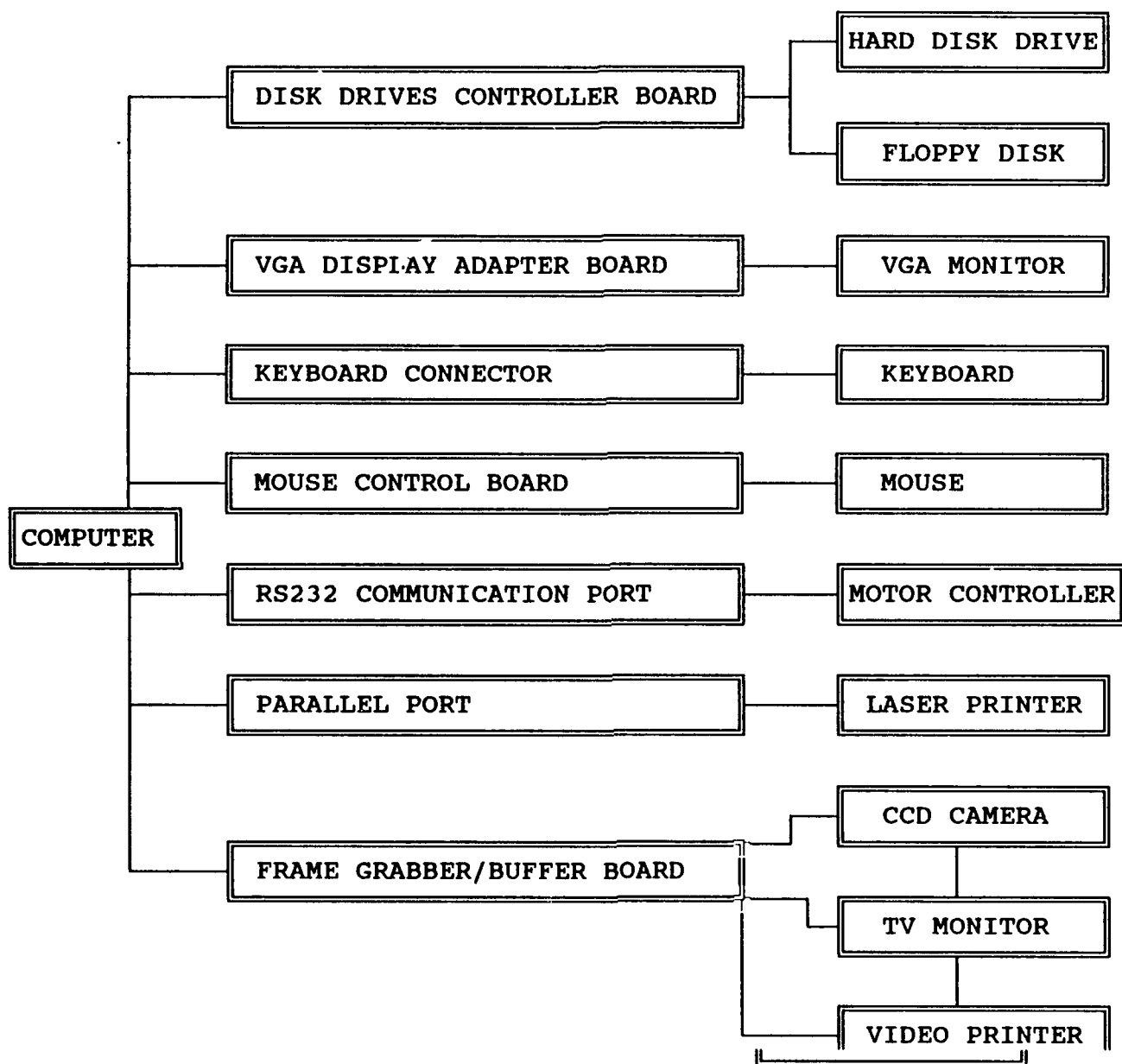


Diagram 1. Block Diagram of the Automated Operation Hardware System

BLOCK DIAGRAM OF THE POSITIONING CONTROL DEVICE

STEPPING MOTOR CONTROLLER SYSTEM

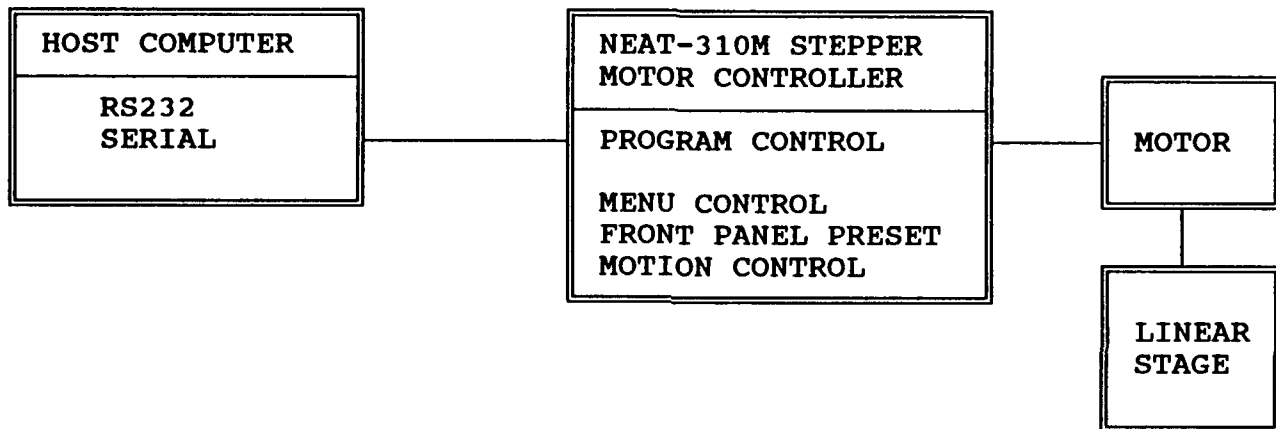


Diagram 2. Block Diagram of the Positioning Control Device

BLOCK DIAGRAM OF THE PHASE MODULATOR CONTROL DEVICE

STEPPING MOTOR CONTROLLER SYSTEM

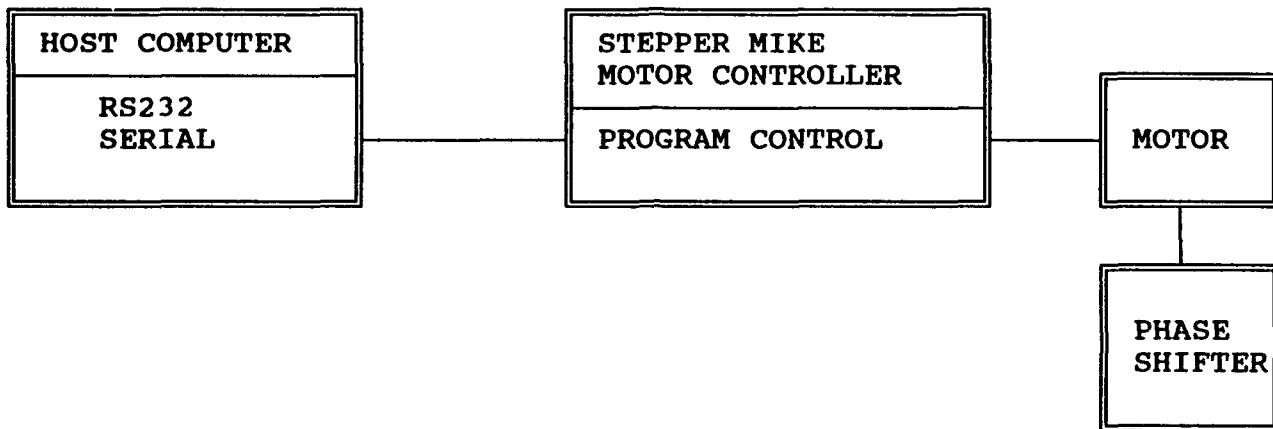


Diagram 3. Block Diagram of the Phase Modulation Control Device

CONNECTION DIAGRAM OF VIDEO INPUT/OUTPUT SYSTEM

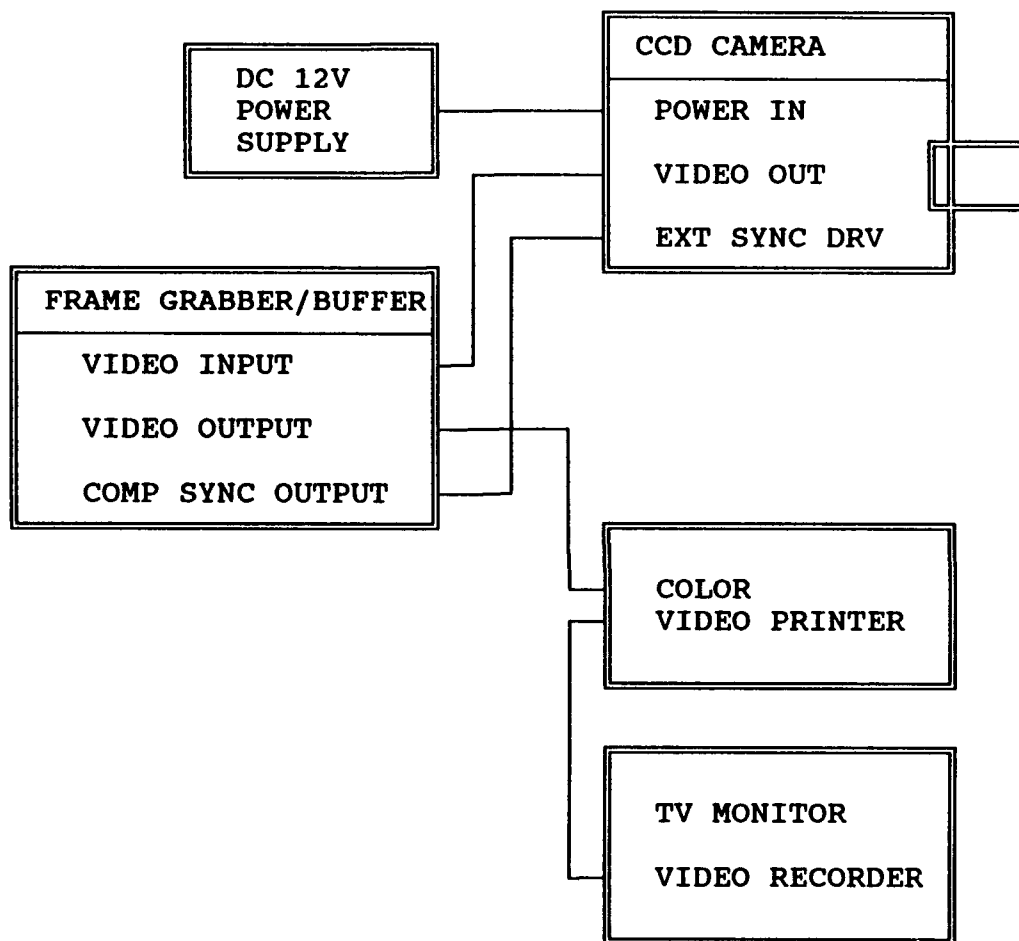
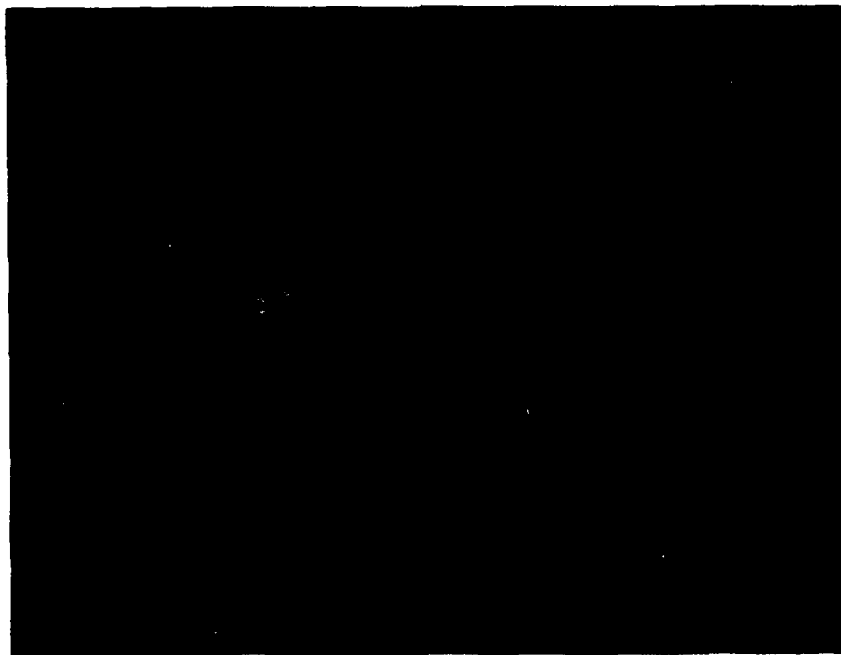


Diagram 4. Block diagram of the video input/output system

(a)



(b)

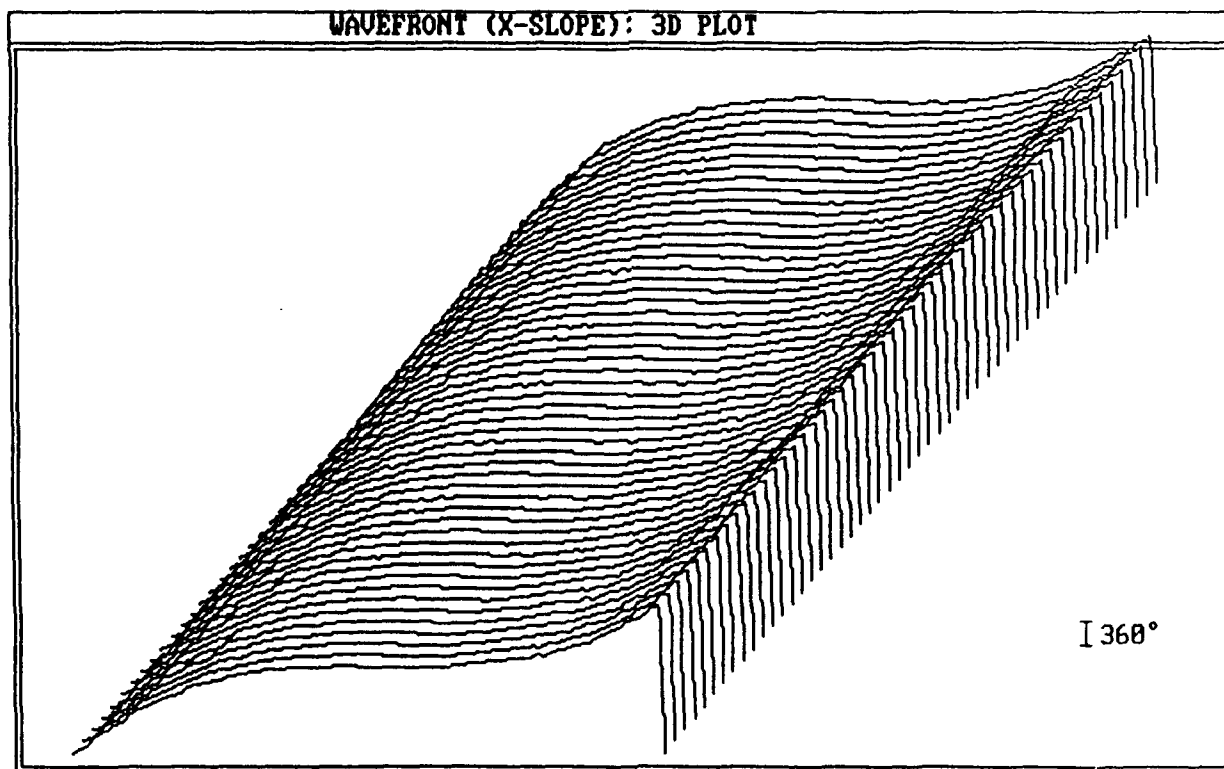


Figure 1: (a). Photograph of subaperture interferogram
(b). 3-D plot of wavefront slope
(X-shear, in focus, aligned)

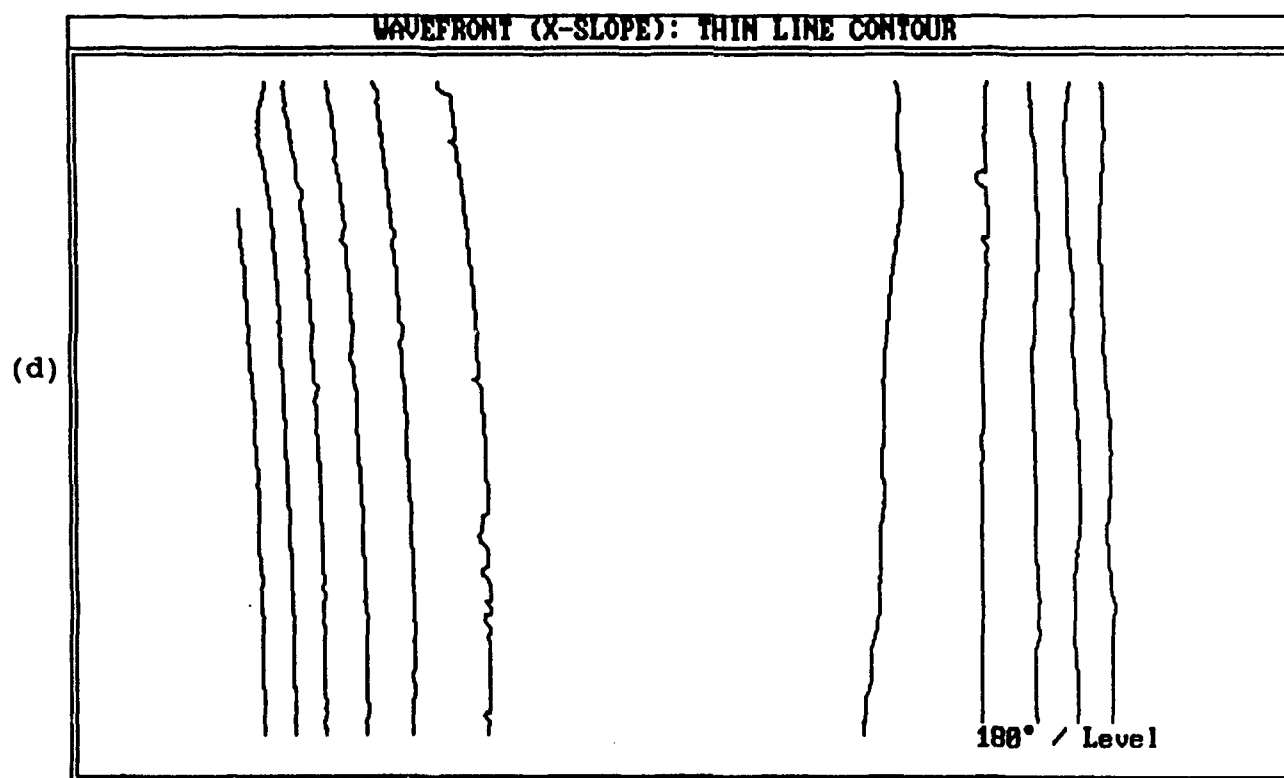
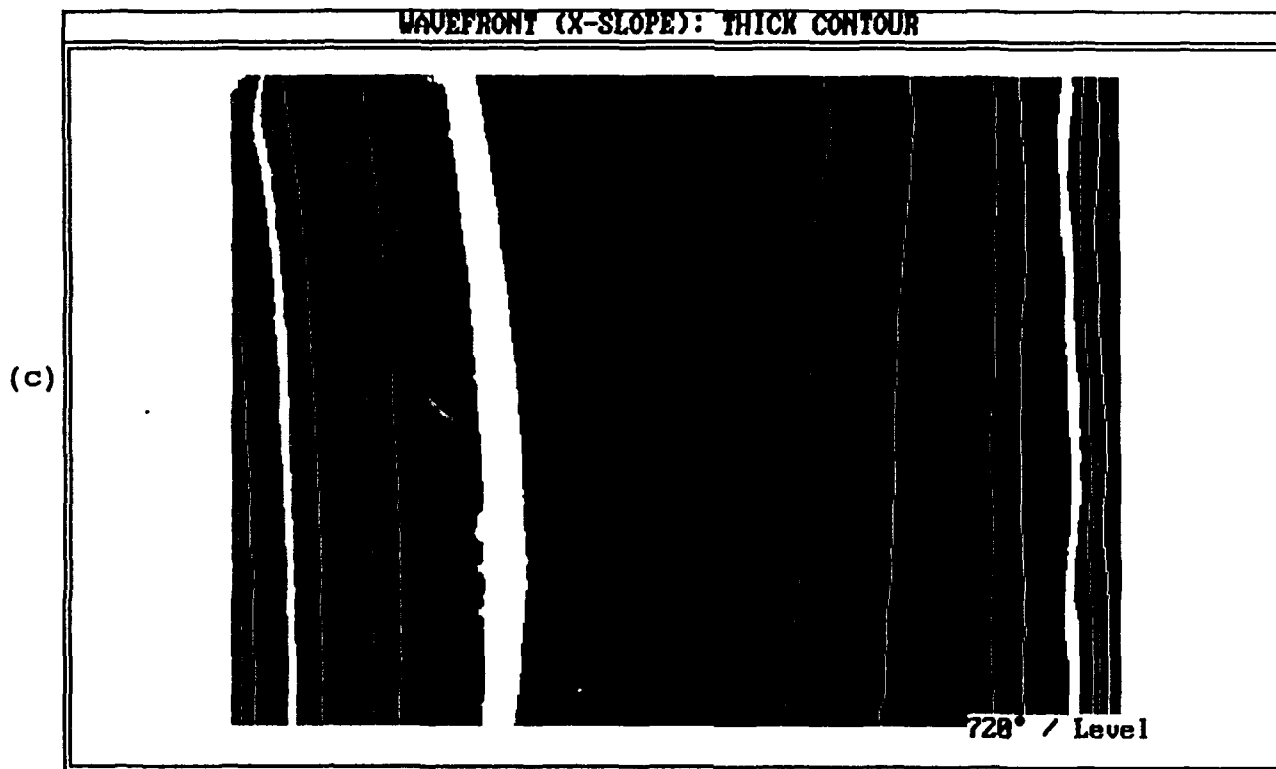
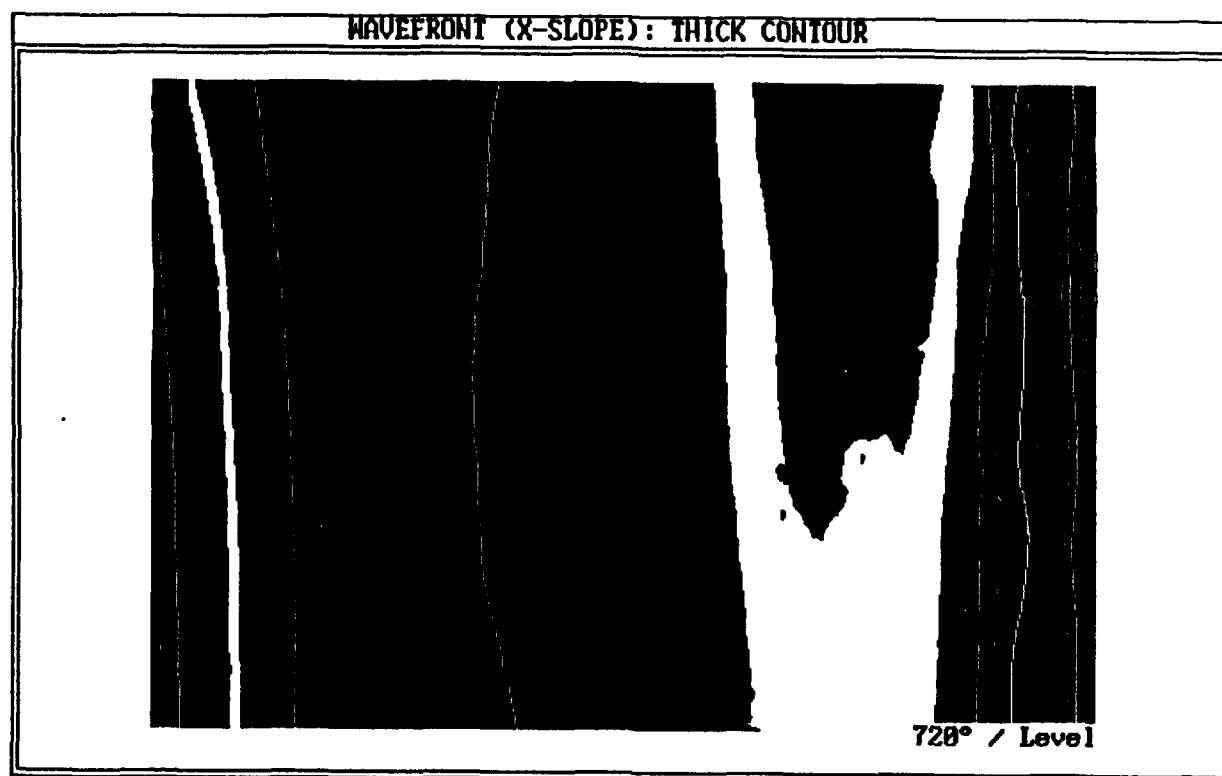


Figure 1: (c, d). Contour maps of wavefront slope
(X-shear, in focus, aligned)

(e)



(f)

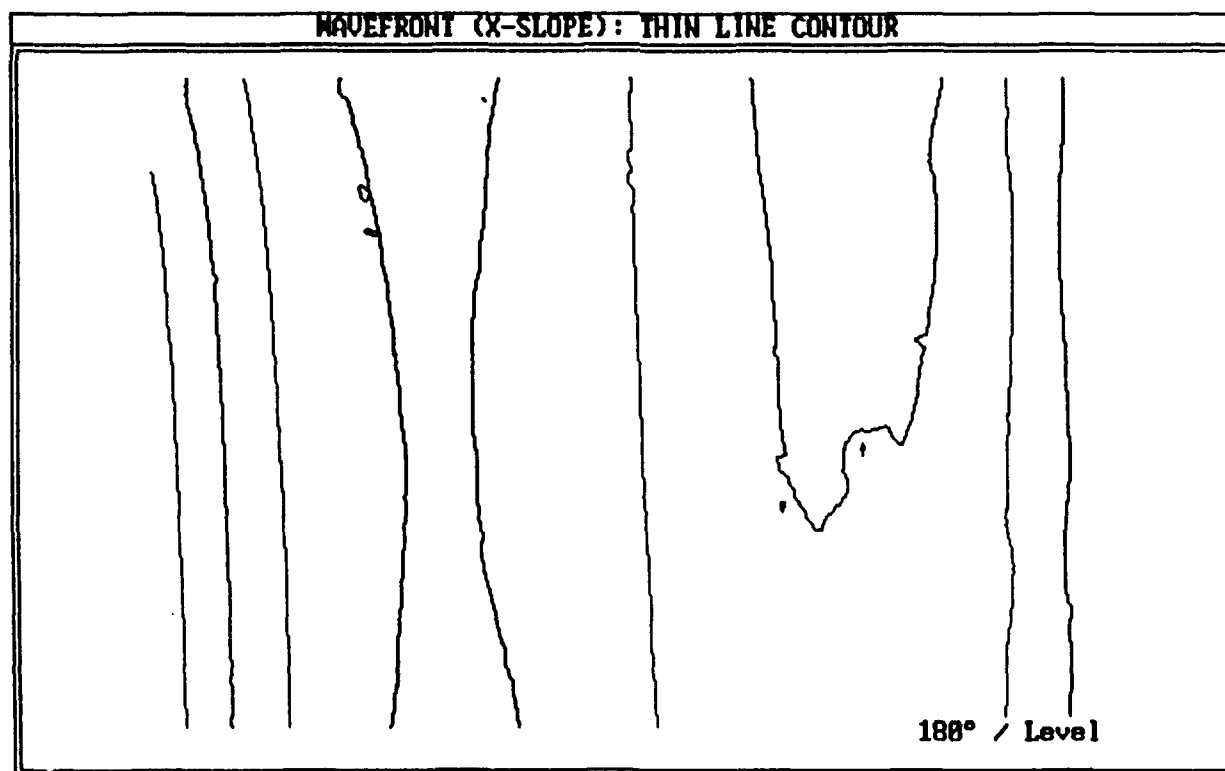
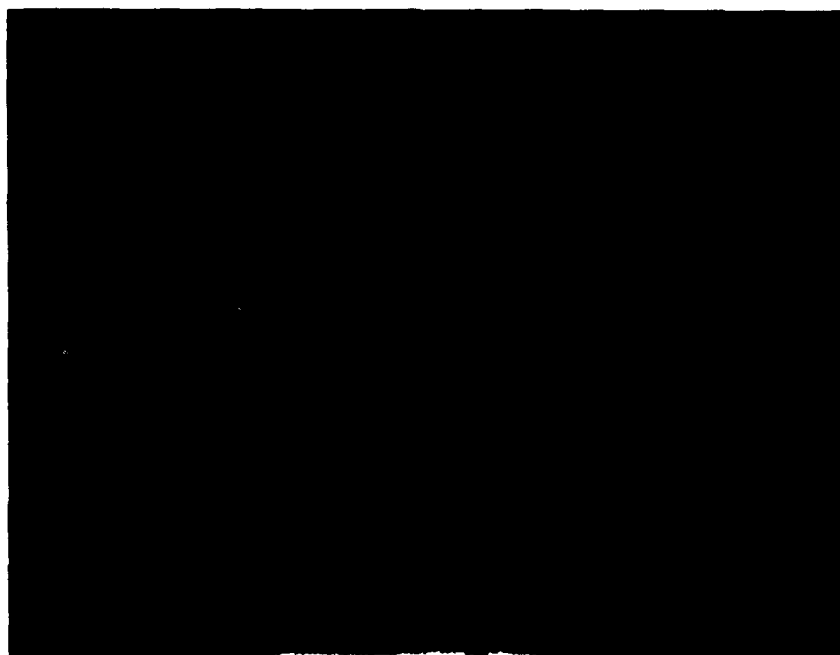


Figure 1: (e, f). Contour maps of wavefront slope, tilt removed (X-shear, in focus, aligned)

(a)



(b)

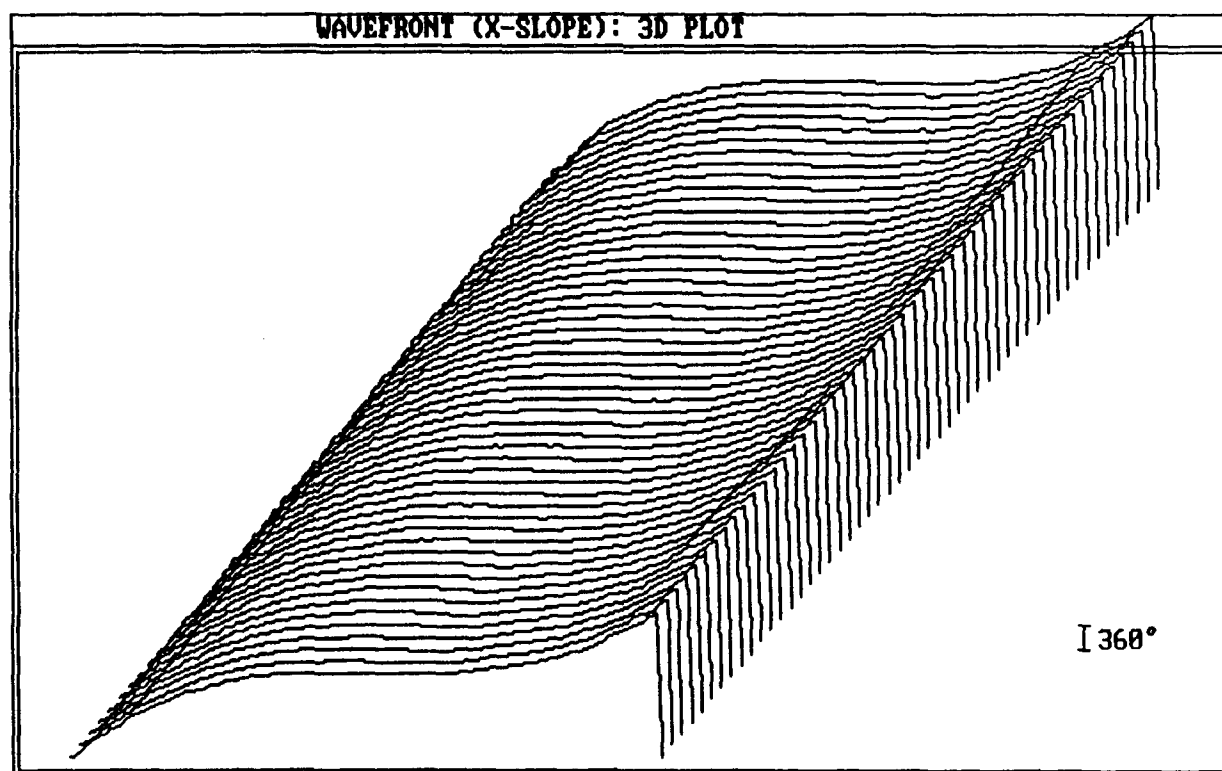
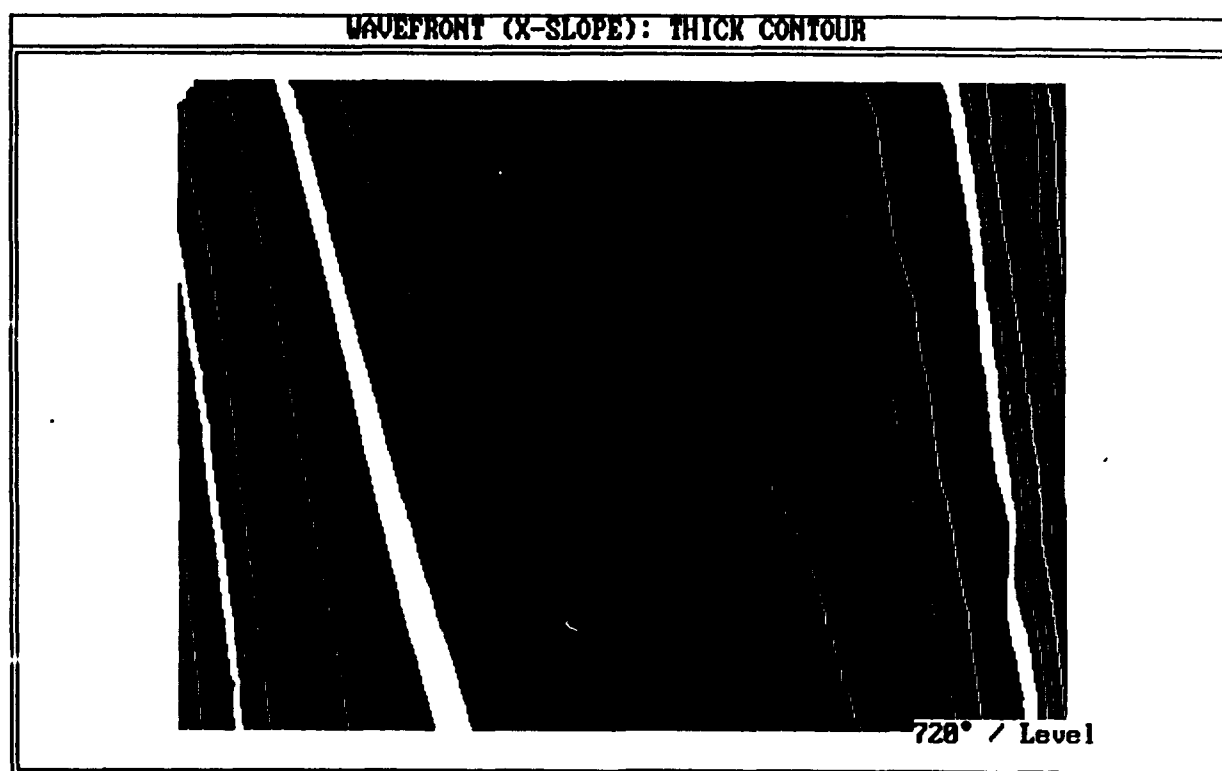


Figure 2: (a). Photograph of subaperture interferogram
(b). 3-D plot of wavefront slope
{X-shear, in focus, small misalignment (positive)}

(c)



(d)

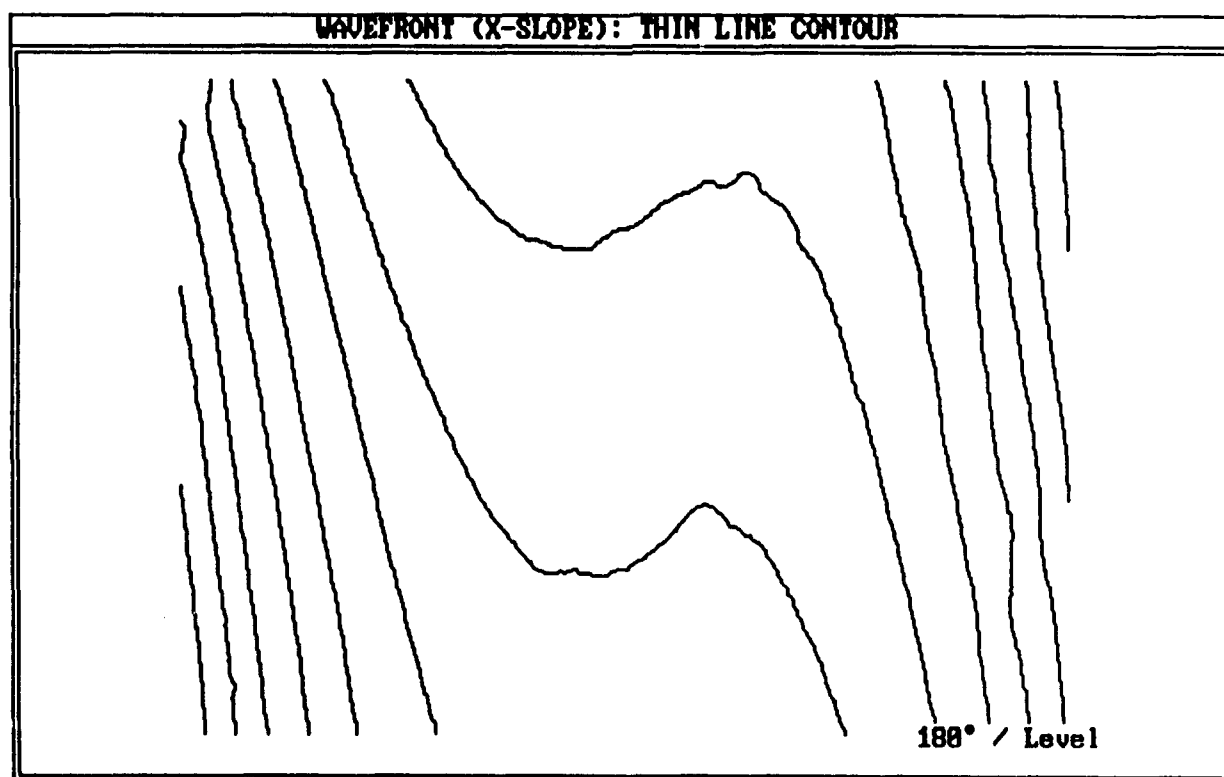
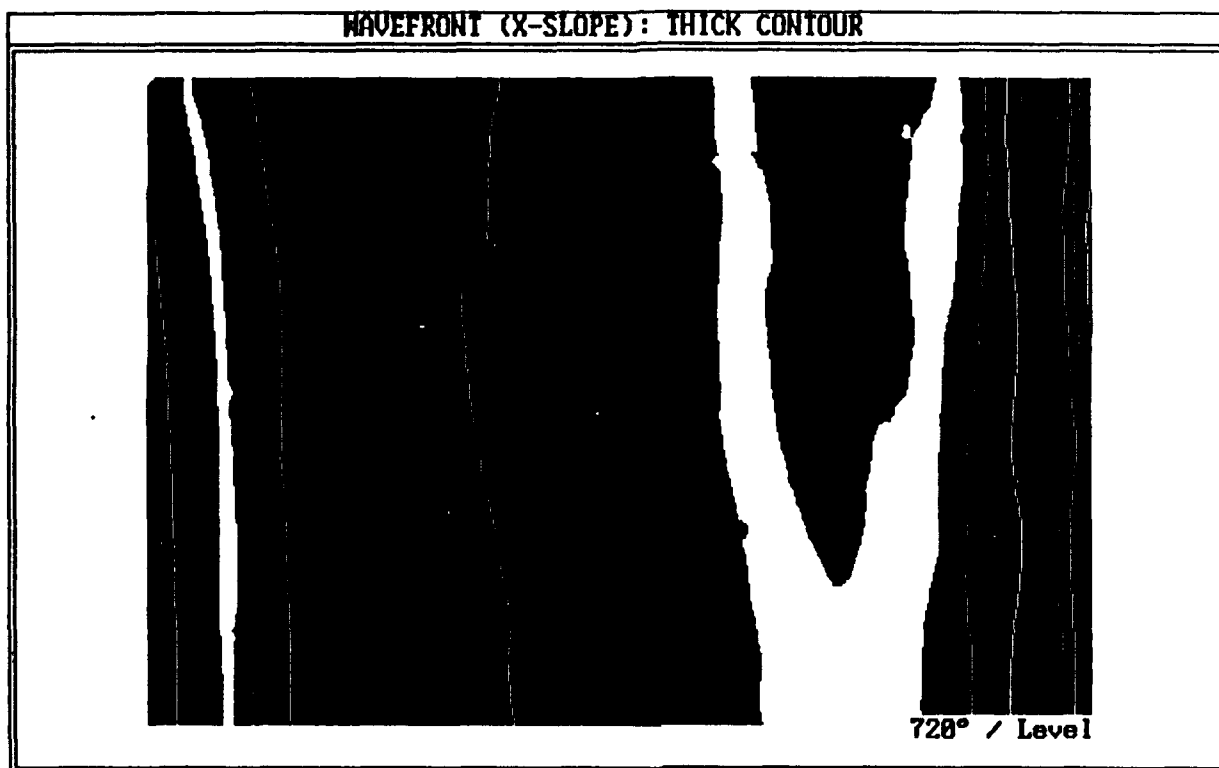


Figure 2: (c, d). Contour maps of wavefront slope
{X-shear, in focus, small misalignment (positive)}

(e)



(f)

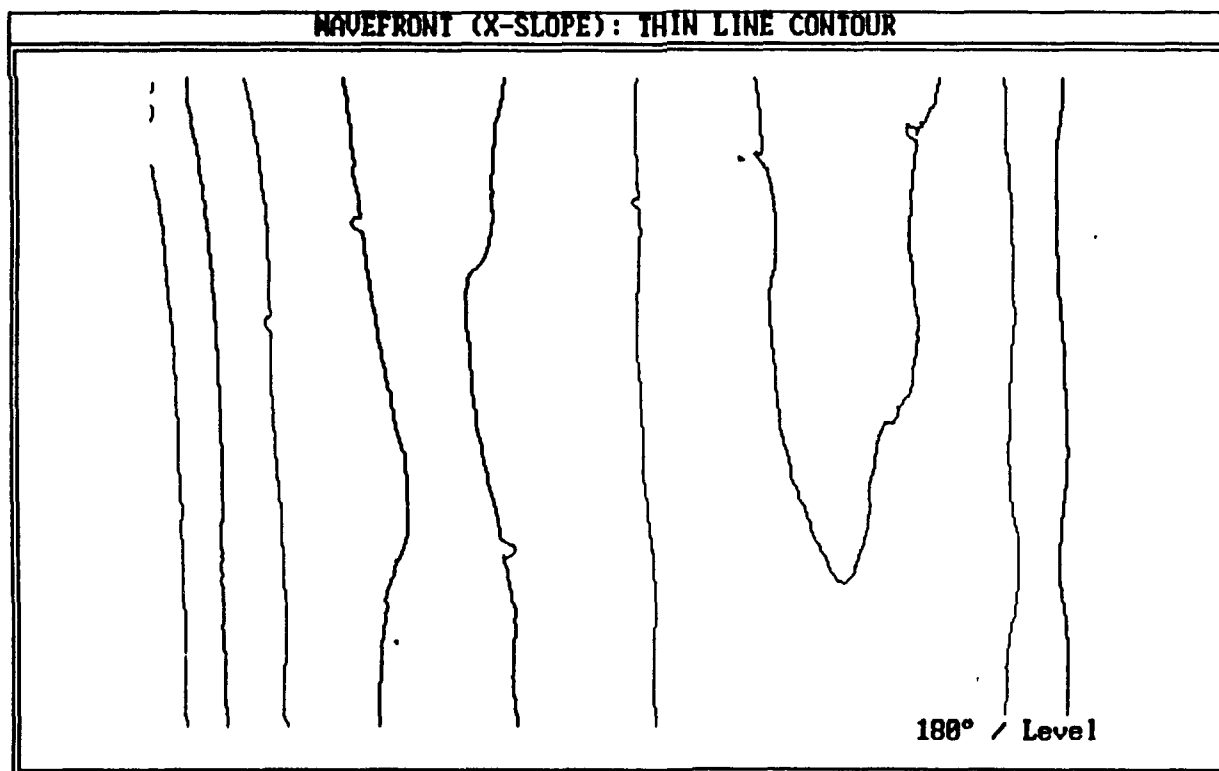


Figure 2: (e, f). Contour maps of wavefront slope, tilt removed
{X-shear, in focus, small misalignment (positive)}

(a)



(b)

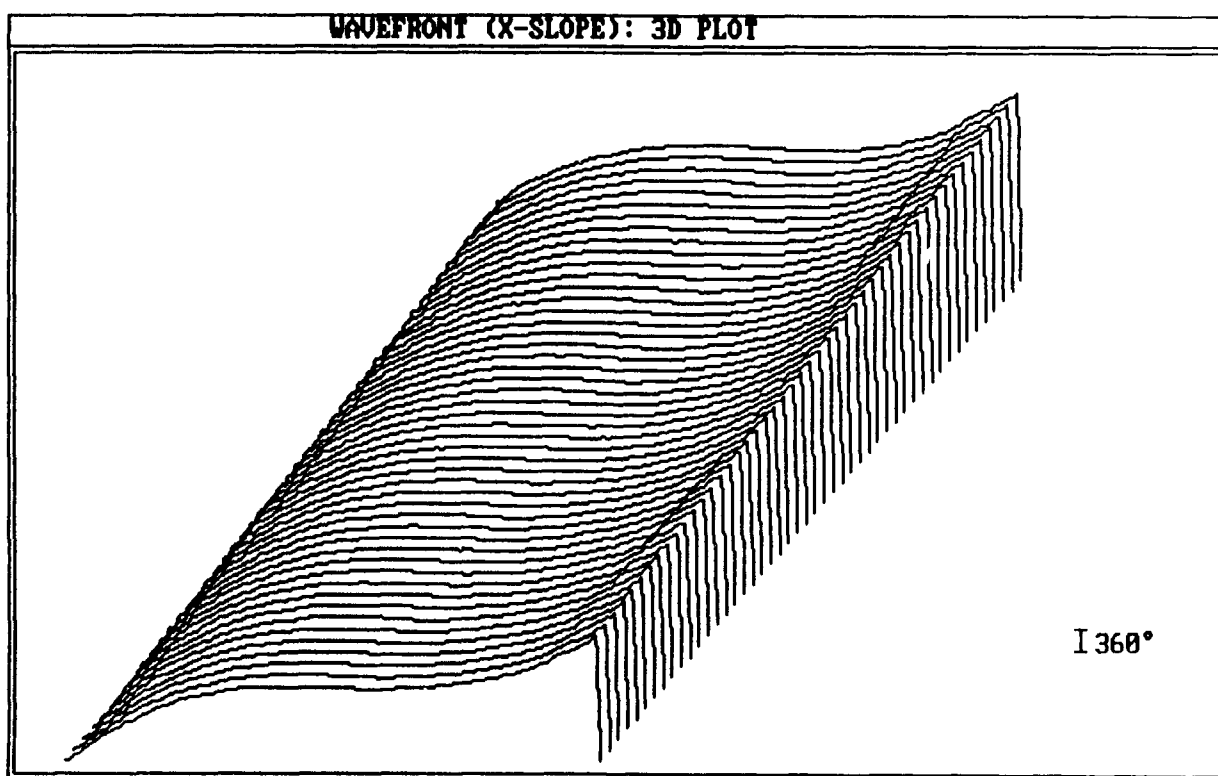
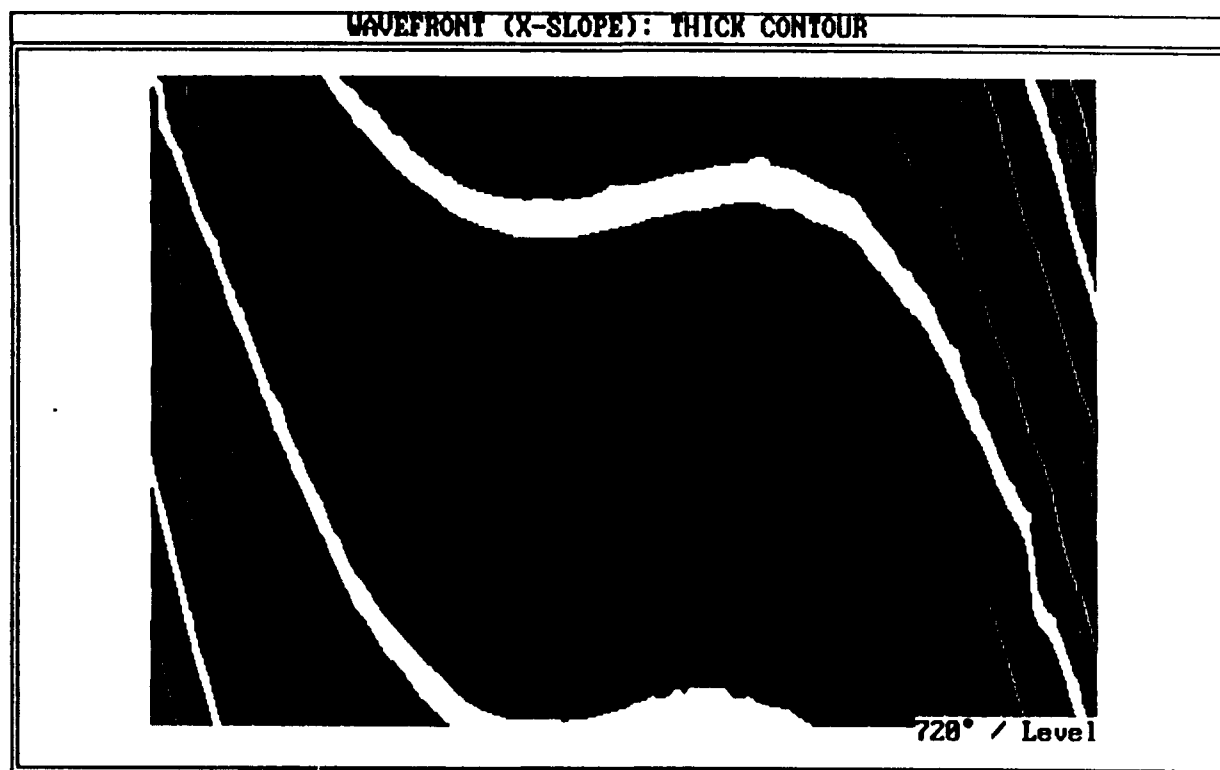


Figure 3: (a). Photograph of subaperture interferogram
(b). 3-D plot of wavefront slope
{X-shear, in focus, medium misalignment (positive)}

(c)



(d)

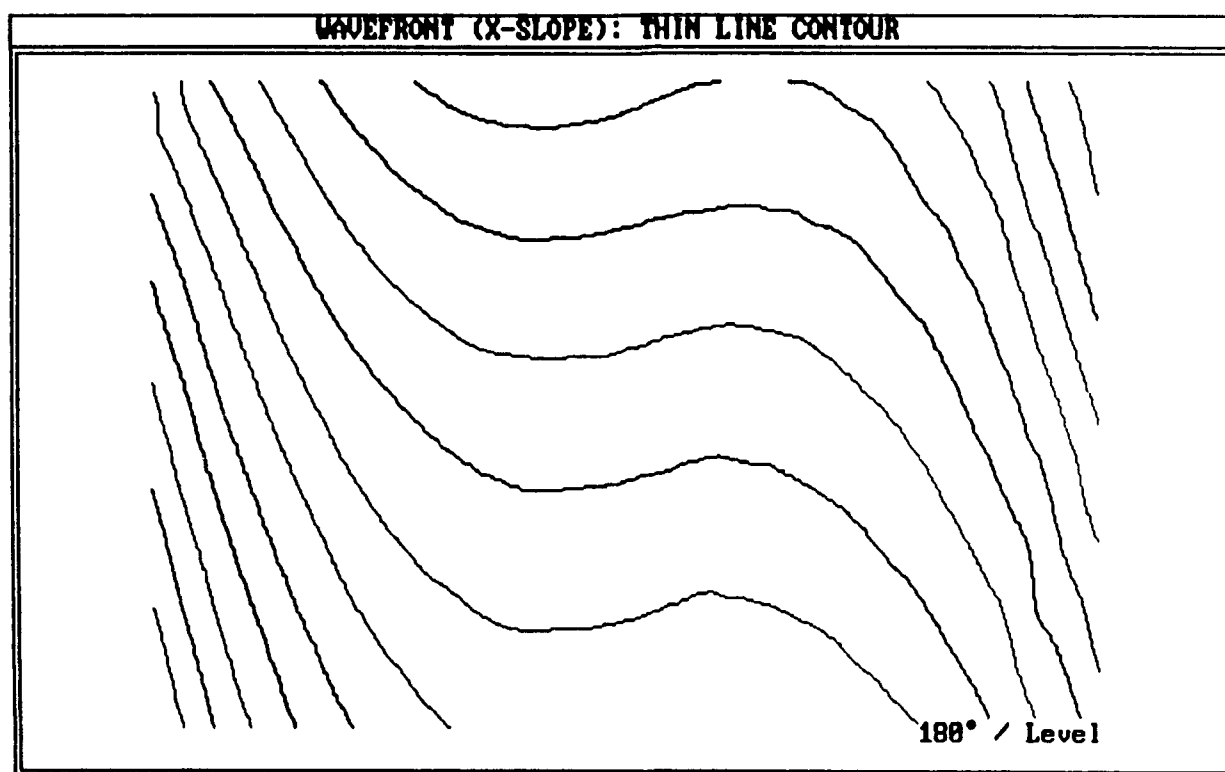
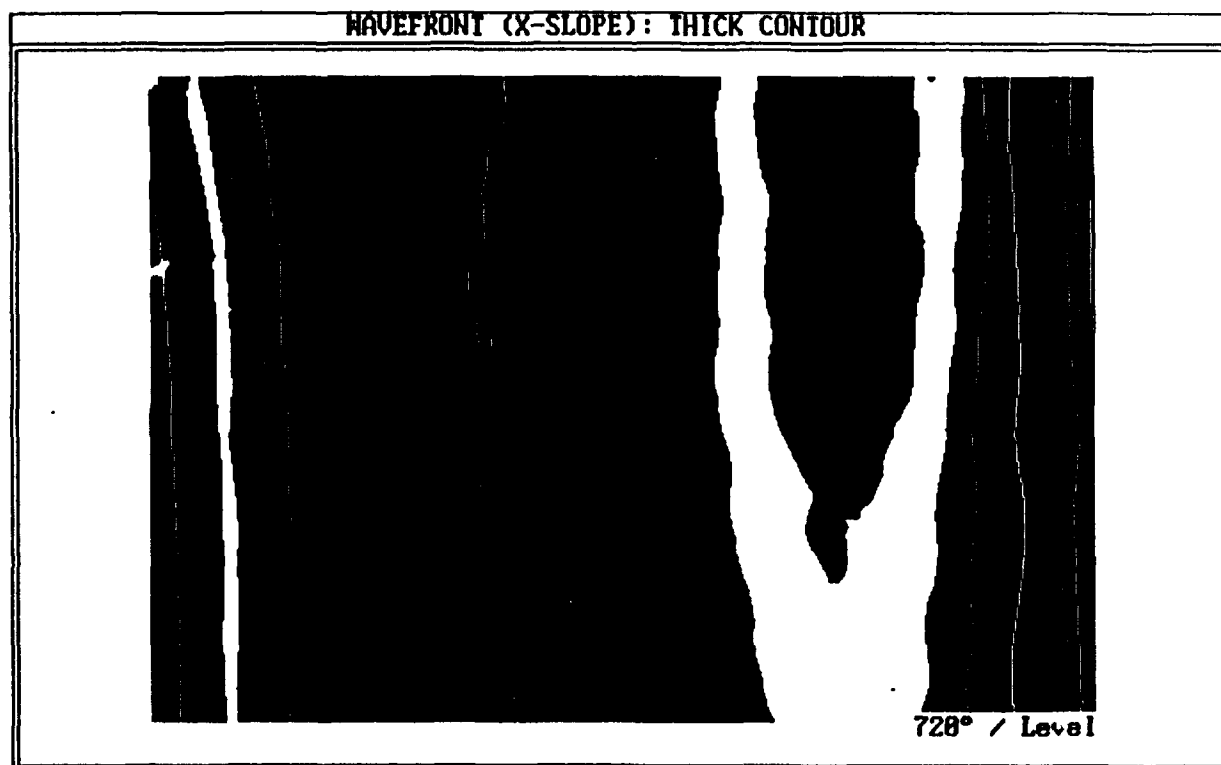


Figure 3: (c, d). Contour maps of wavefront slope
{X-shear, in focus, medium misalignment (positive)}

(e)



(f)

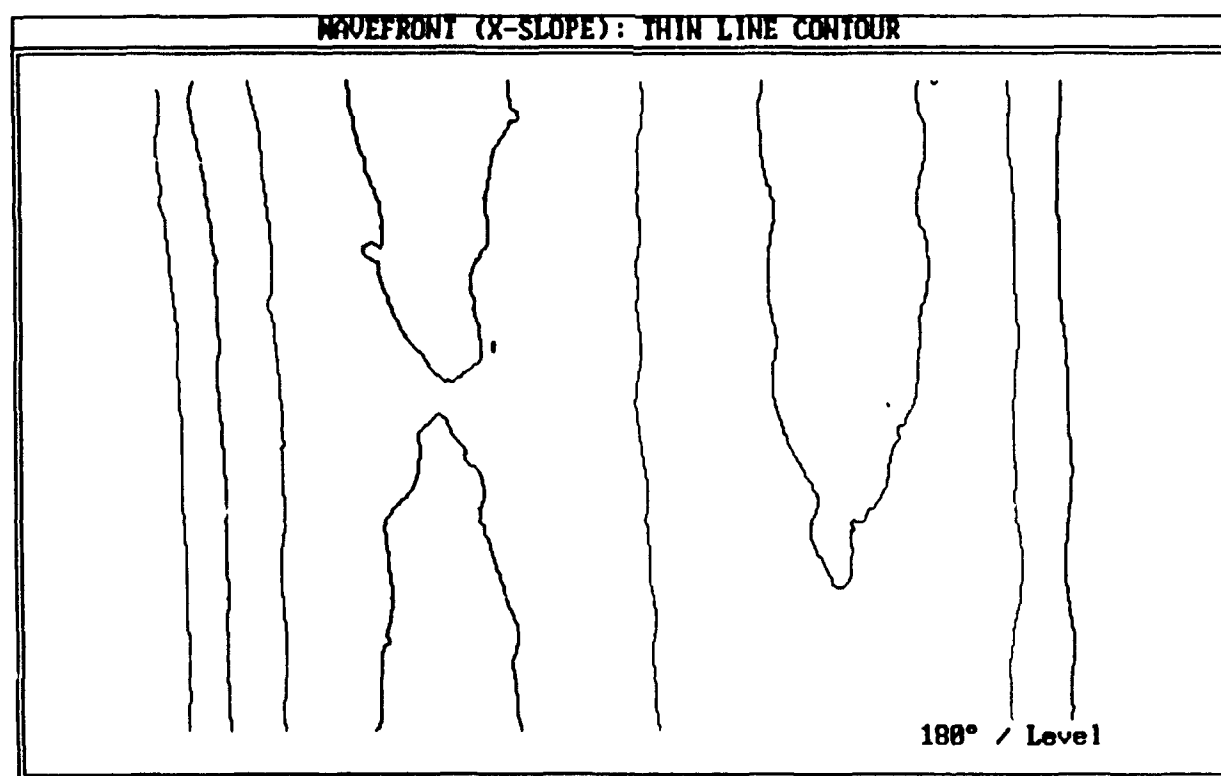
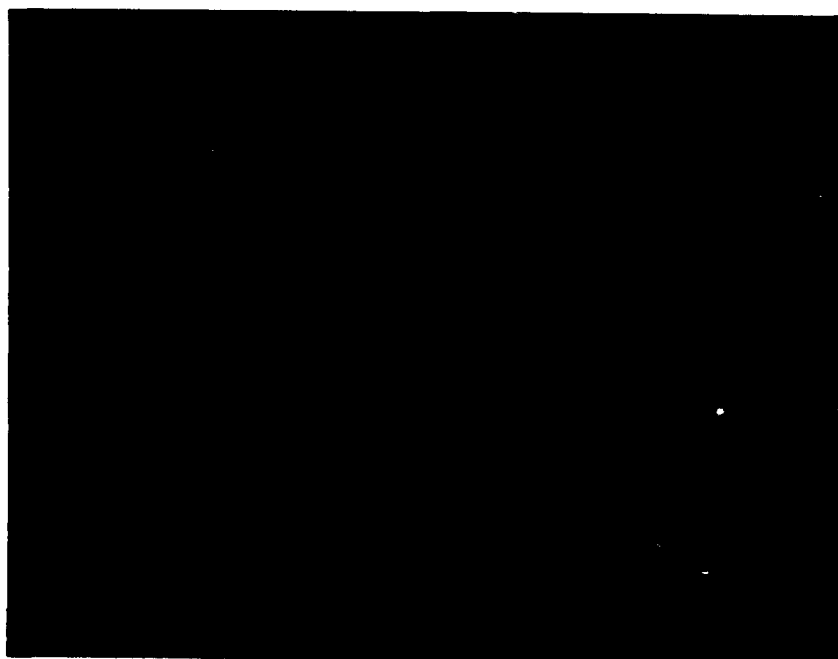


Figure 3: (e, f). Contour maps of wavefront slope, tilt removed
{X-shear, in focus, medium misalignment (positive)}

(a)



(b)

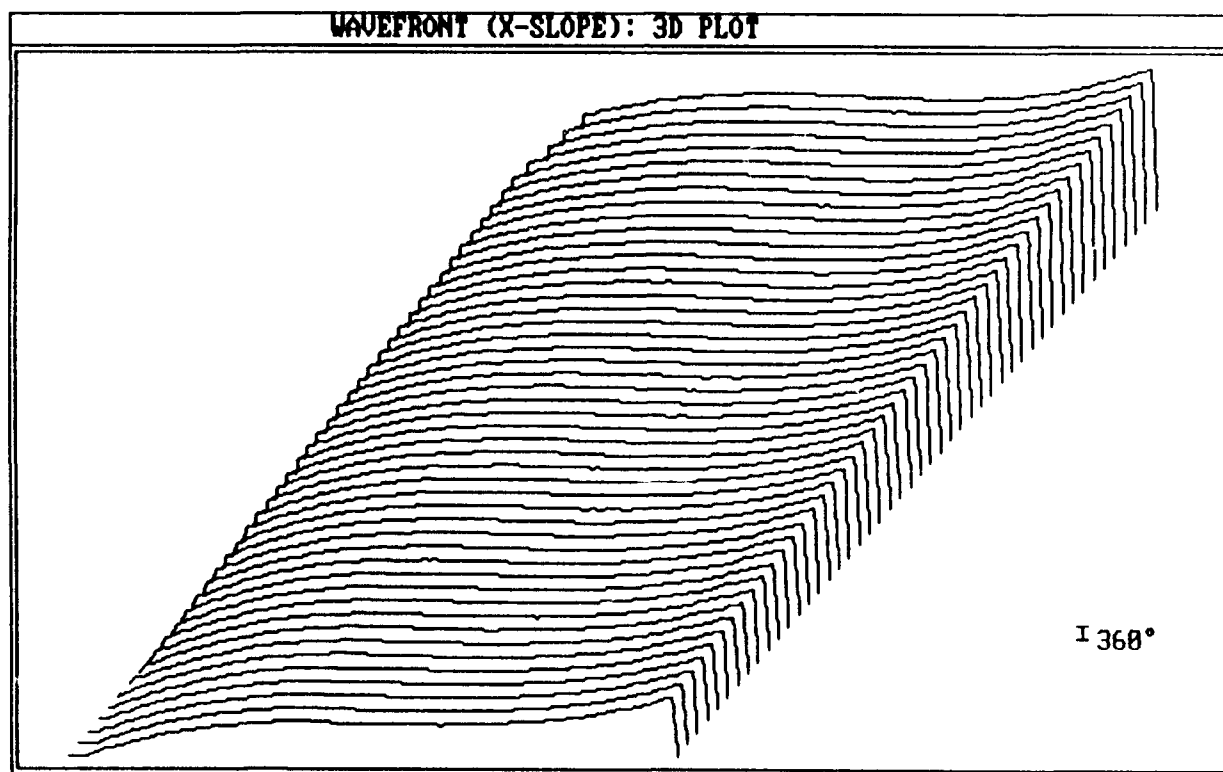
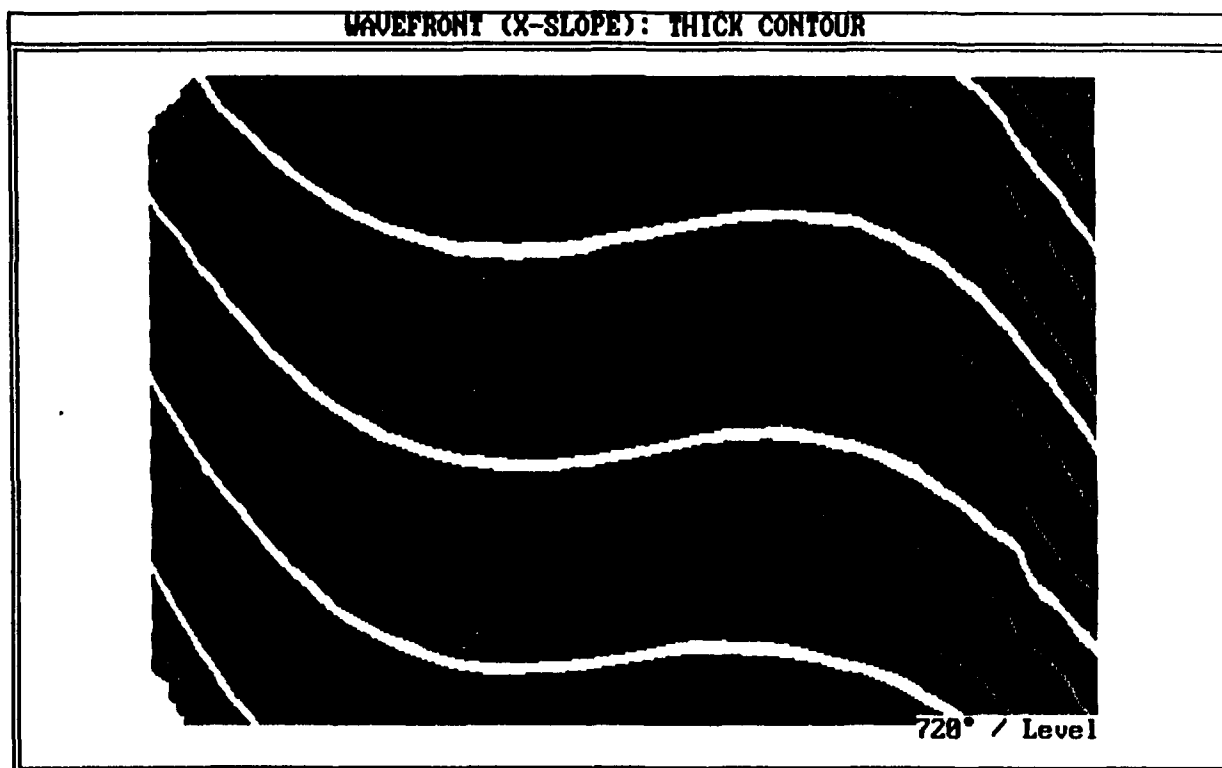


Figure 4: (a). Photograph of subaperture interferogram
(b). 3-D plot of wavefront slope
{X-shear, in focus, large misalignment (positive)}

(c)



(d)

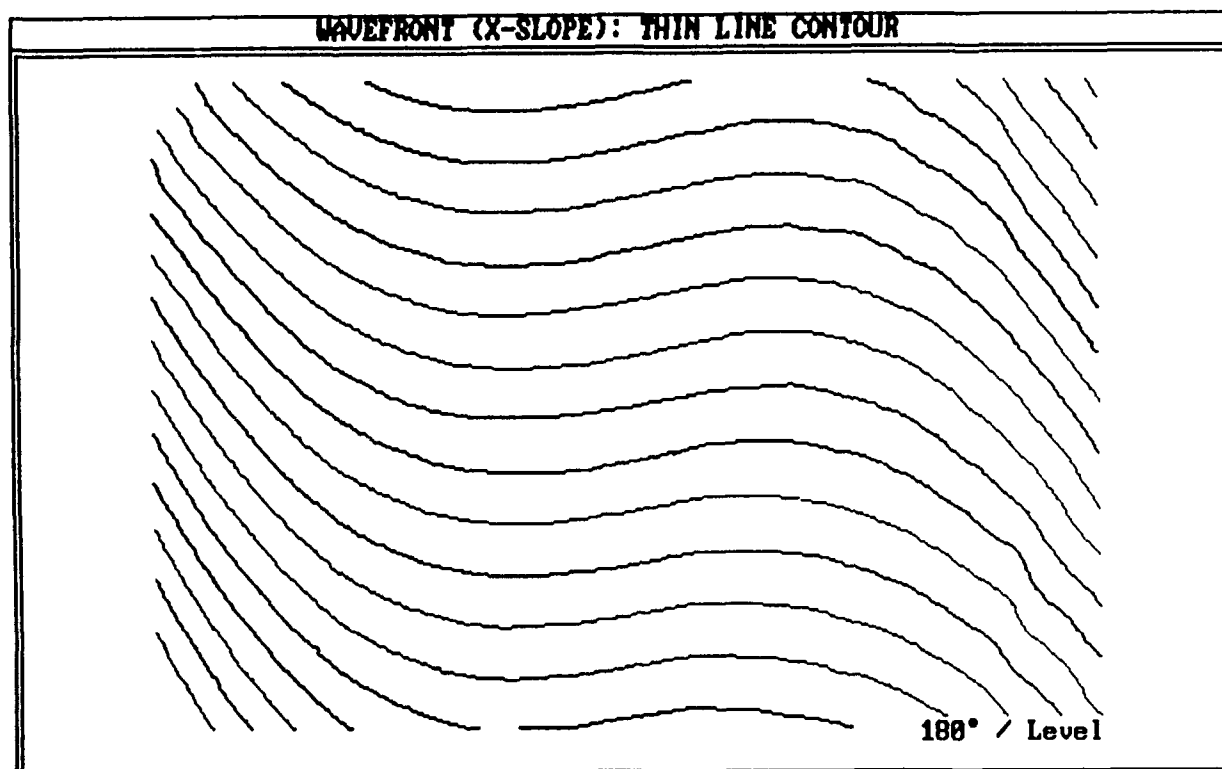
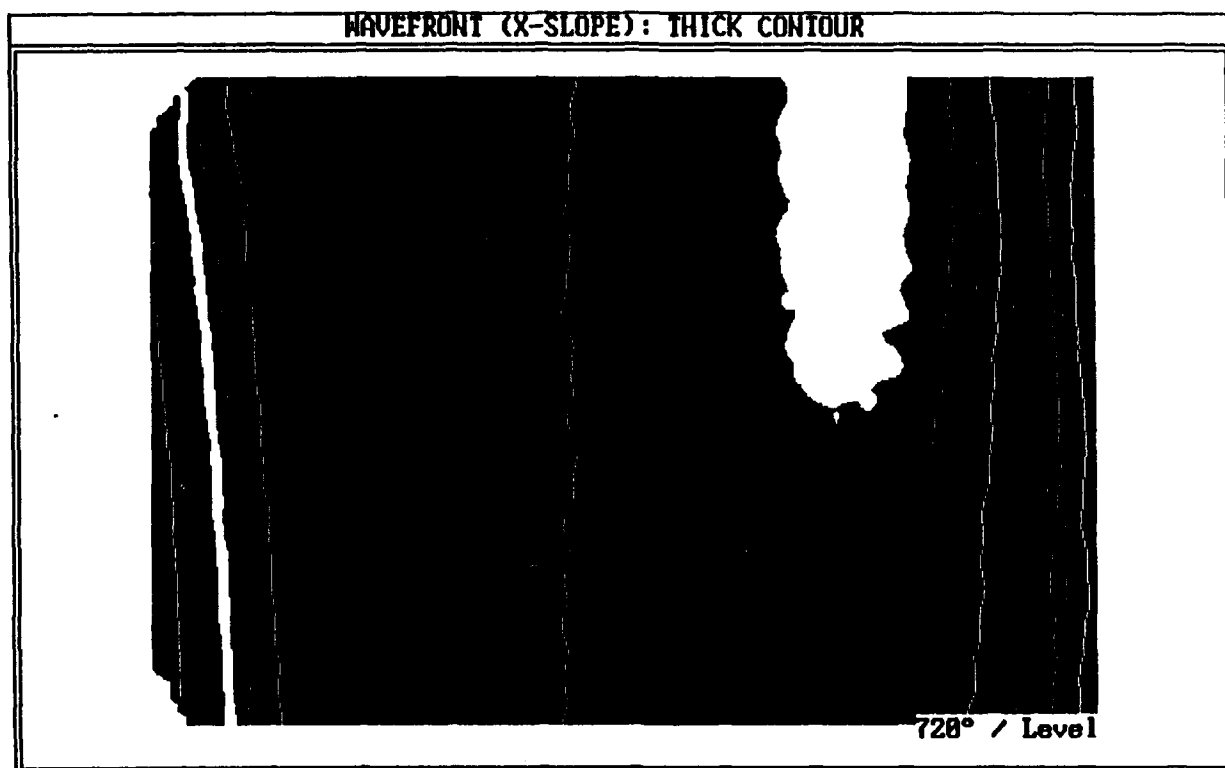


Figure 4: (c, d). Contour maps of wavefront slope
{X-shear, in focus, large misalignment (positive)}

(e)



(f)

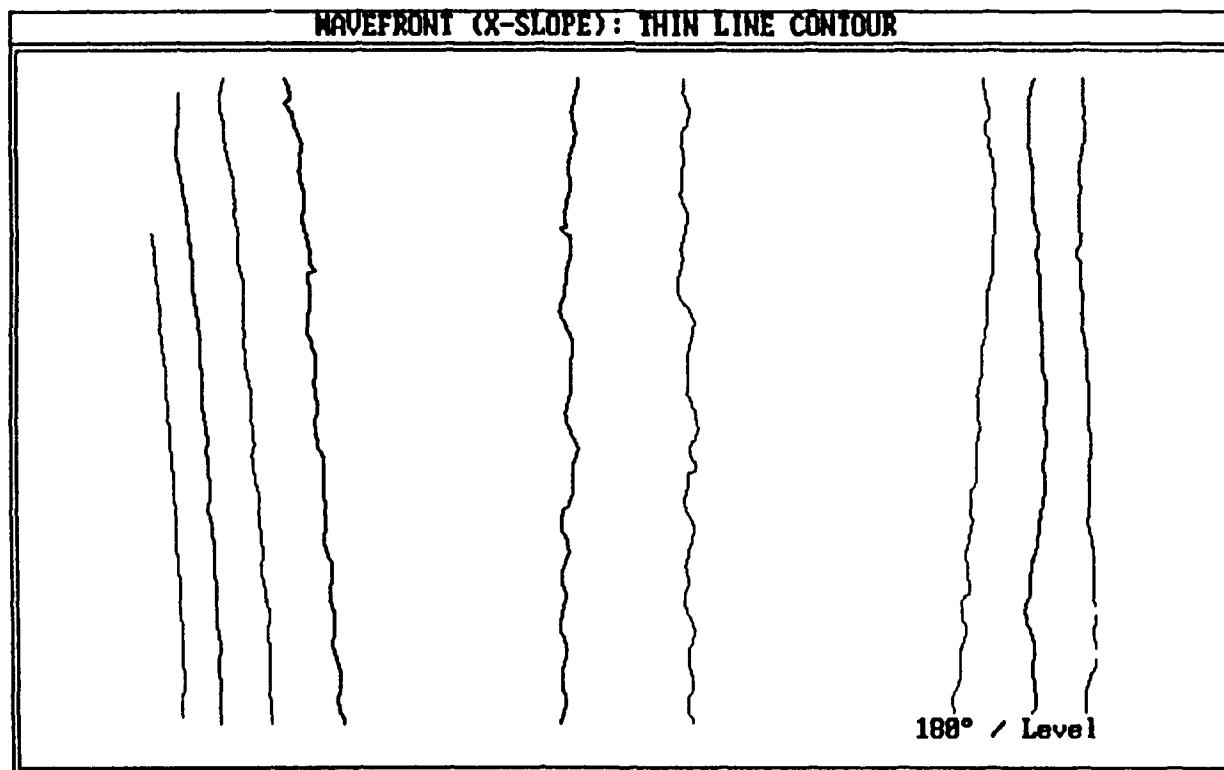
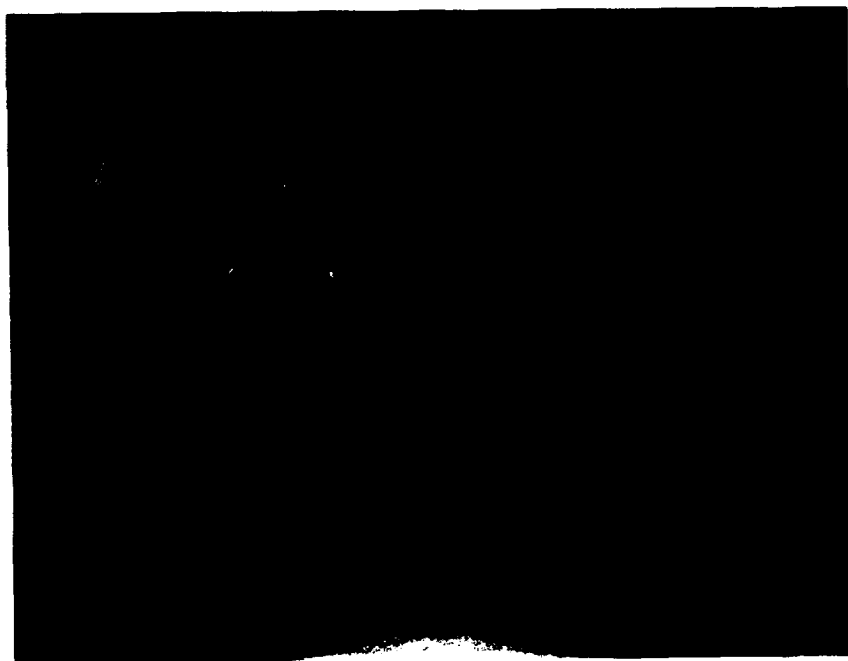


Figure 4: (e, f). Contour maps of wavefront slope, tilt removed
{X-shear, in focus, large misalignment (positive)}

(a)



(b)

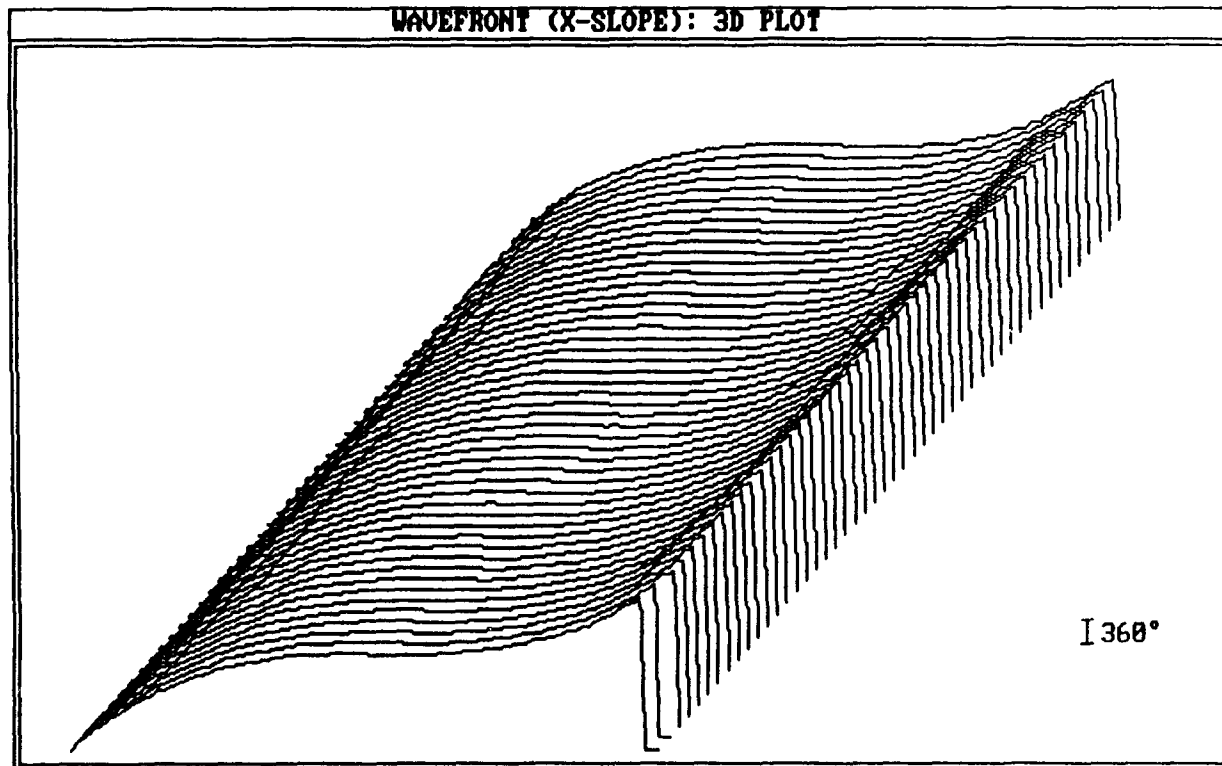
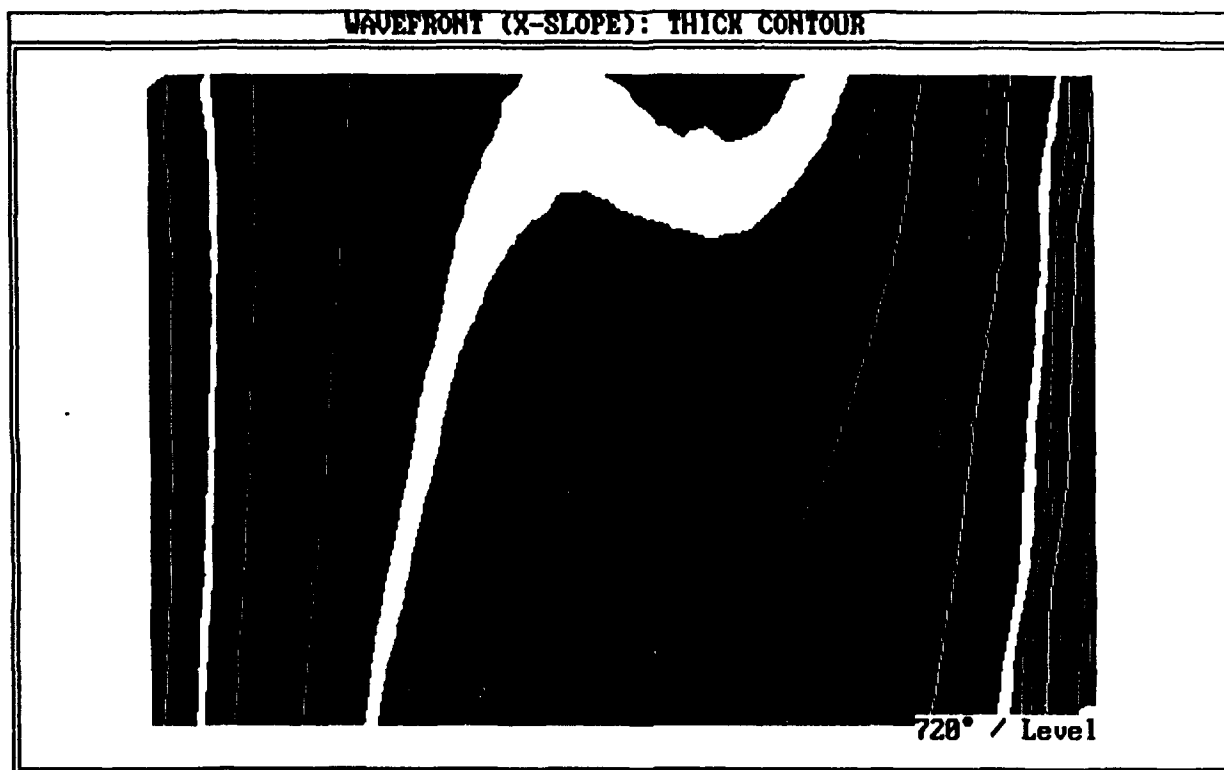


Figure 5: (a). Photograph of subaperture interferogram
(b). 3-D plot of wavefront slope
{X-shear, in focus, small misalignment (negative)}

(c)



(d)

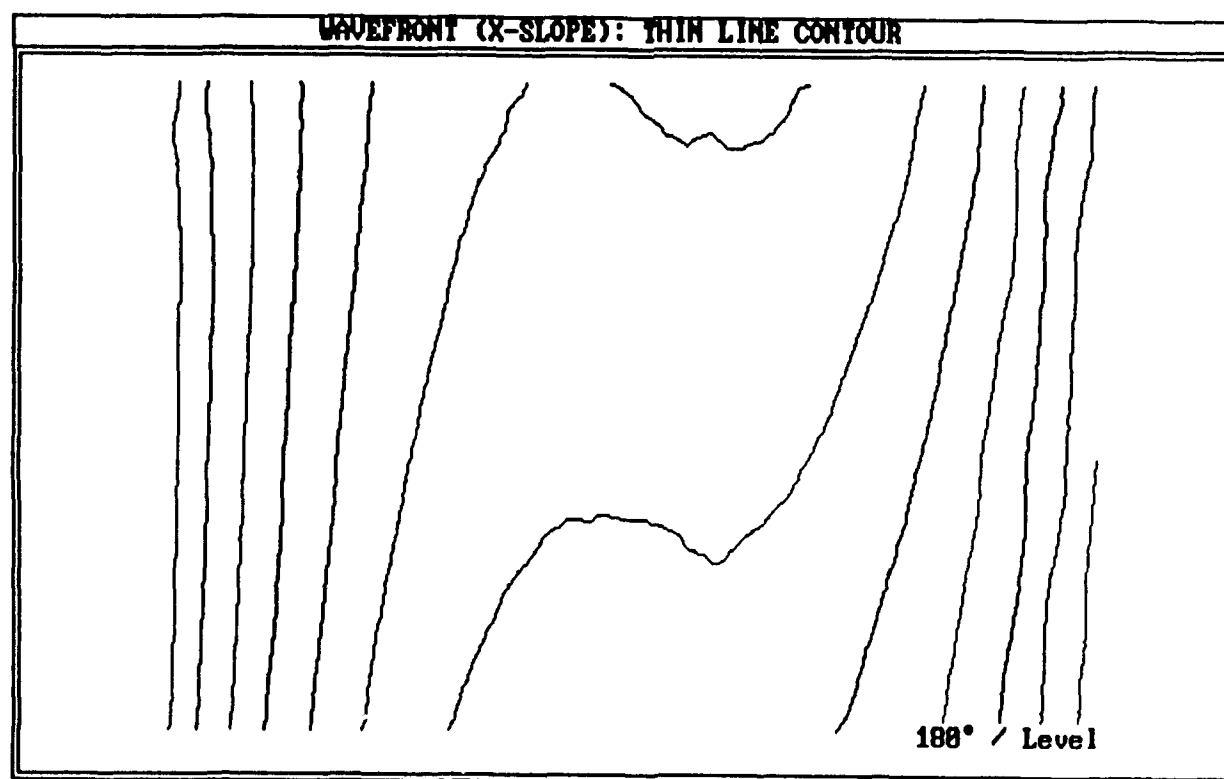
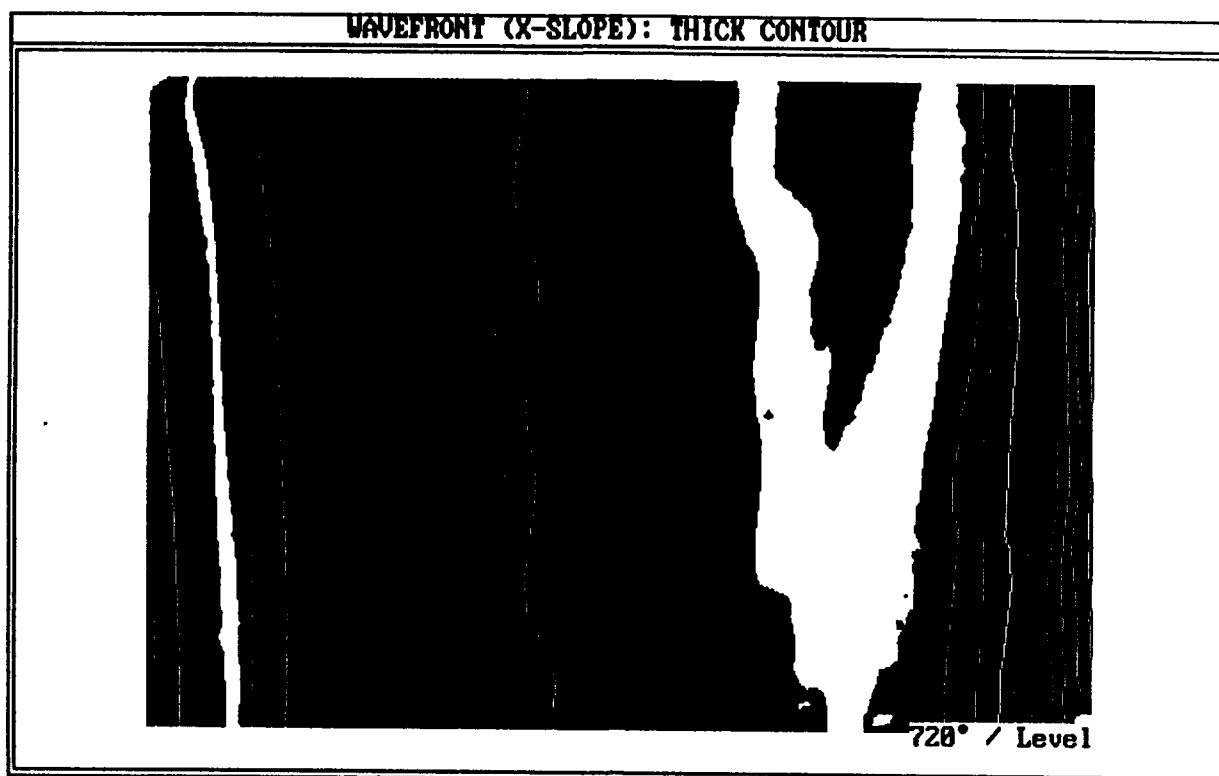


Figure 5: (c, d). Contour maps of wavefront slope
{X-shear, in focus, small misalignment (negative)}

(e)



(f)

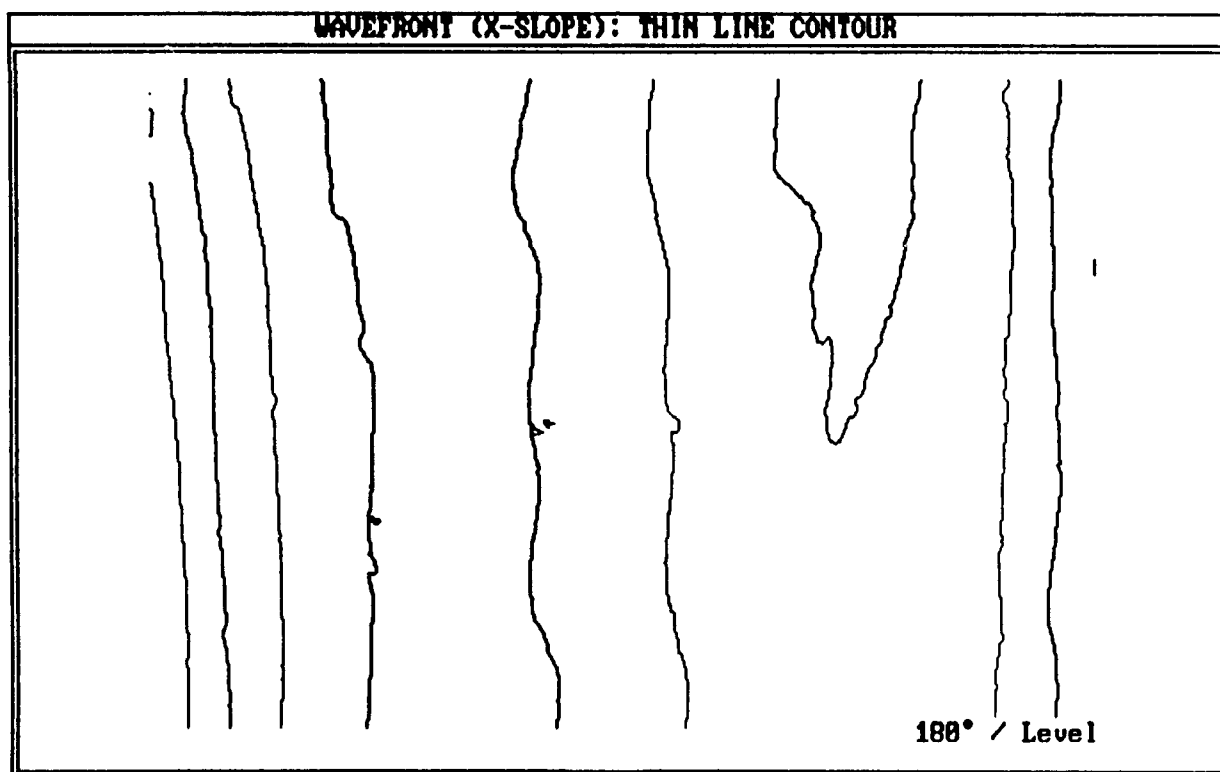


Figure 5: (e, f). Contour maps of wavefront slope, tilt removed
{X-shear, in focus, small misalignment (negative)}

(a)



(b)

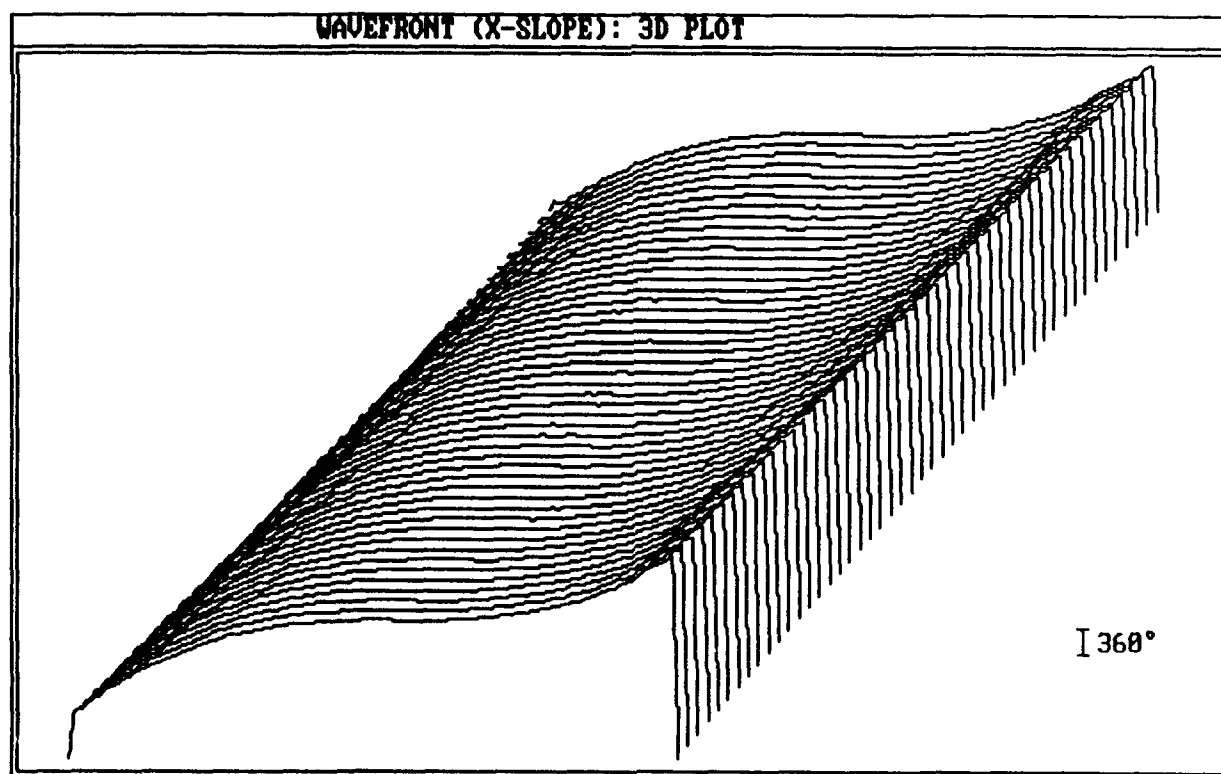
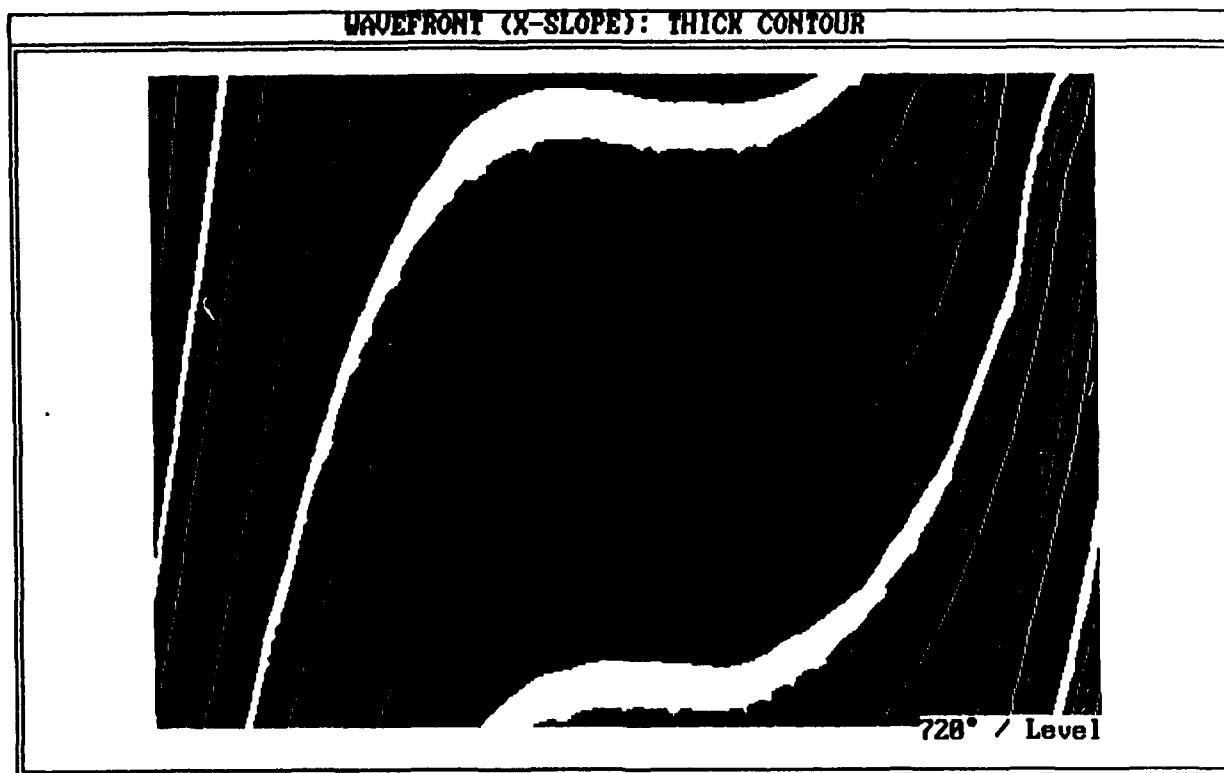


Figure 6: (a). Photograph of subaperture interferogram
(b). 3-D plot of wavefront slope
{X-shear, in focus, medium misalignment (negative)}

(c)



(d)

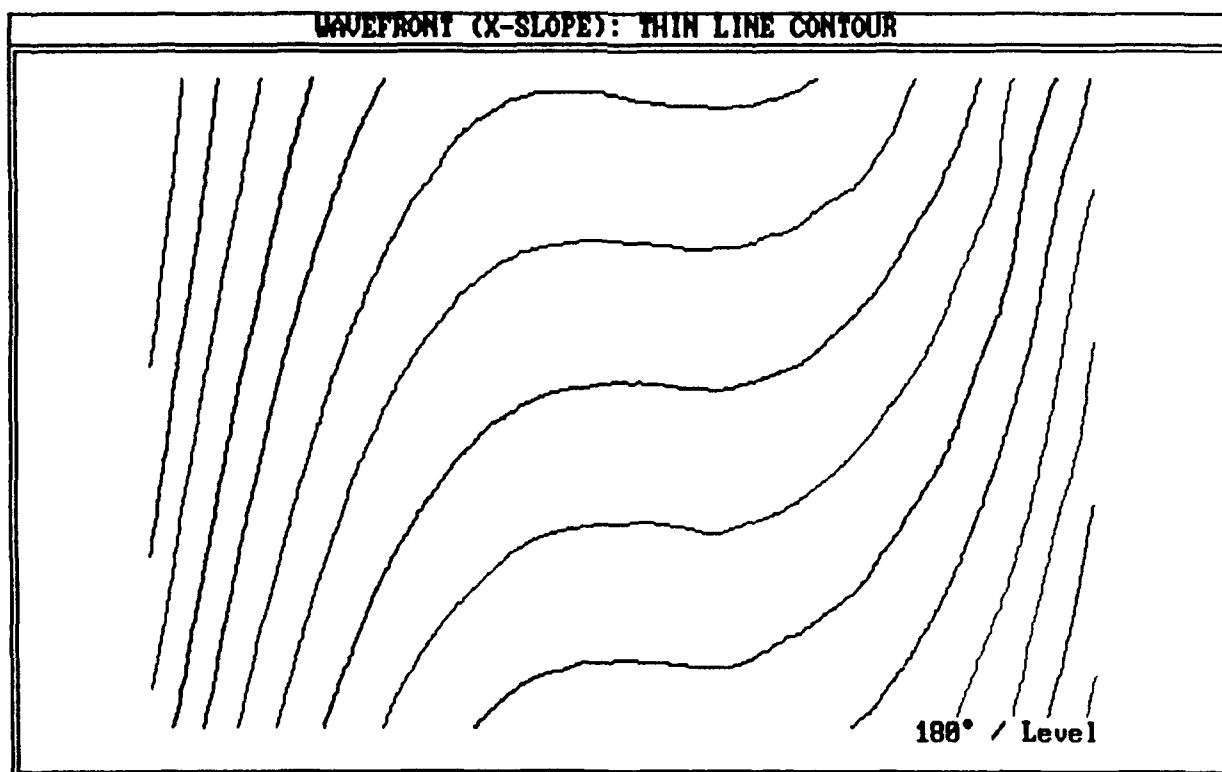
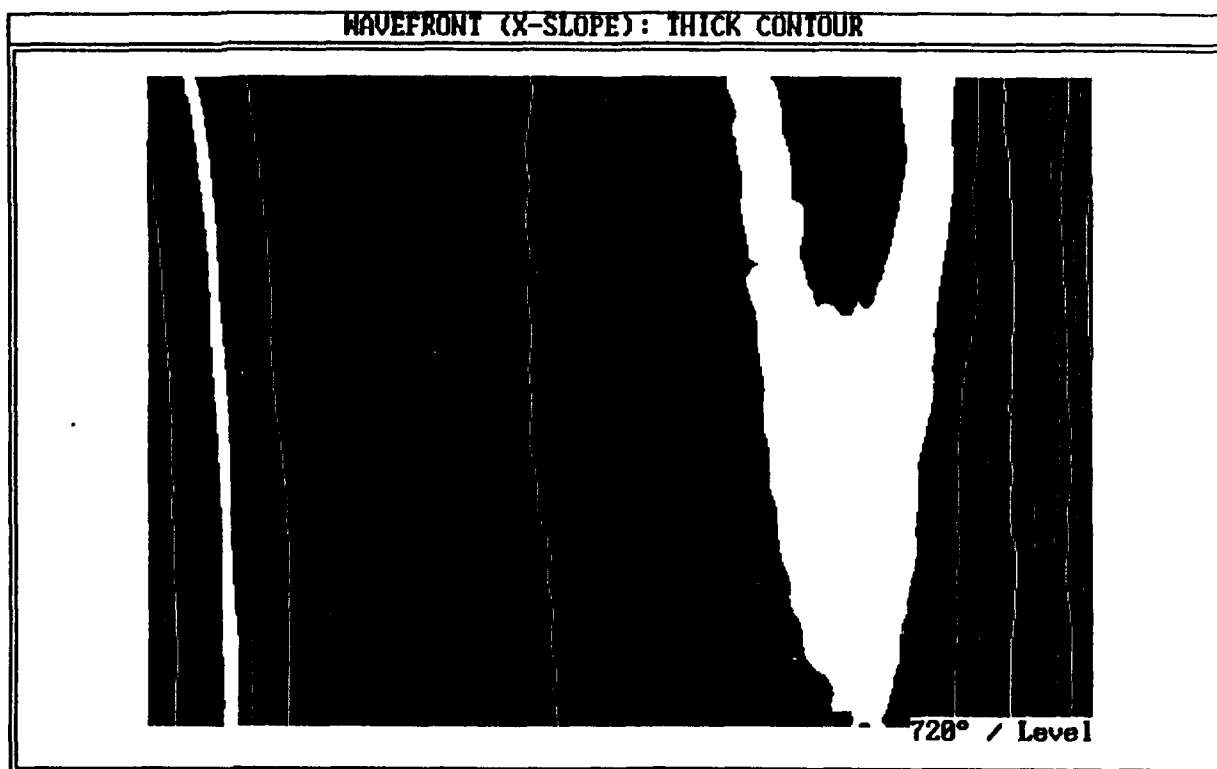


Figure 6: (c, d). Contour maps of wavefront slope
{X-shear, in focus, medium misalignment (negative)}

(e)



(f)

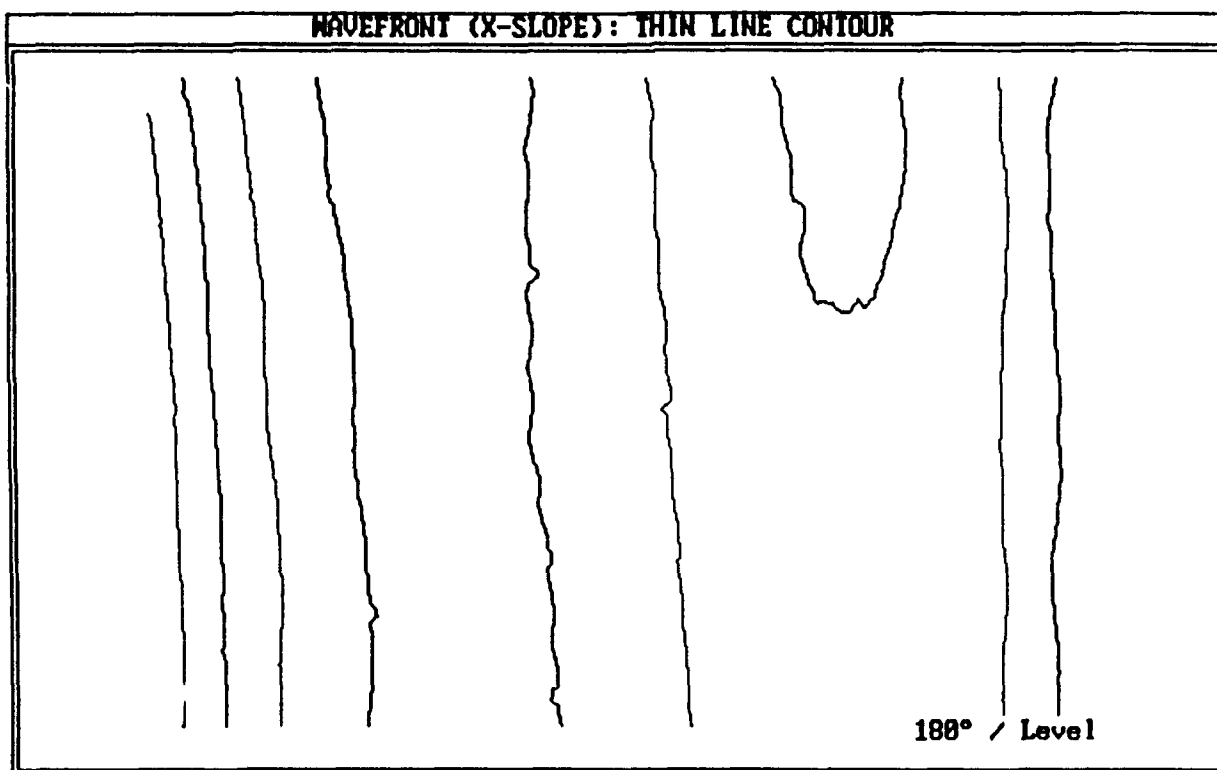


Figure 6: (e, f). Contour maps of wavefront slope, tilt removed
{X-shear, in focus, medium misalignment (negative)}

(a)



(b)

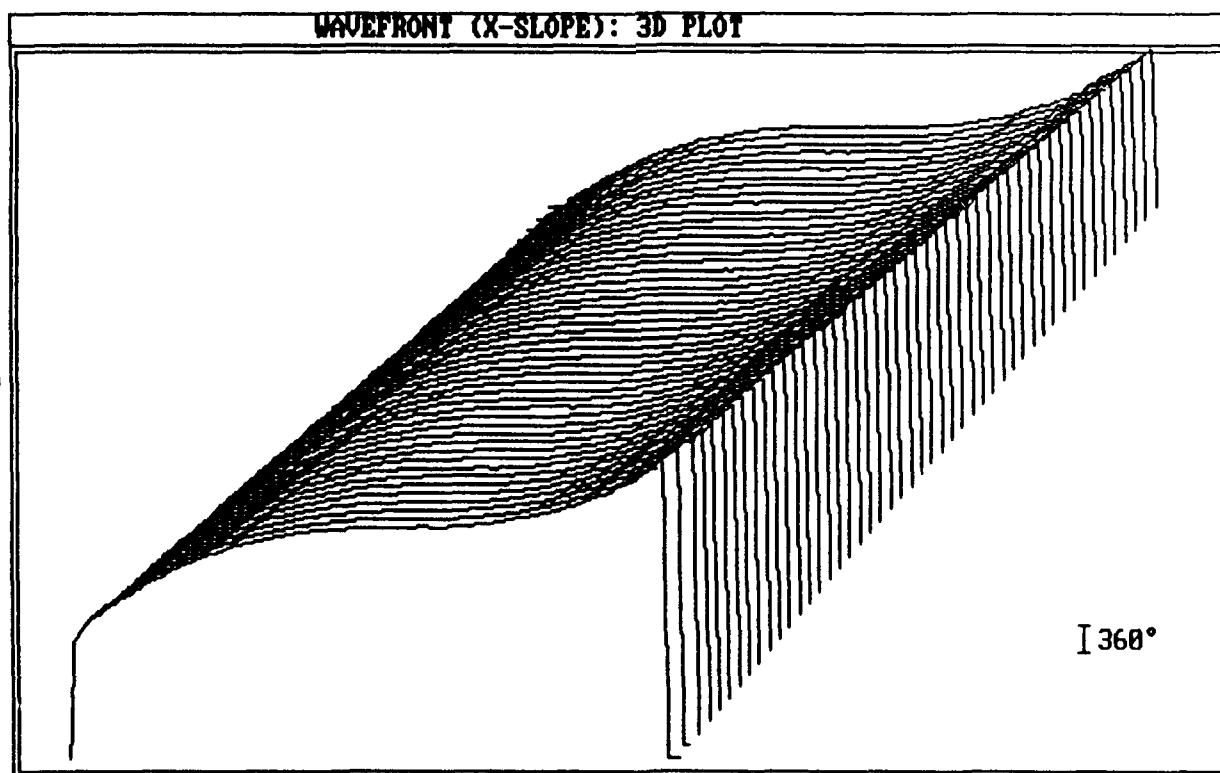


Figure 7: (a). Photograph of subaperture interferogram
(b). 3-D plot of wavefront slope
{X-shear, in focus, large misalignment (negative)}

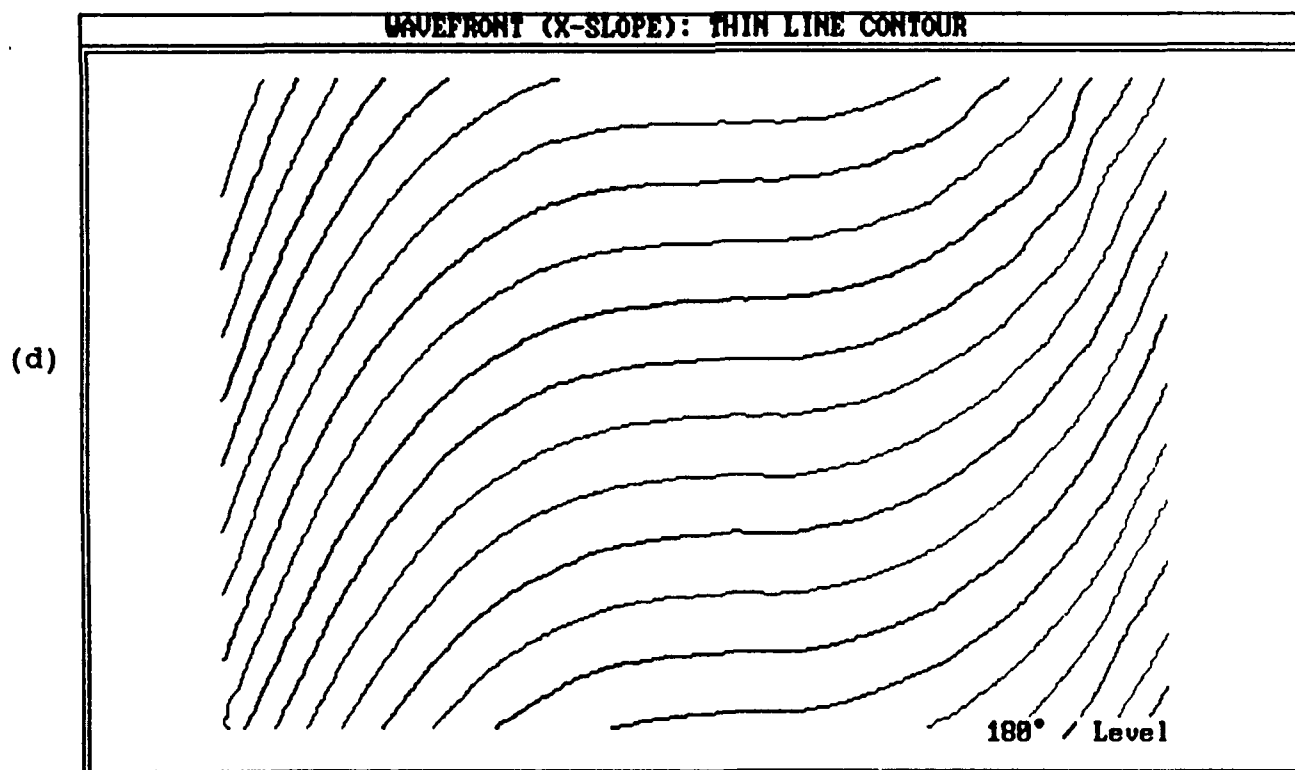
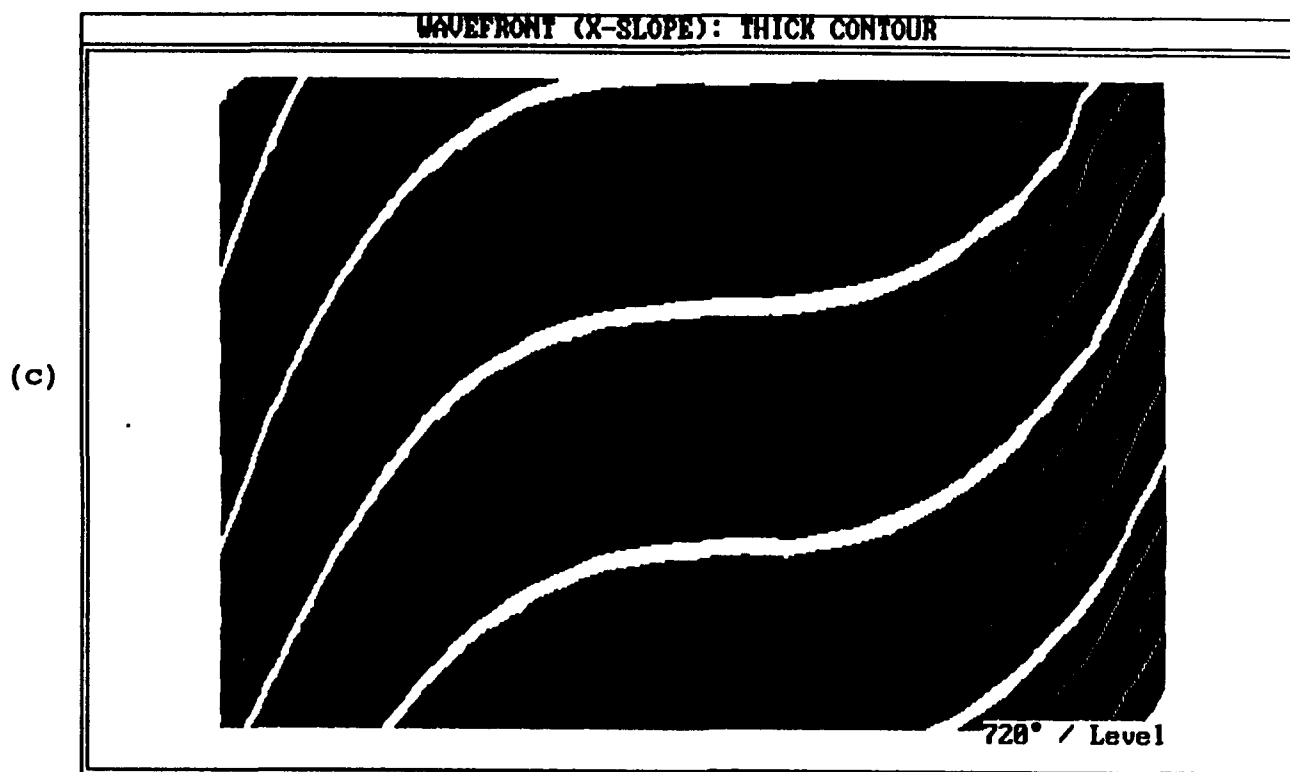
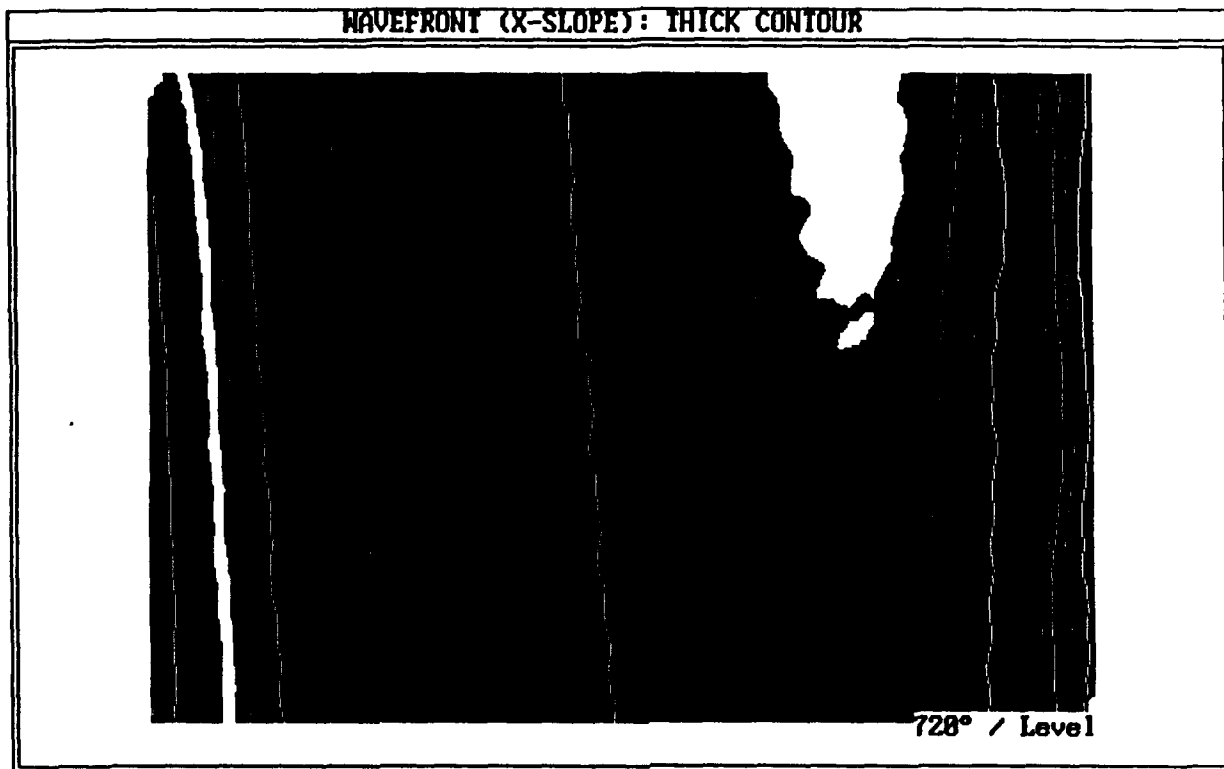


Figure 7: (c, d). Contour maps of wavefront slope
{X-shear, in focus, large misalignment (negative)}

(e)



(f)

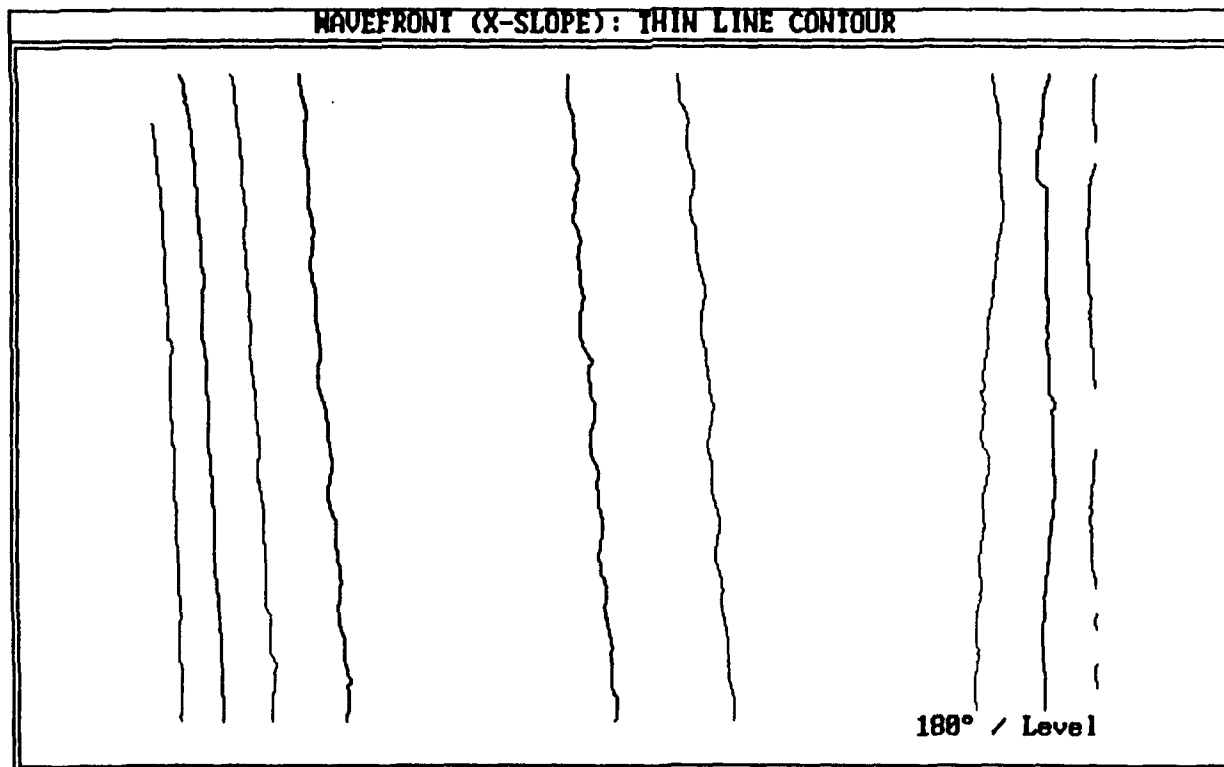
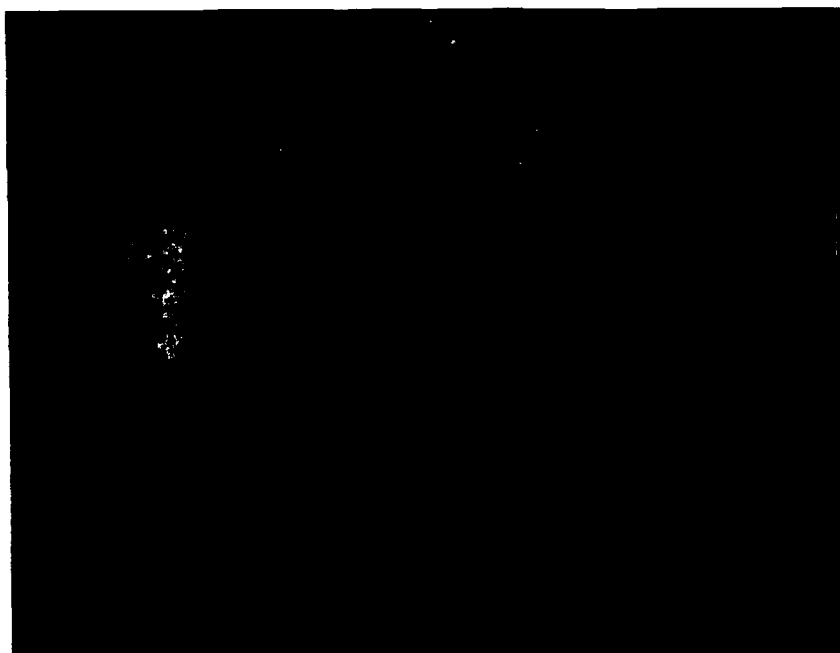


Figure 7: (e, f). Contour maps of wavefront slope, tilt removed
{X-shear, in focus, large misalignment (negative)}

(a)



(b)

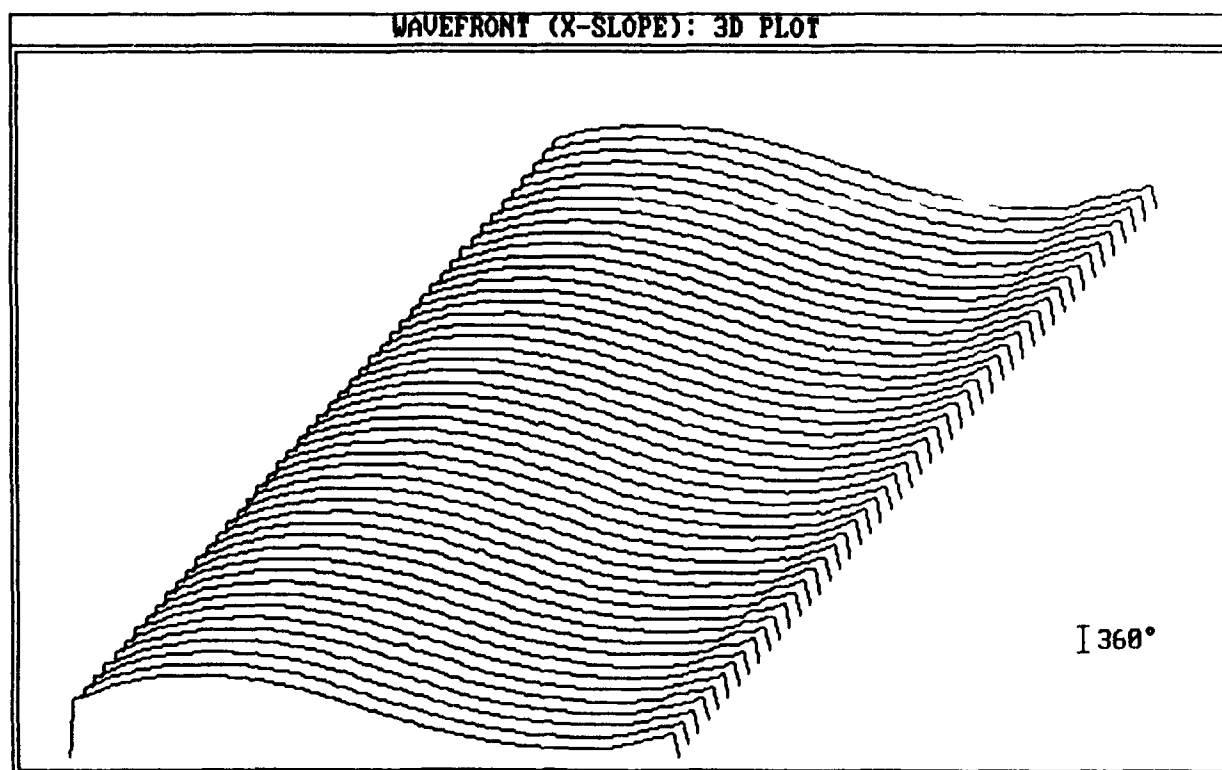
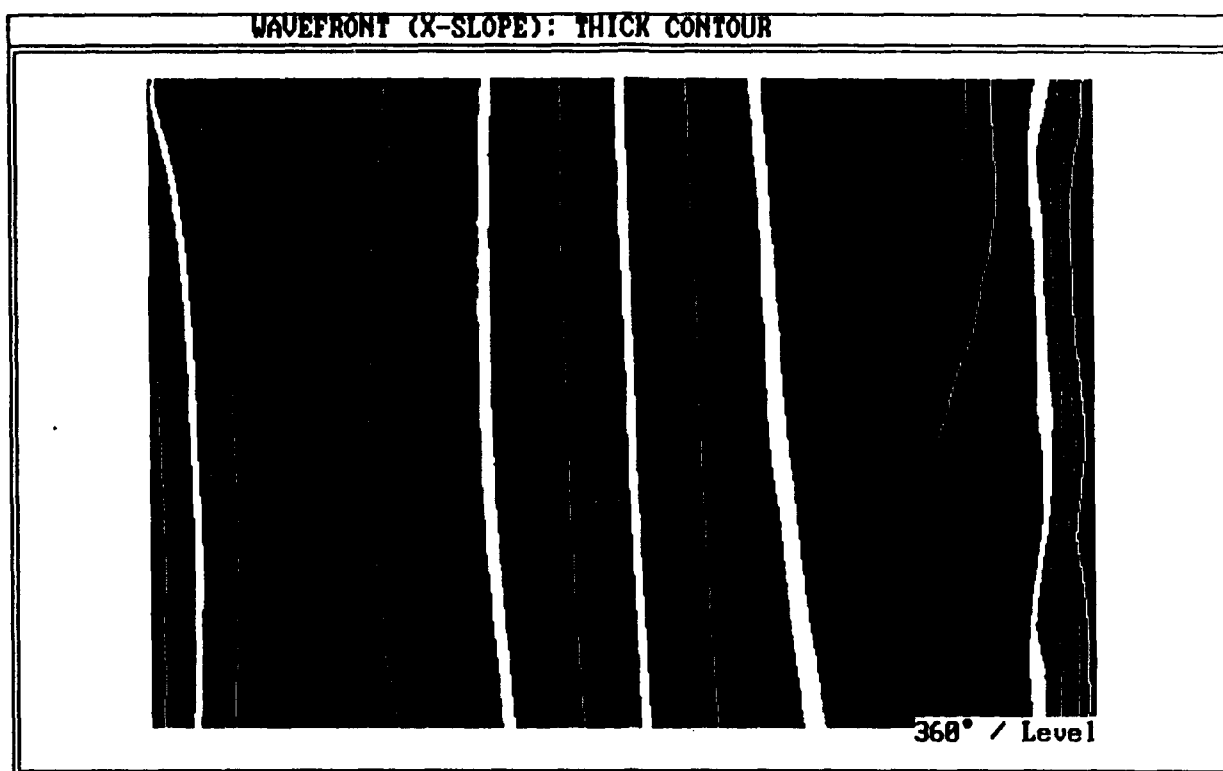


Figure 8: (a). Photograph of subaperture interferogram
(b). 3-D plot of wavefront slope
(X-shear, off focus, aligned)

(c)



(d)

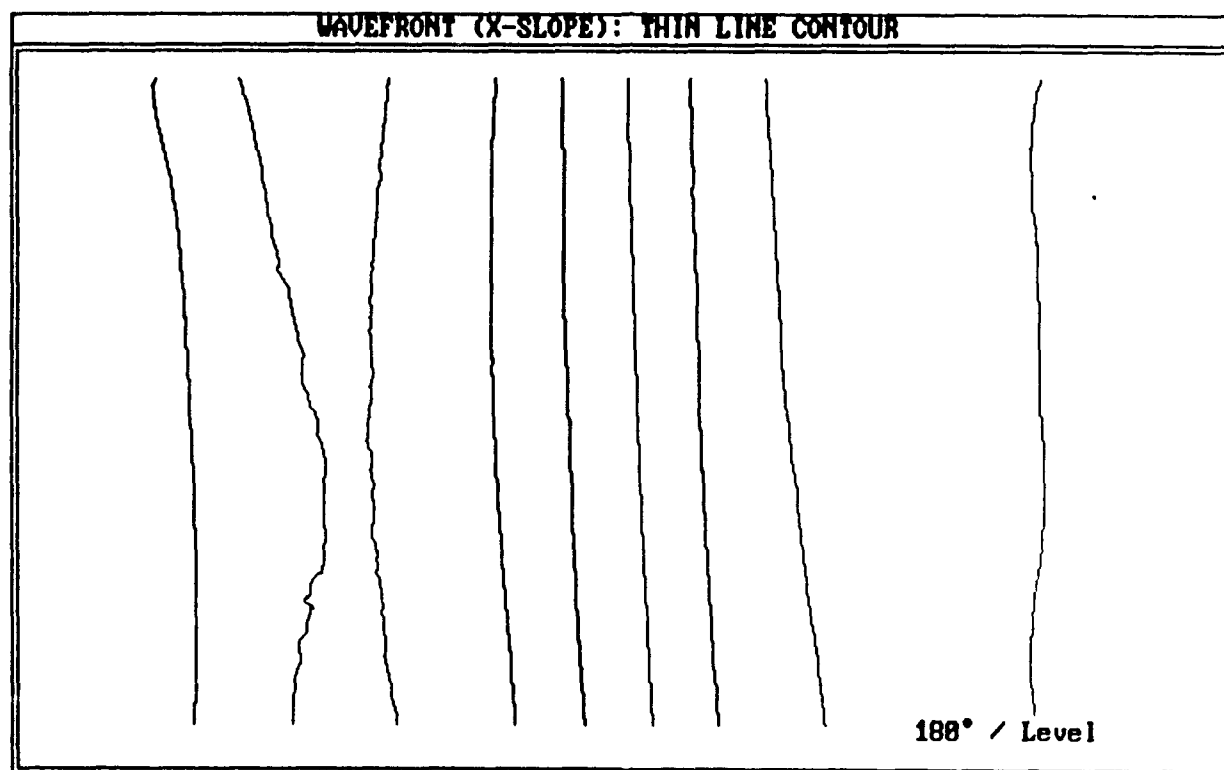
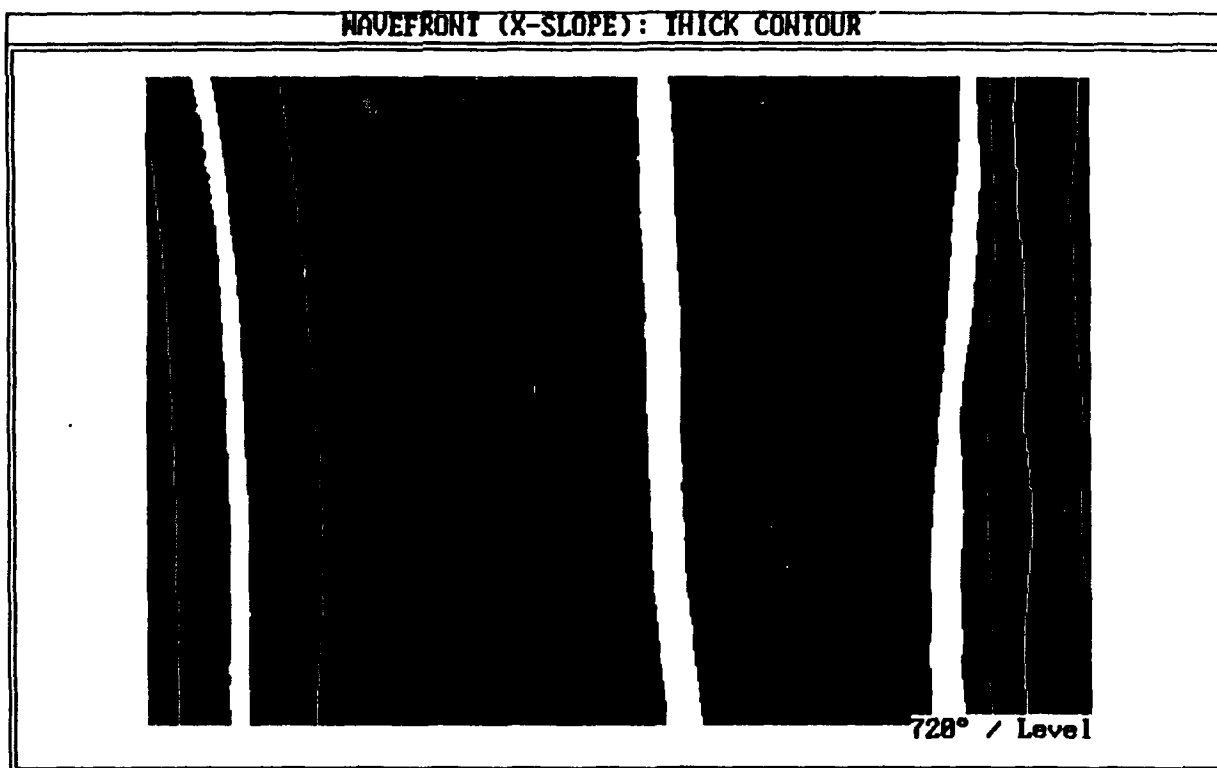


Figure 8: (c, d). Contour maps of wavefront slope (X-shear, off focus, aligned)

(e)



(f)

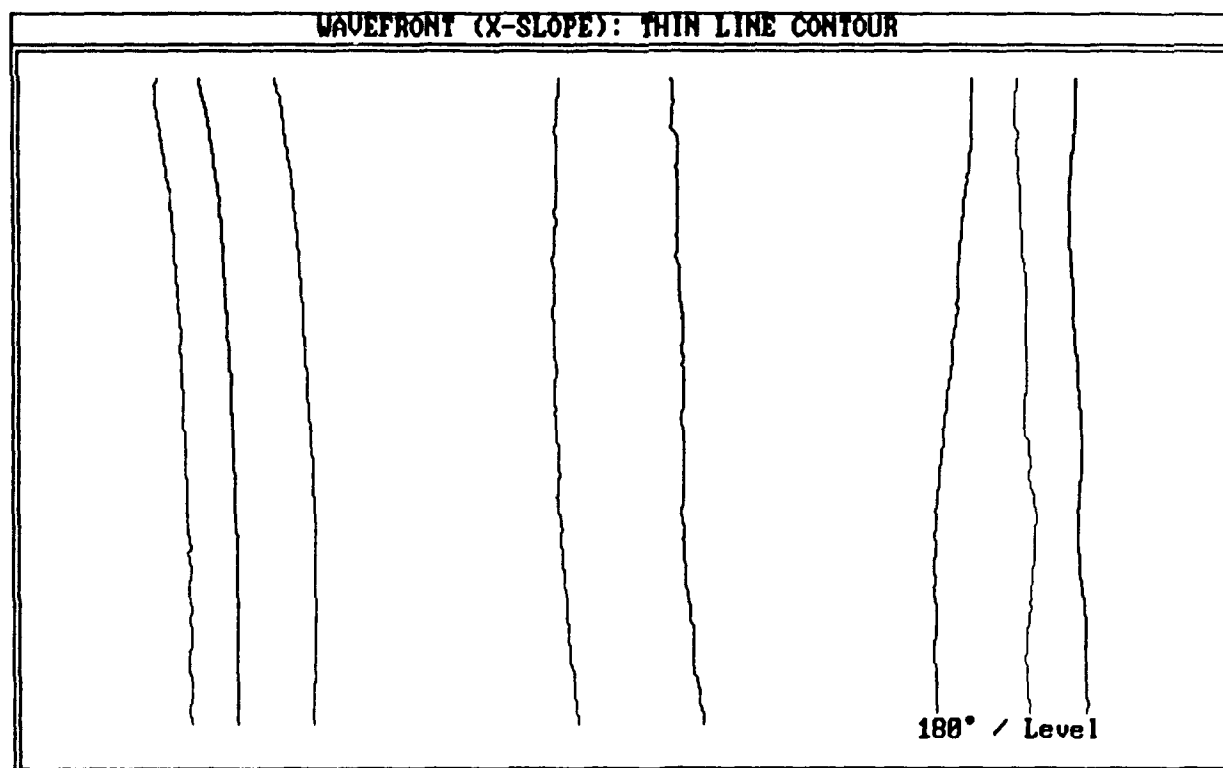
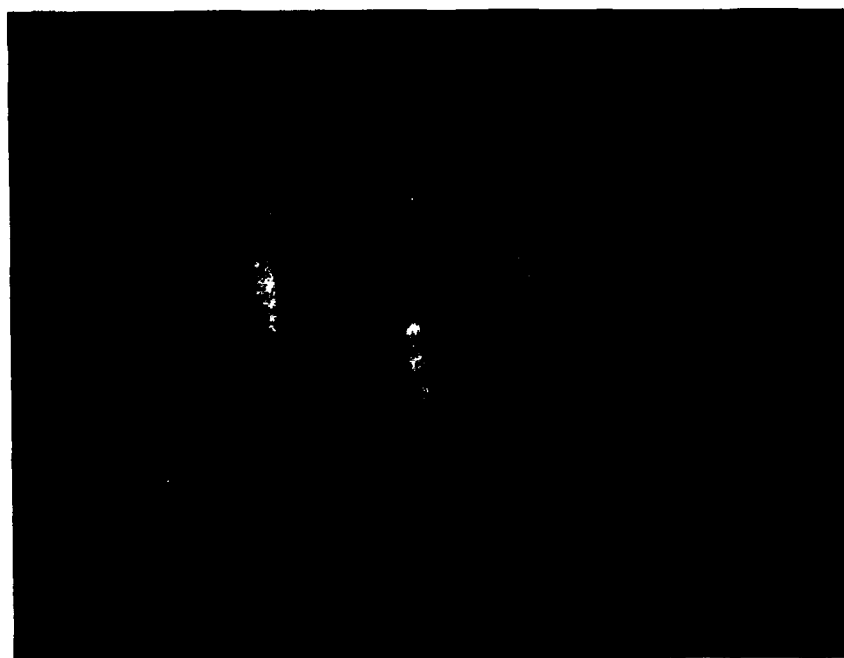


Figure 8: (e, f). Contour maps of wavefront slope, tilt removed (X-shear, off focus, aligned)

(a)



(b)

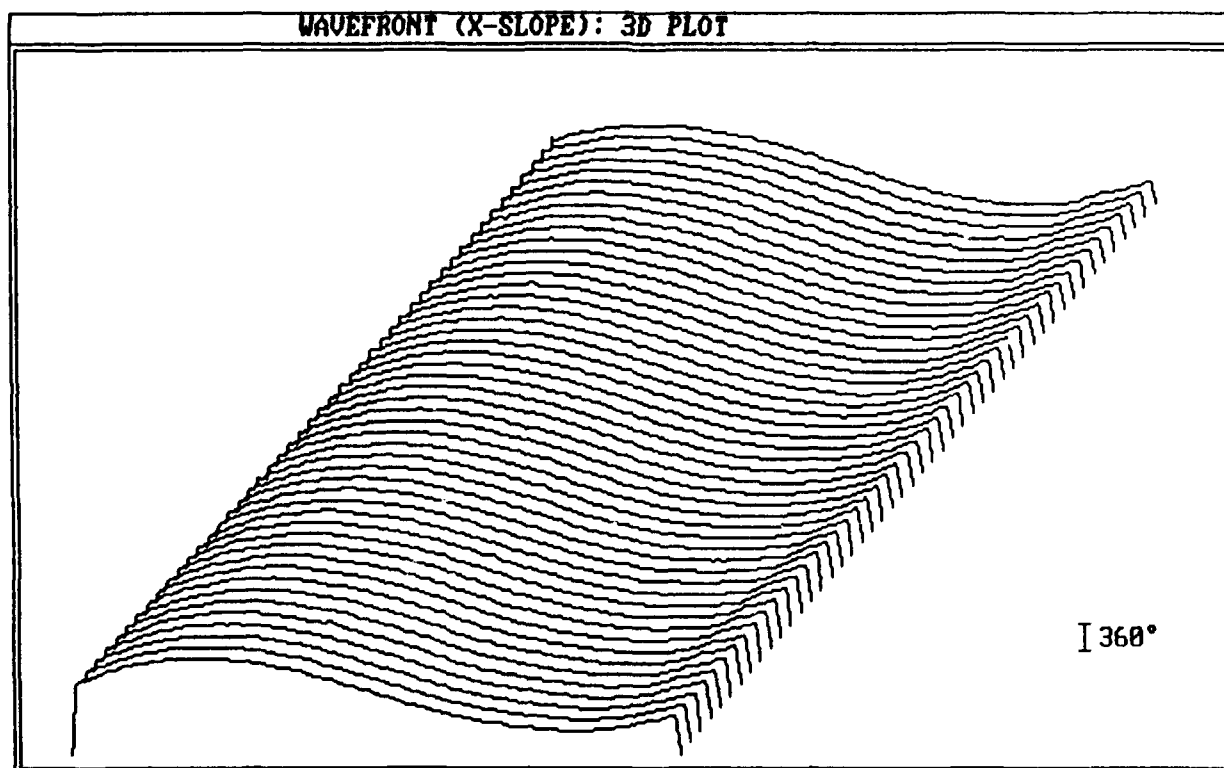


Figure 9: (a). Photograph of subaperture interferogram
(b). 3-D plot of wavefront slope
{X-shear, off focus, small misalignment (positive)}

WAVEFRONT (X-SLOPE): THICK CONTOUR

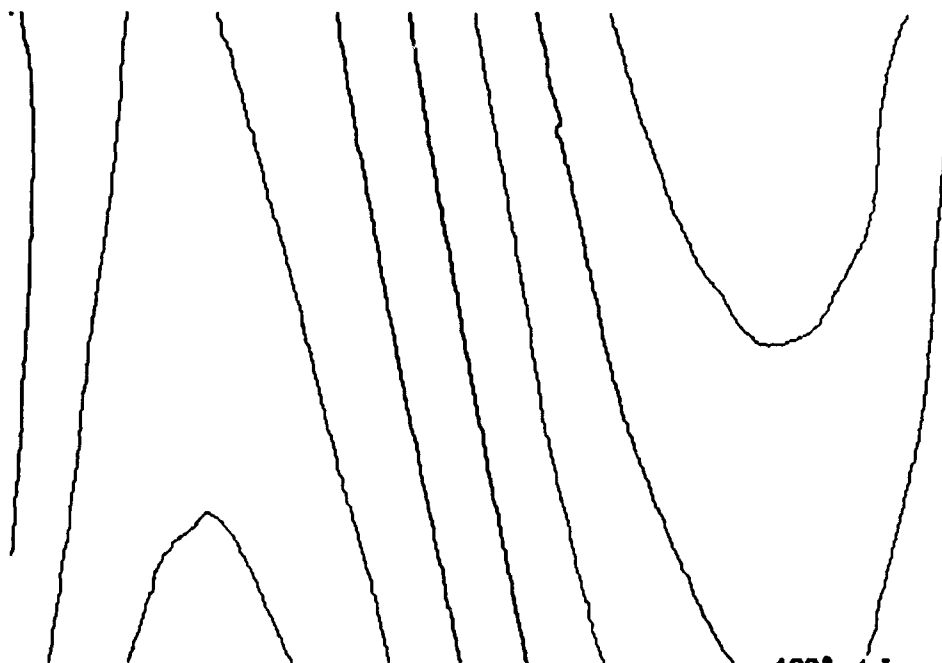
(c)



360° / Level

WAVEFRONT (X-SLOPE): THIN LINE CONTOUR

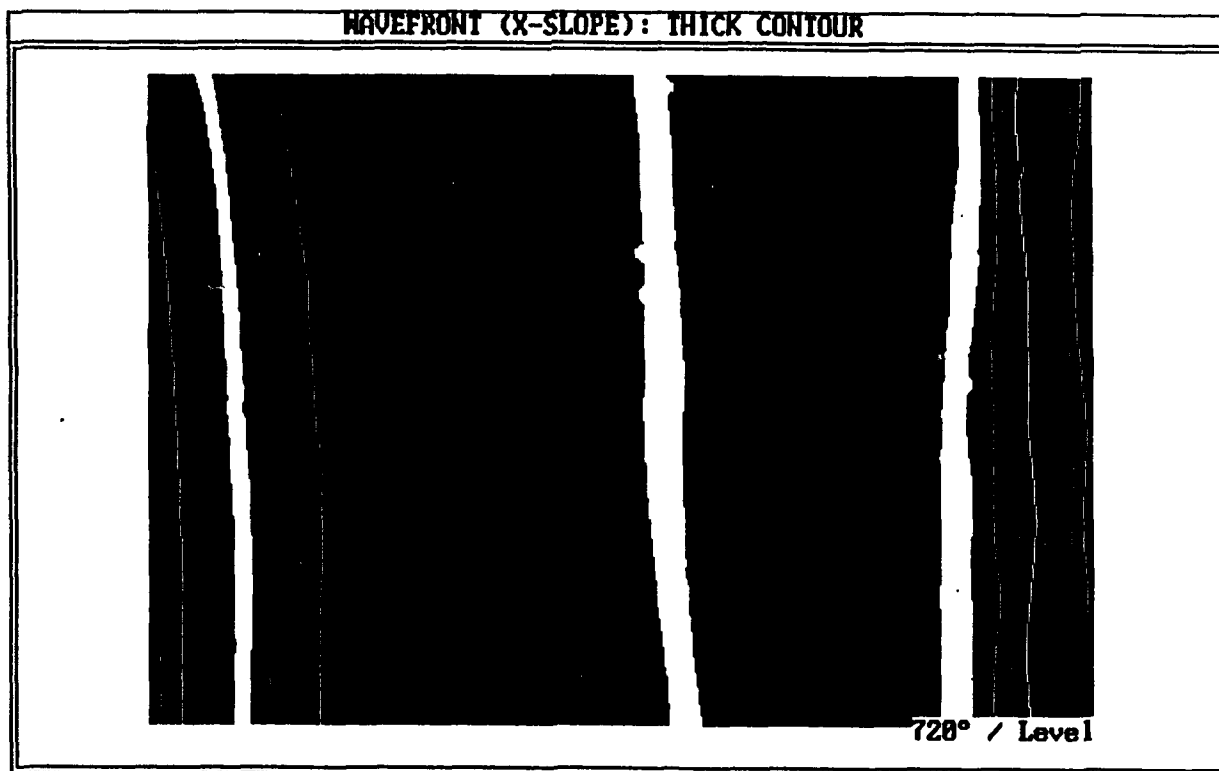
(d)



180° / Level

Figure 9: (c, d). Contour maps of wavefront slope
{X-shear, off focus, small misalignment (positive)}

(e)



(f)

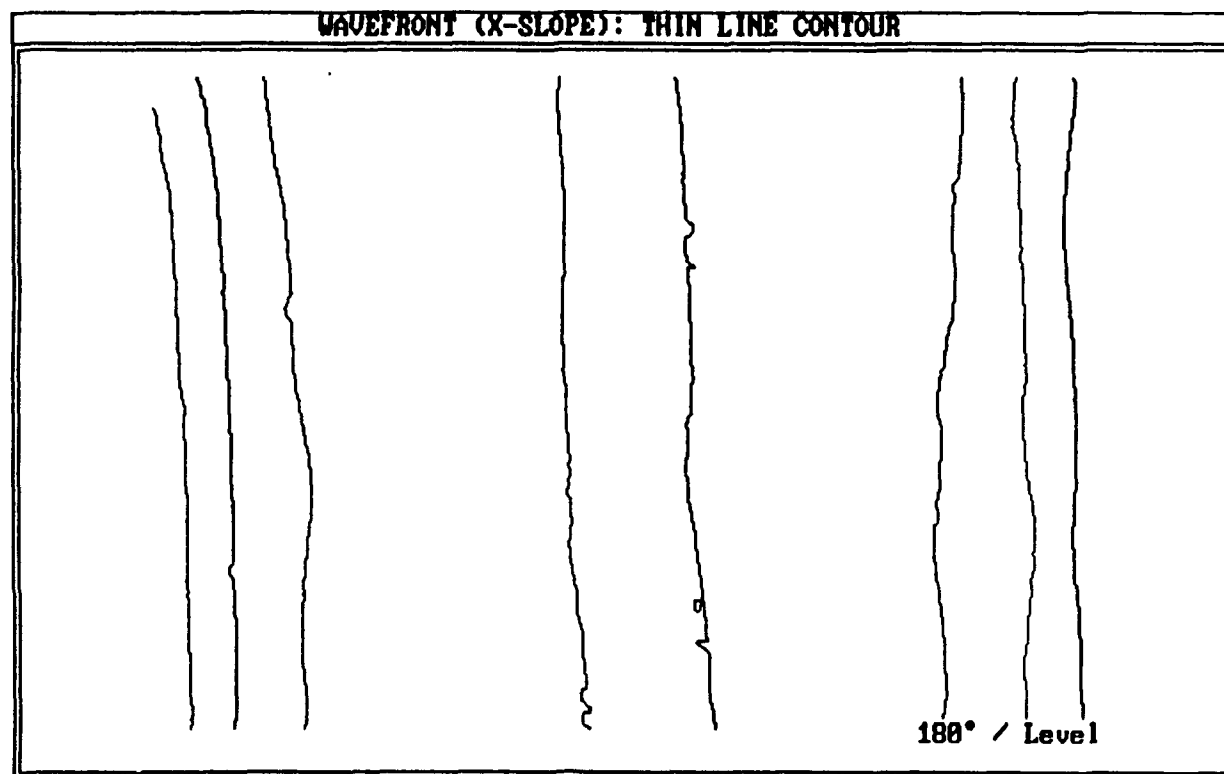
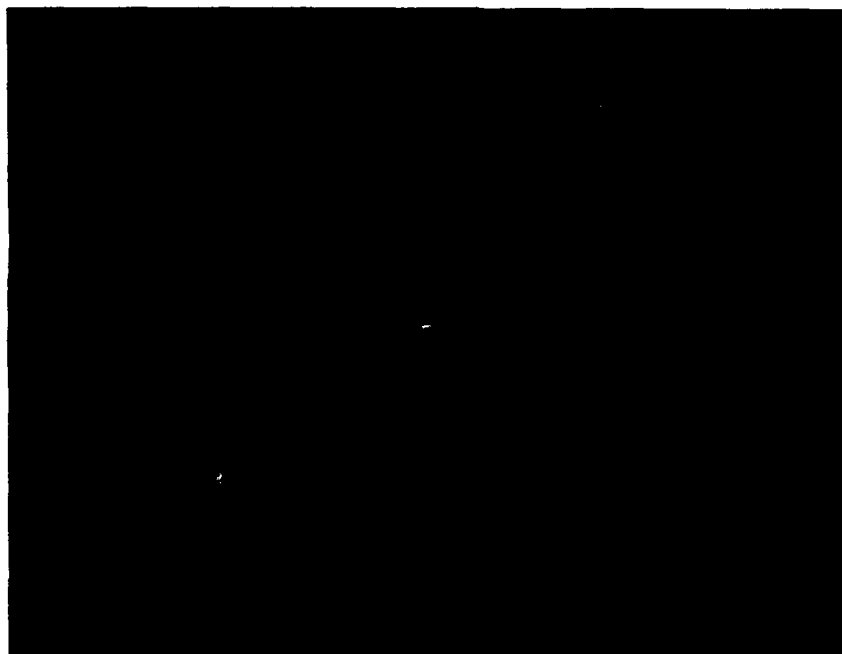


Figure 9: (e, f). Contour maps of wavefront slope, tilt removed
{X-shear, off focus, small misalignment (positive)}

(a)



(b)

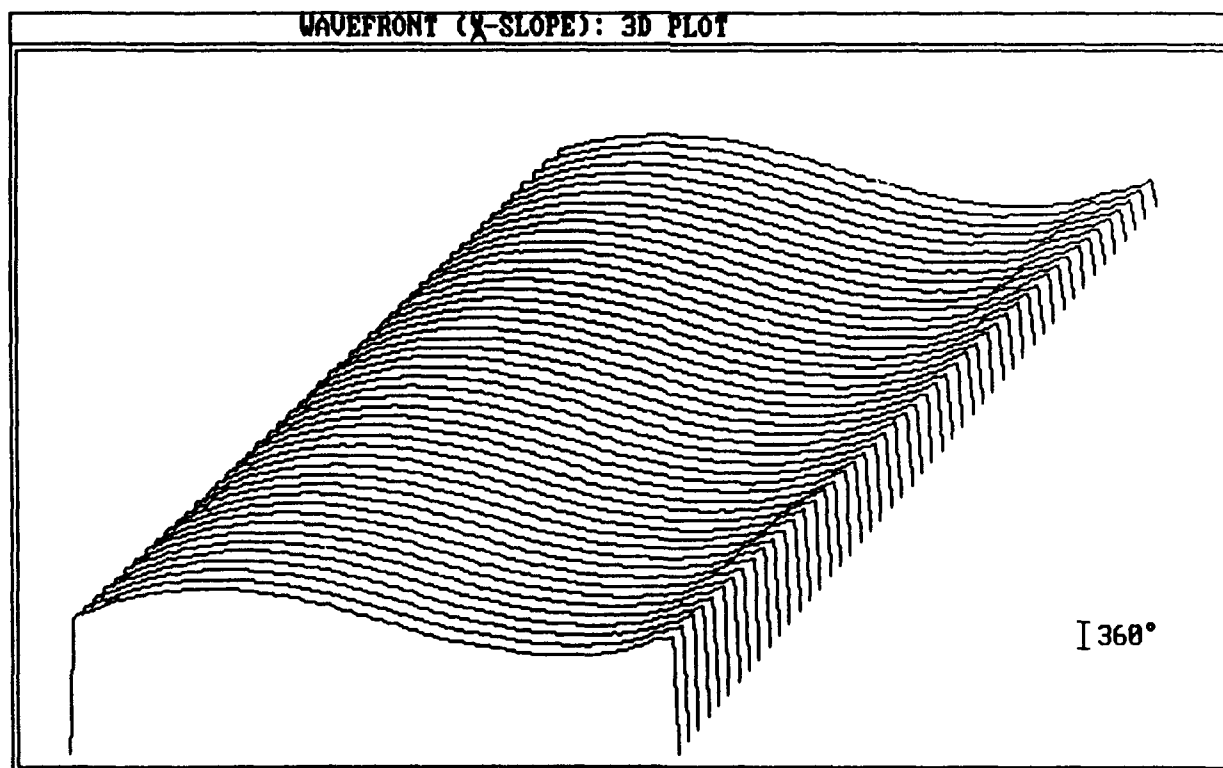
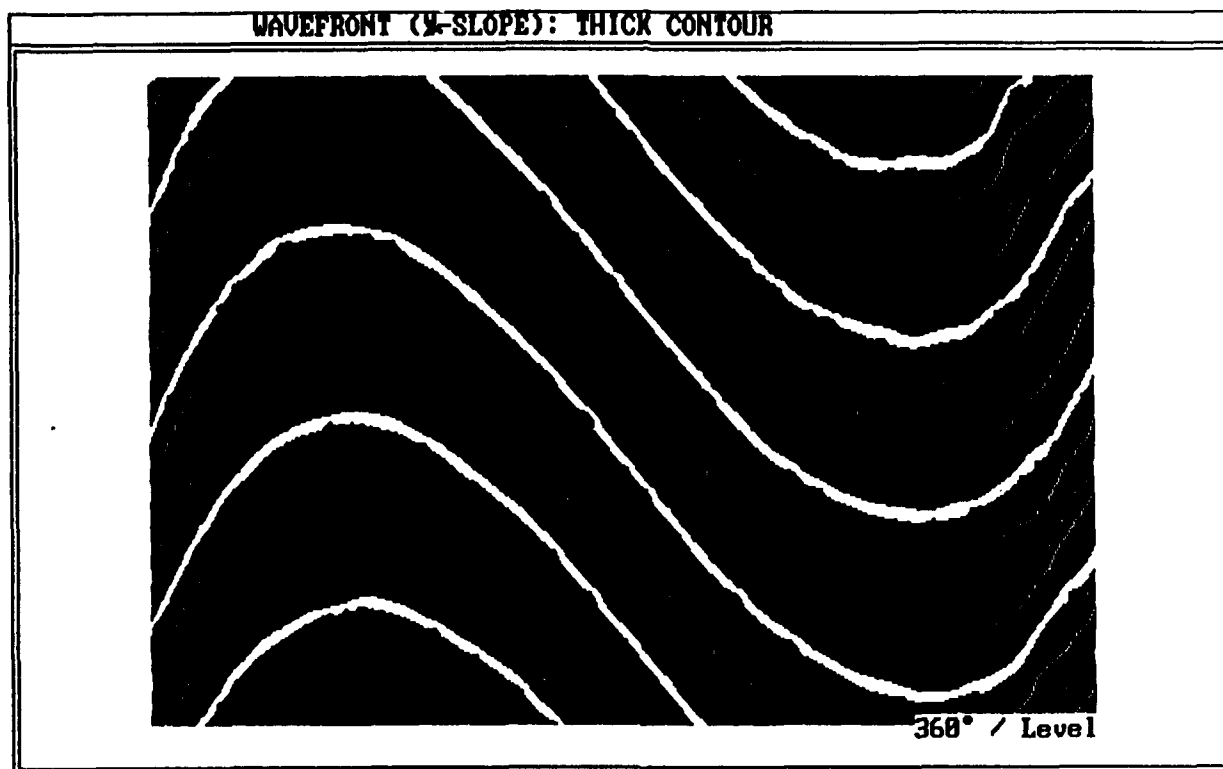


Figure 10: (a). Photograph of subaperture interferogram
(b). 3-D plot of wavefront slope
{X-shear, off focus, large misalignment (positive)}

(c)



(d)

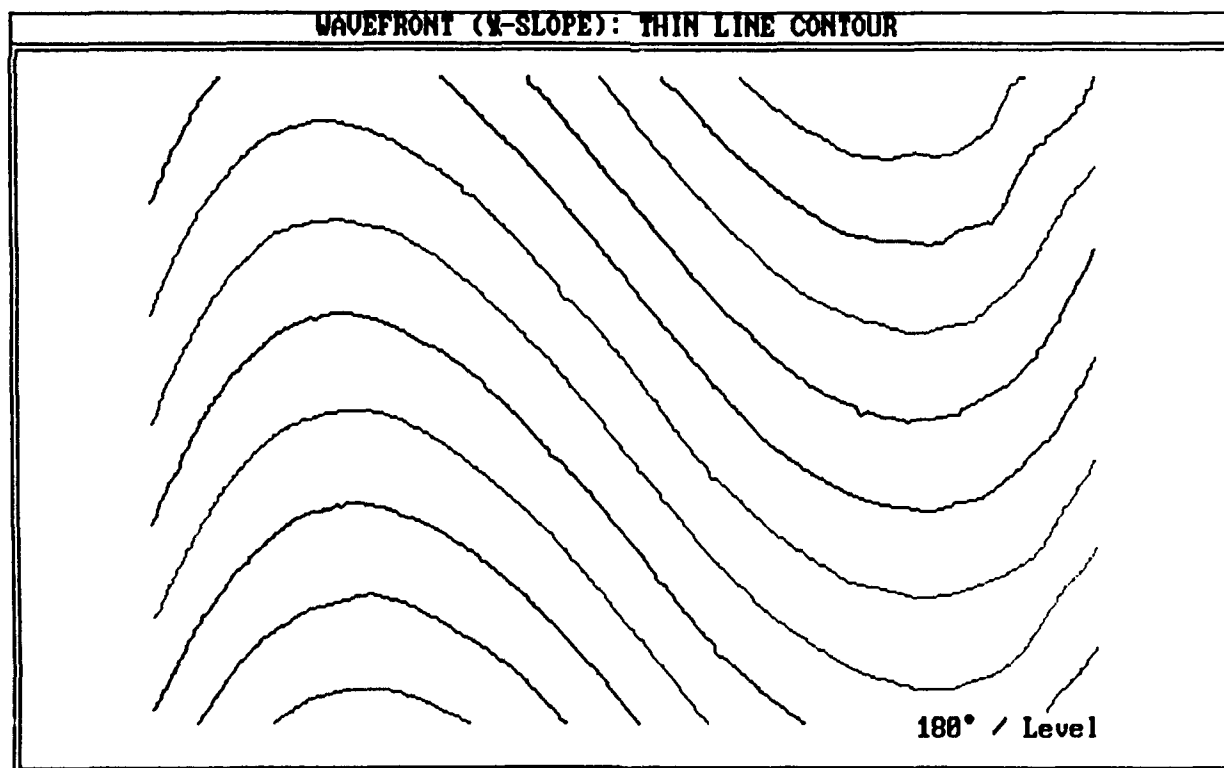
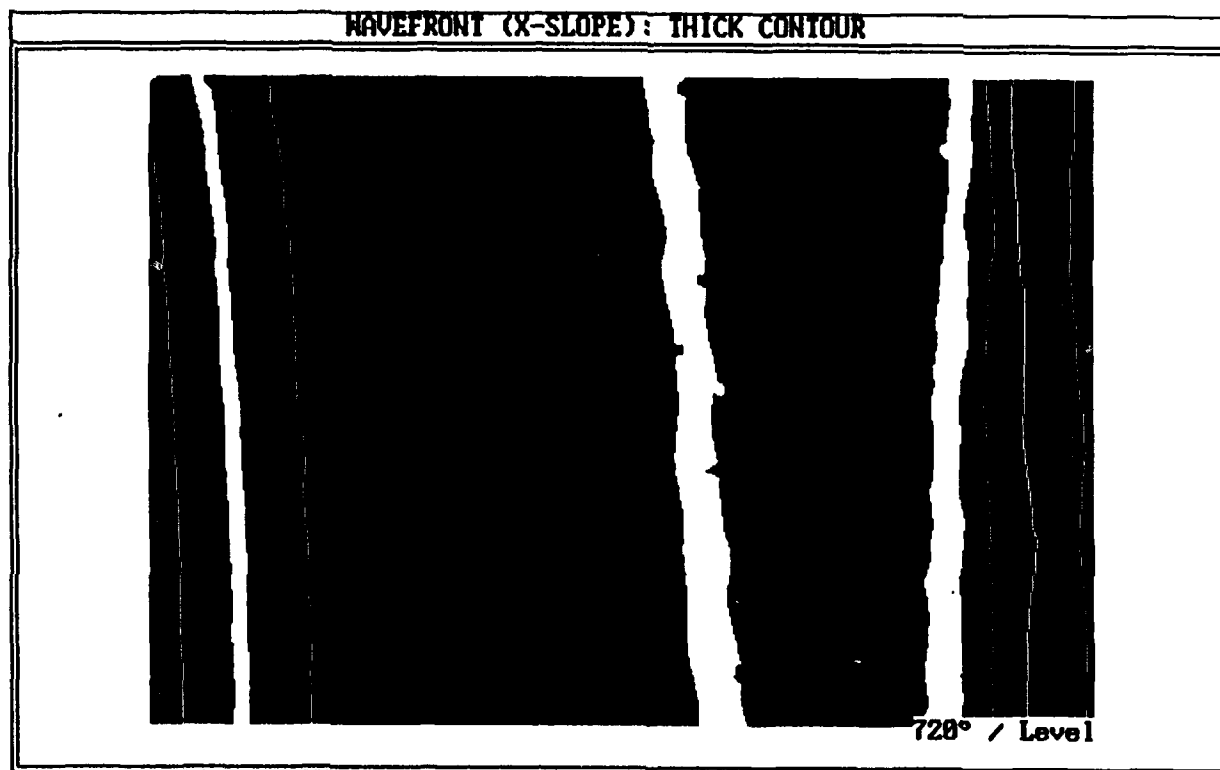


Figure 10: (c, d). Contour maps of wavefront slope
{X-shear, off focus, large misalignment (positive)}

(e)



(f)

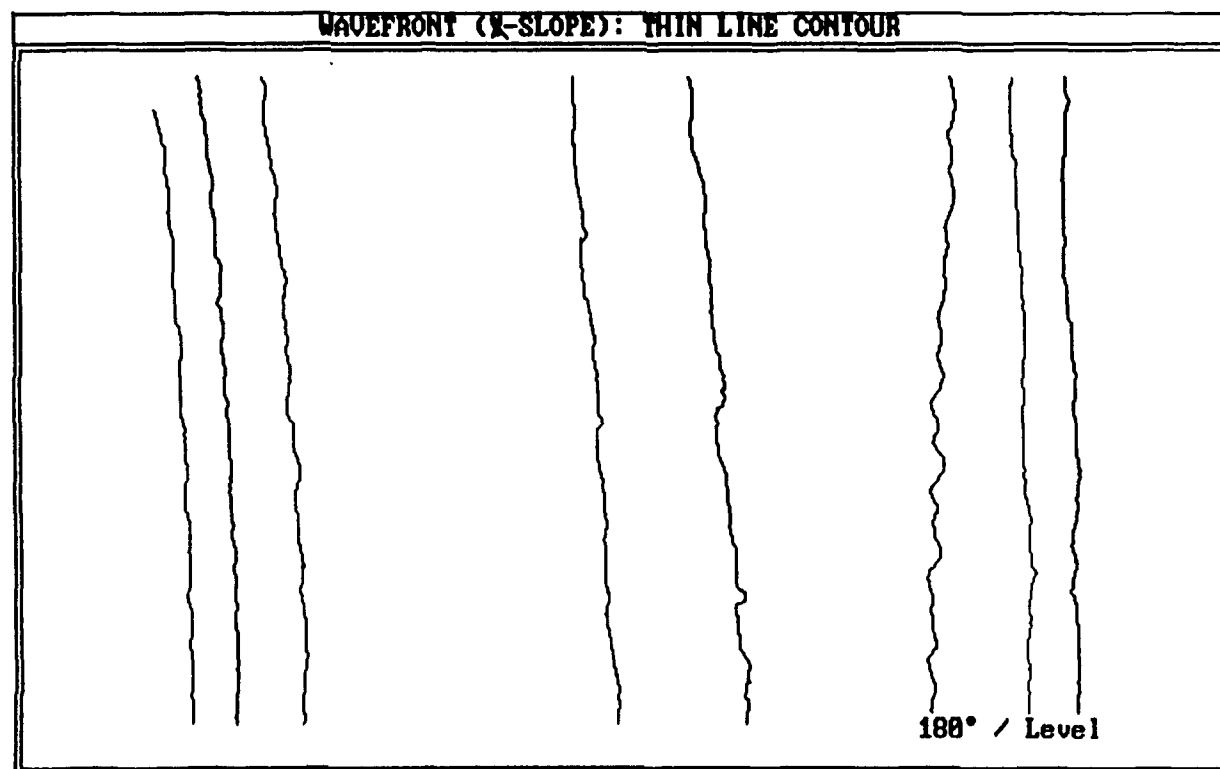


Figure 10: (e, f). Contour maps of wavefront slope, tilt removed
{X-shear, off focus, large misalignment (positive)}

(a)



(b)

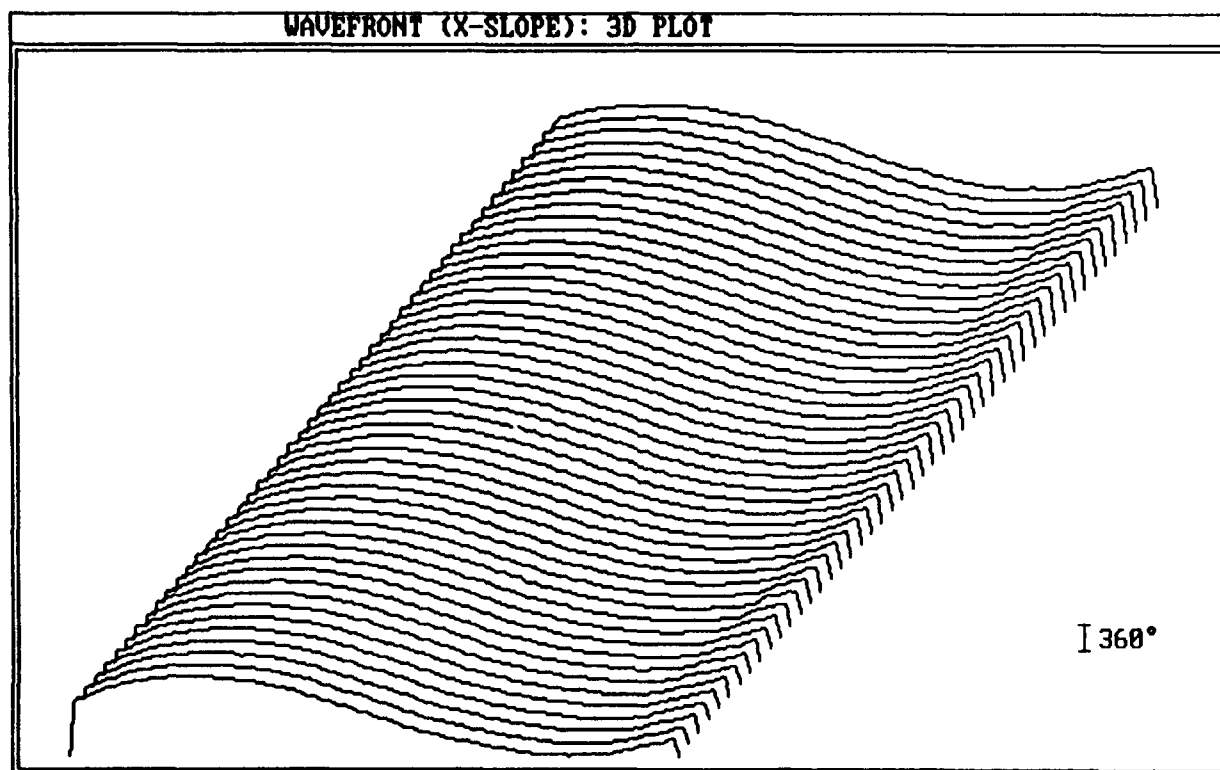
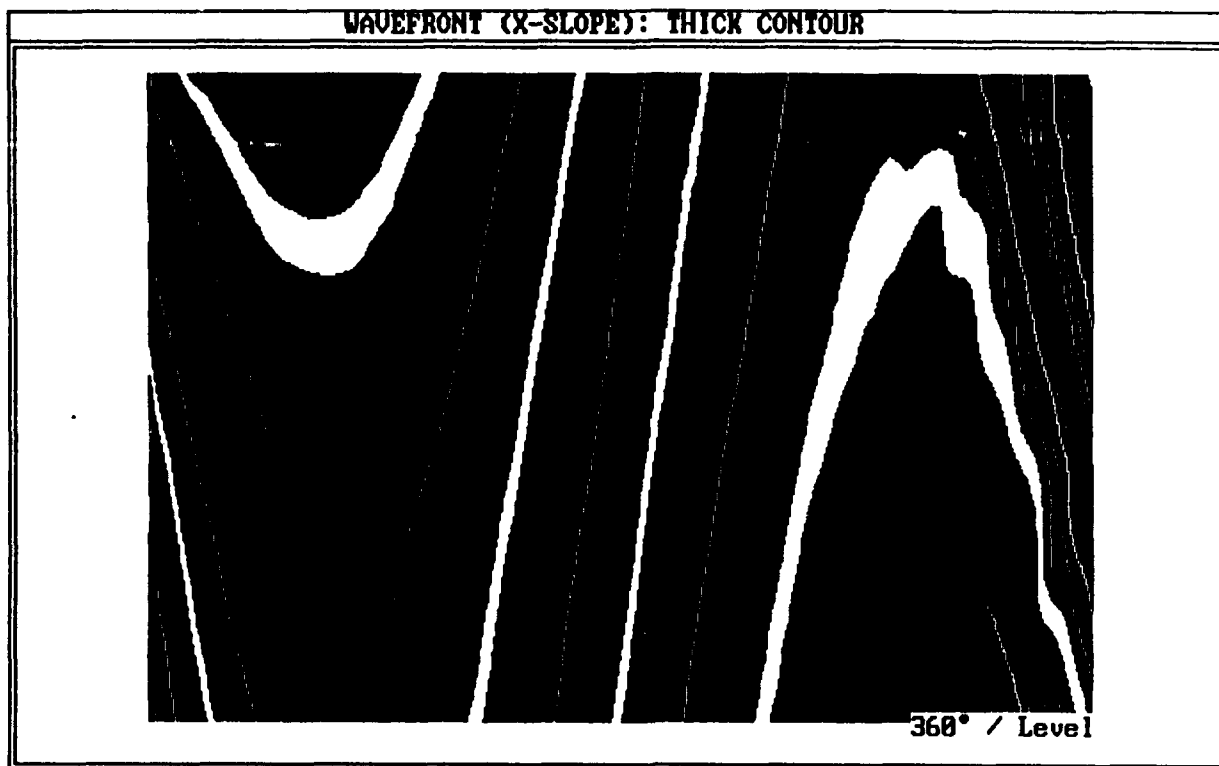


Figure 11: (a). Photograph of subaperture interferogram
(b). 3-D plot of wavefront slope
{X-shear, off focus, small misalignment (negative)}

(c)



(d)

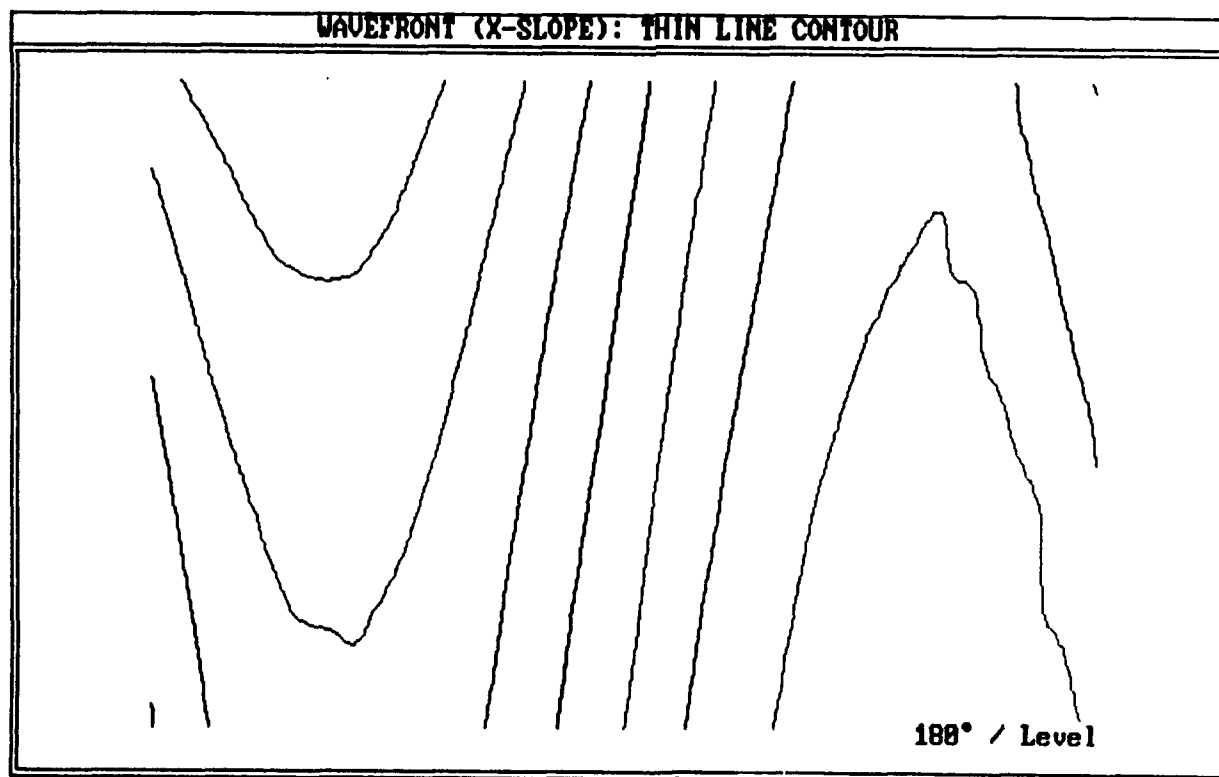
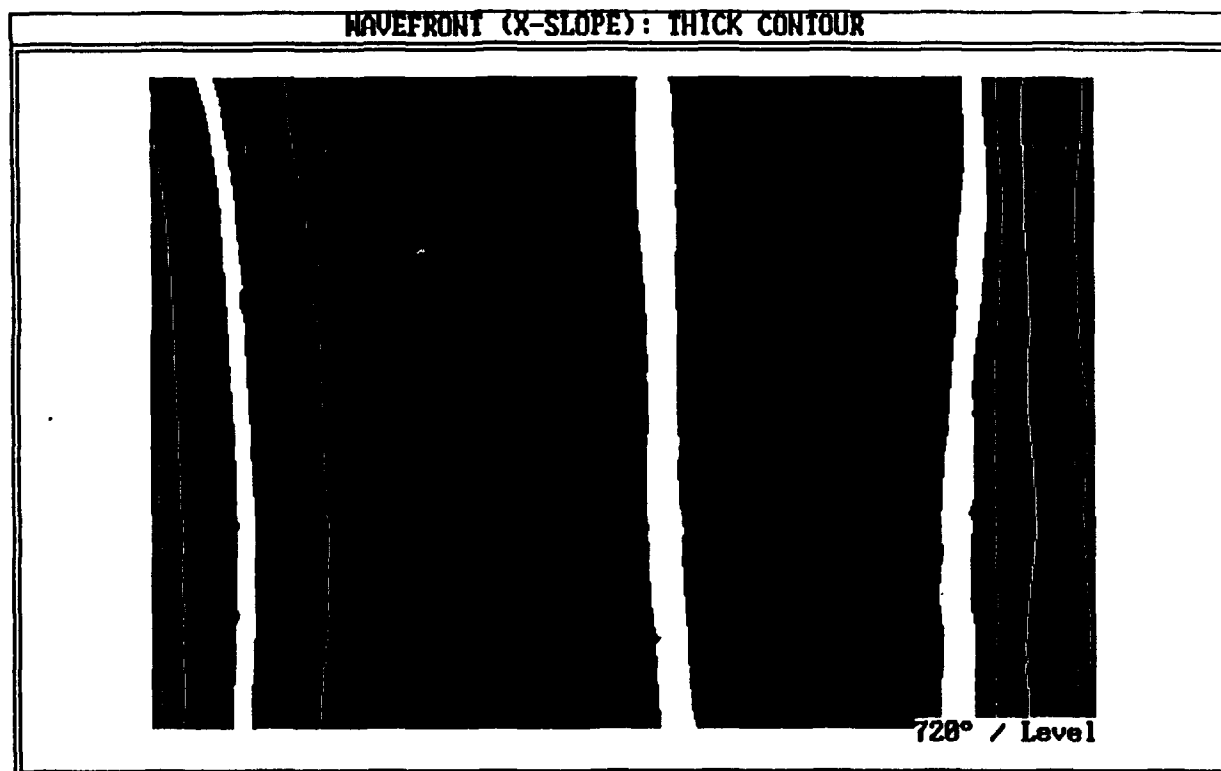


Figure 11: (c, d). Contour maps of wavefront slope
{X-shear, off focus, small misalignment (negative)}

(e)



(f)

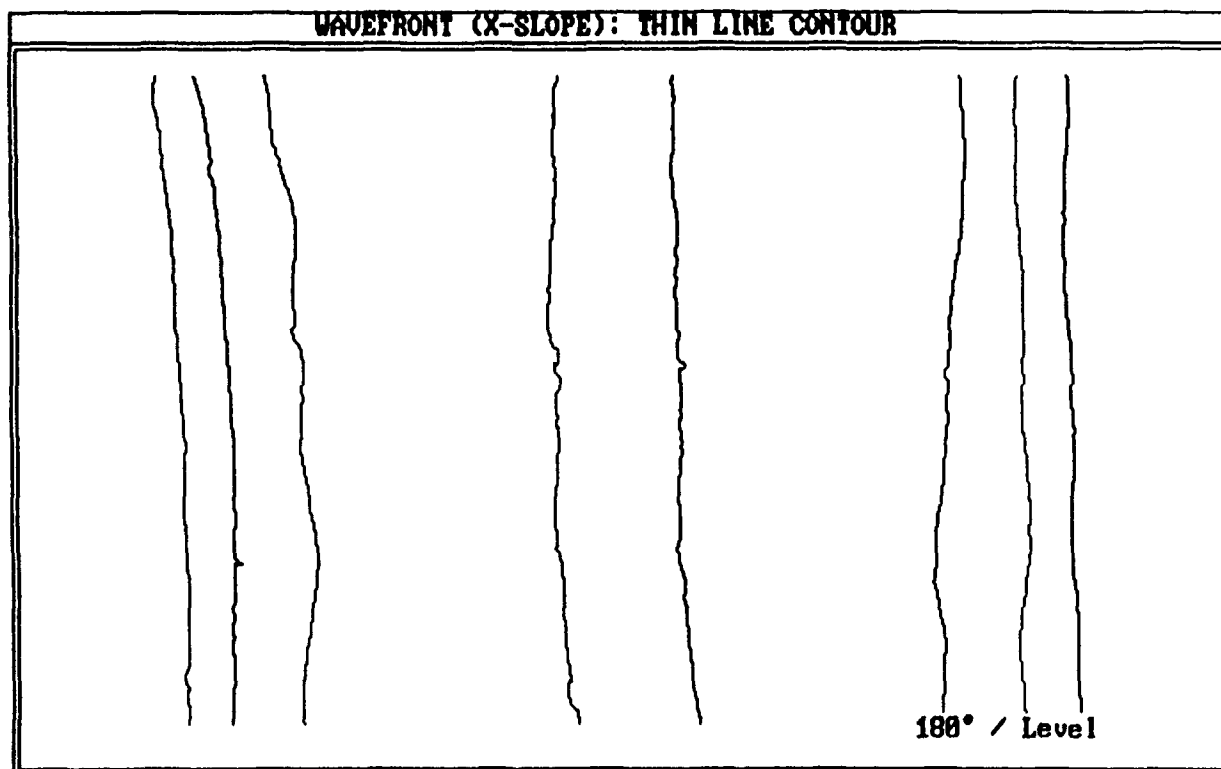


Figure 11: (e, f). Contour maps of wavefront slope, tilt removed
{X-shear, off focus, small misalignment (negative)}

(a)



(b)

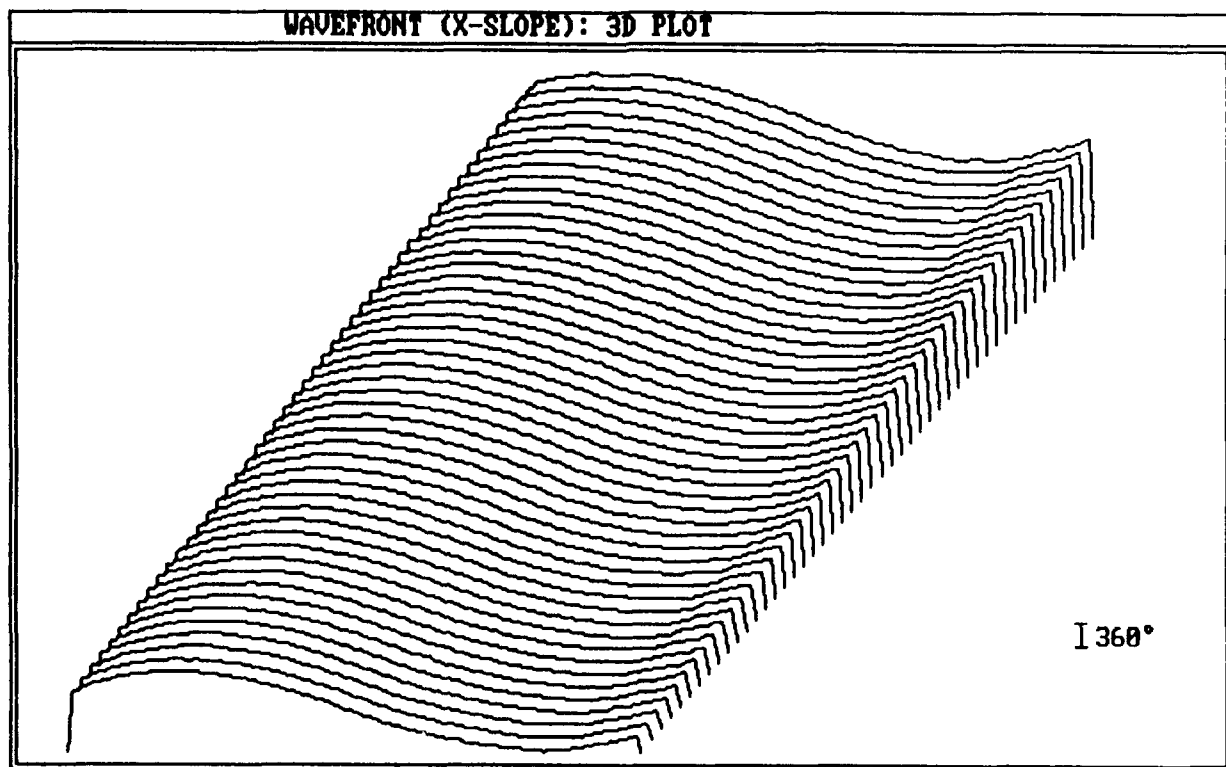
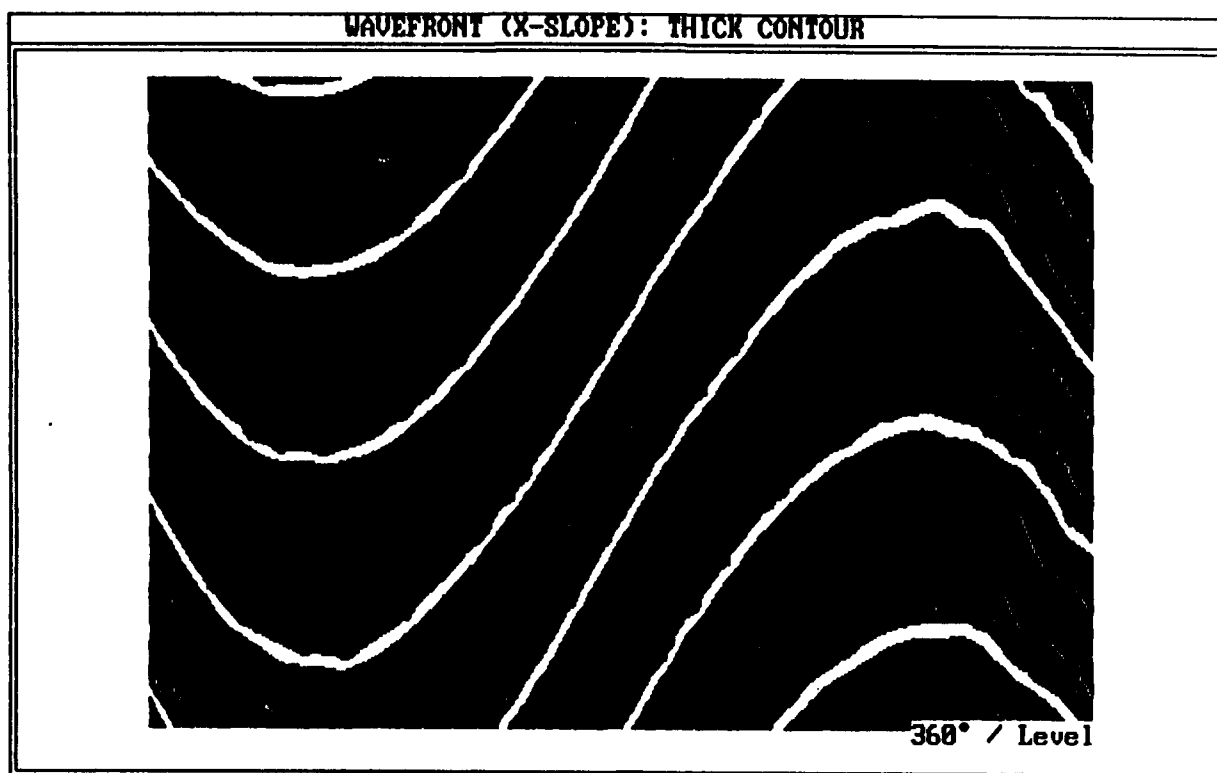


Figure 12: (a). Photograph of subaperture interferogram
(b). 3-D plot of wavefront slope
{X-shear, off focus, large misalignment (negative)}

(c)



(d)

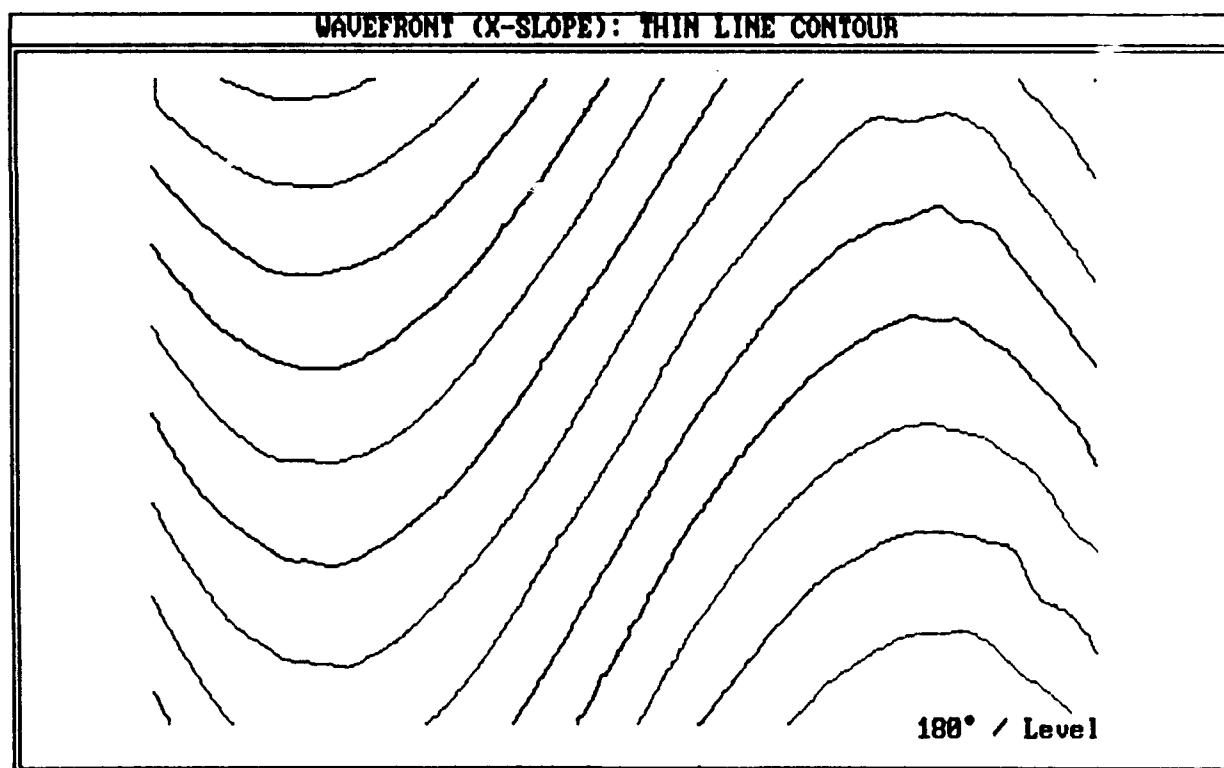
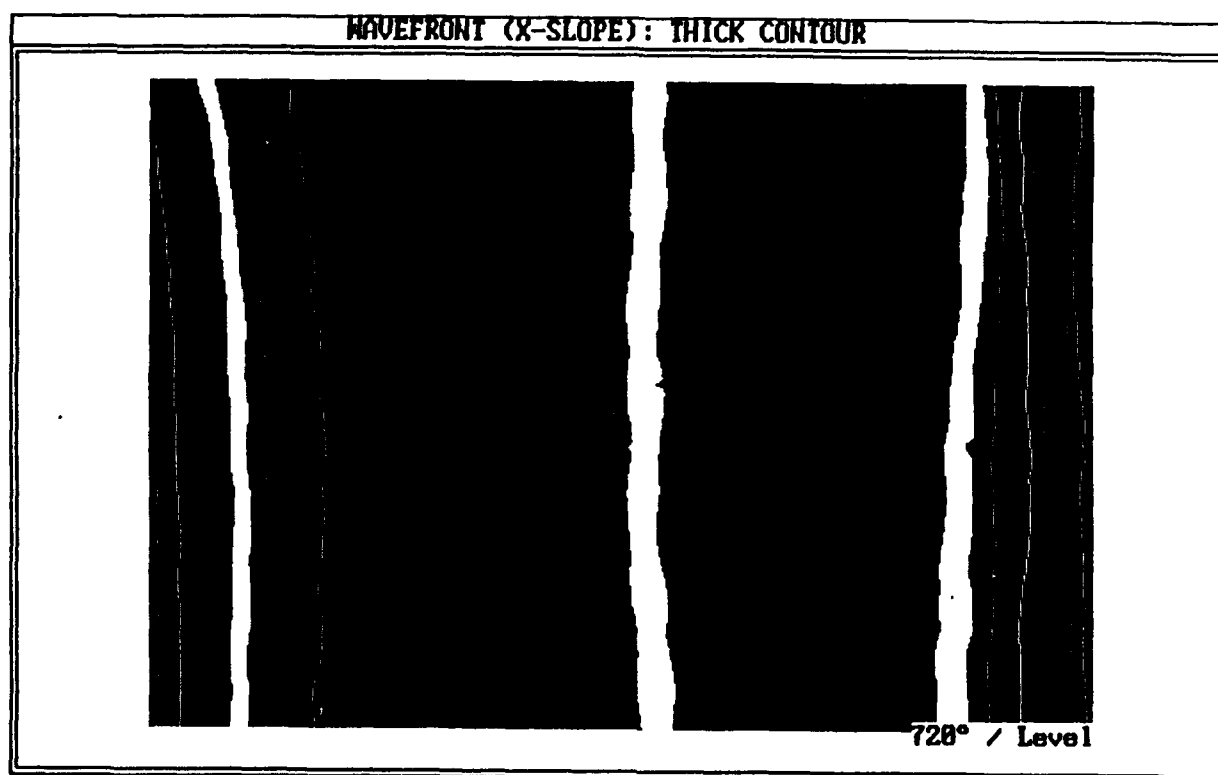


Figure 12: (c, d). Contour maps of wavefront slope
{X-shear, off focus, large misalignment (negative)}

(e)



(f)

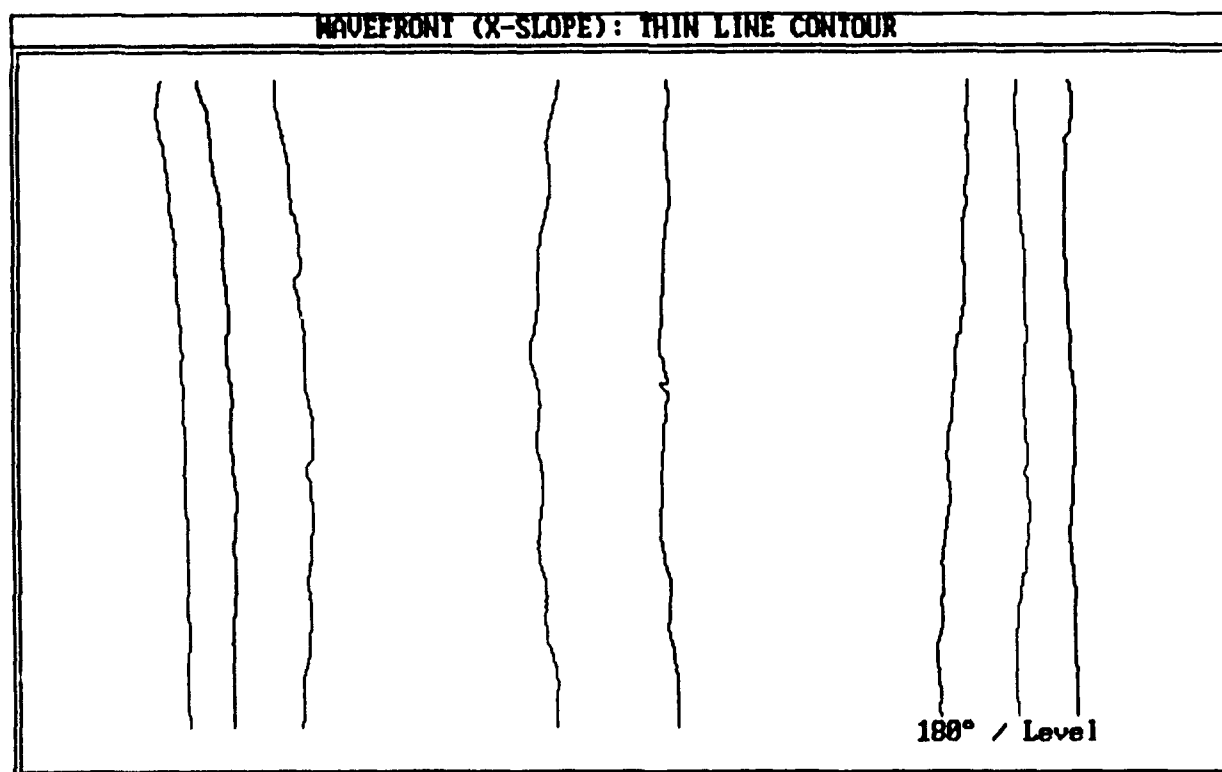
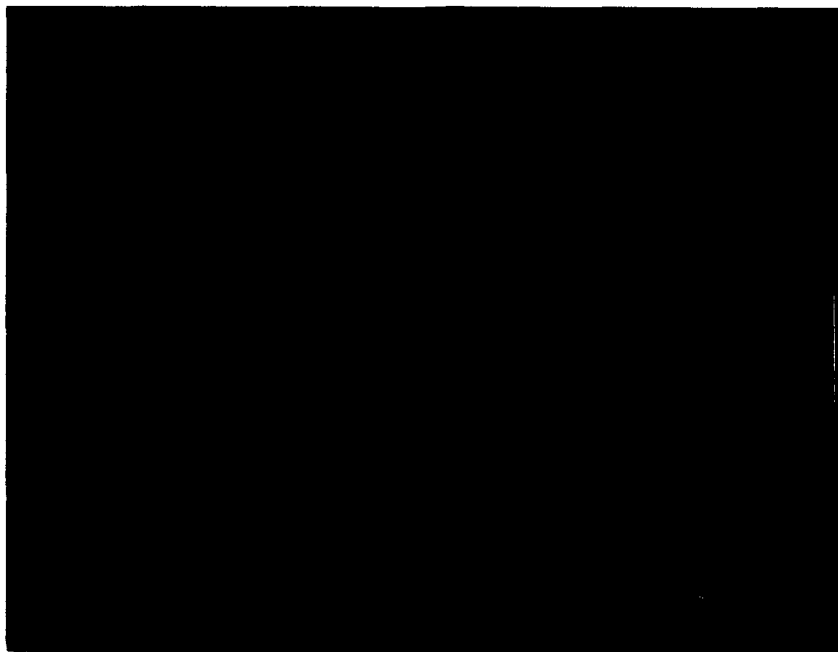


Figure 12: (e, f). Contour maps of wavefront slope, tilt removed
{X-shear, off focus, large misalignment (negative)}

(a)



(b)

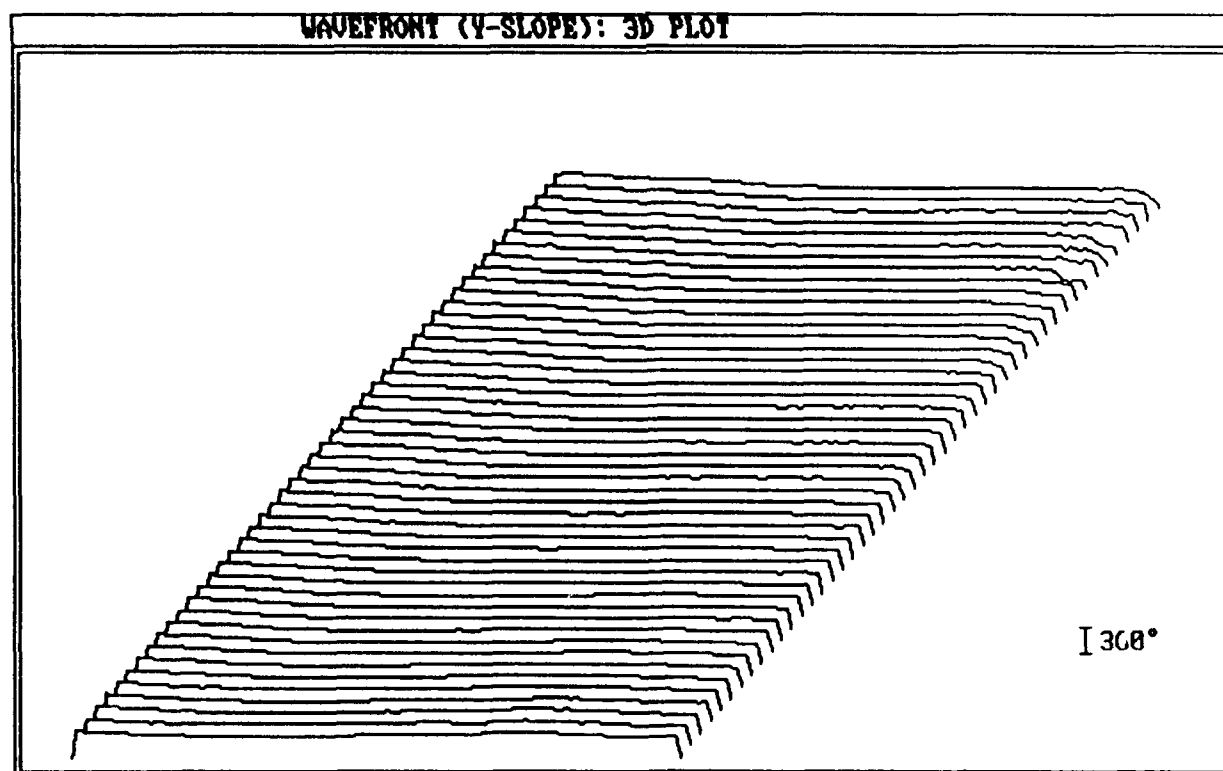
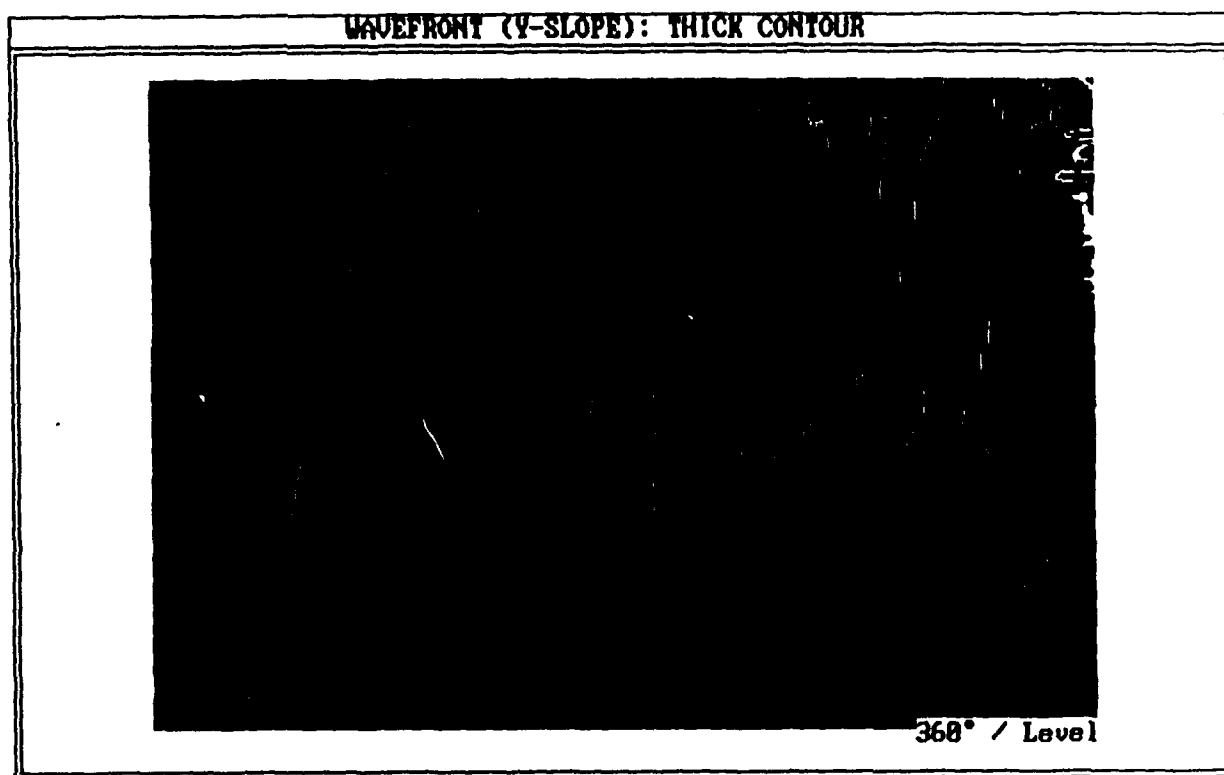


Figure 13: (a). Photograph of subaperture interferogram
(b). 3-D plot of wavefront slope
(Y-shear, in focus, aligned)

(c)



(d)

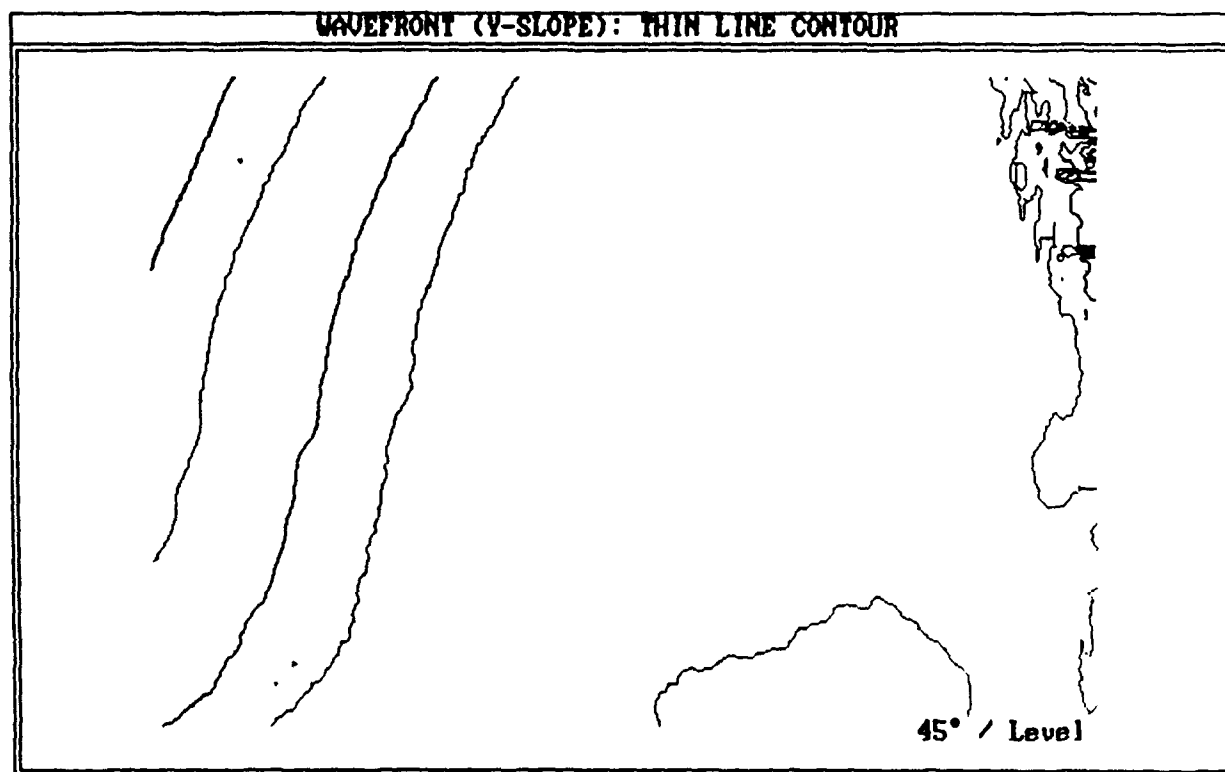
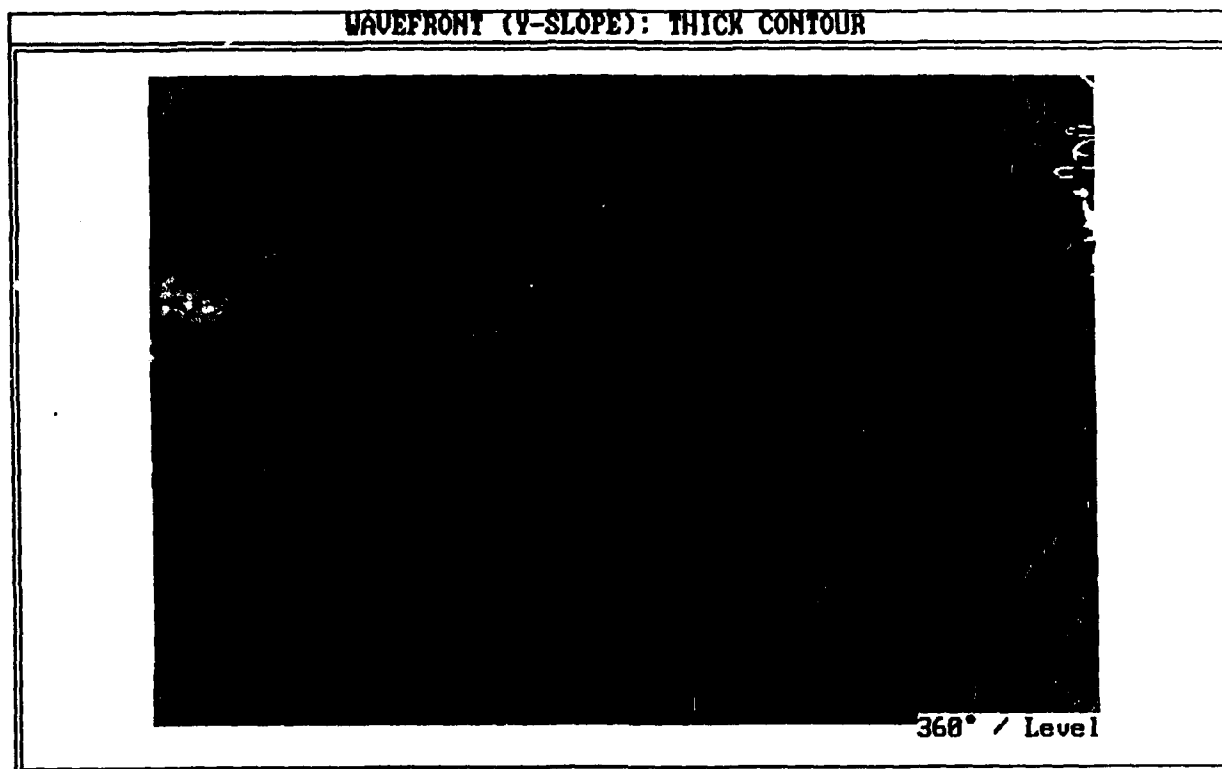


Figure 13: (c, d). Contour maps of wavefront slope (Y-shear, in focus, aligned)

(e)



(f)

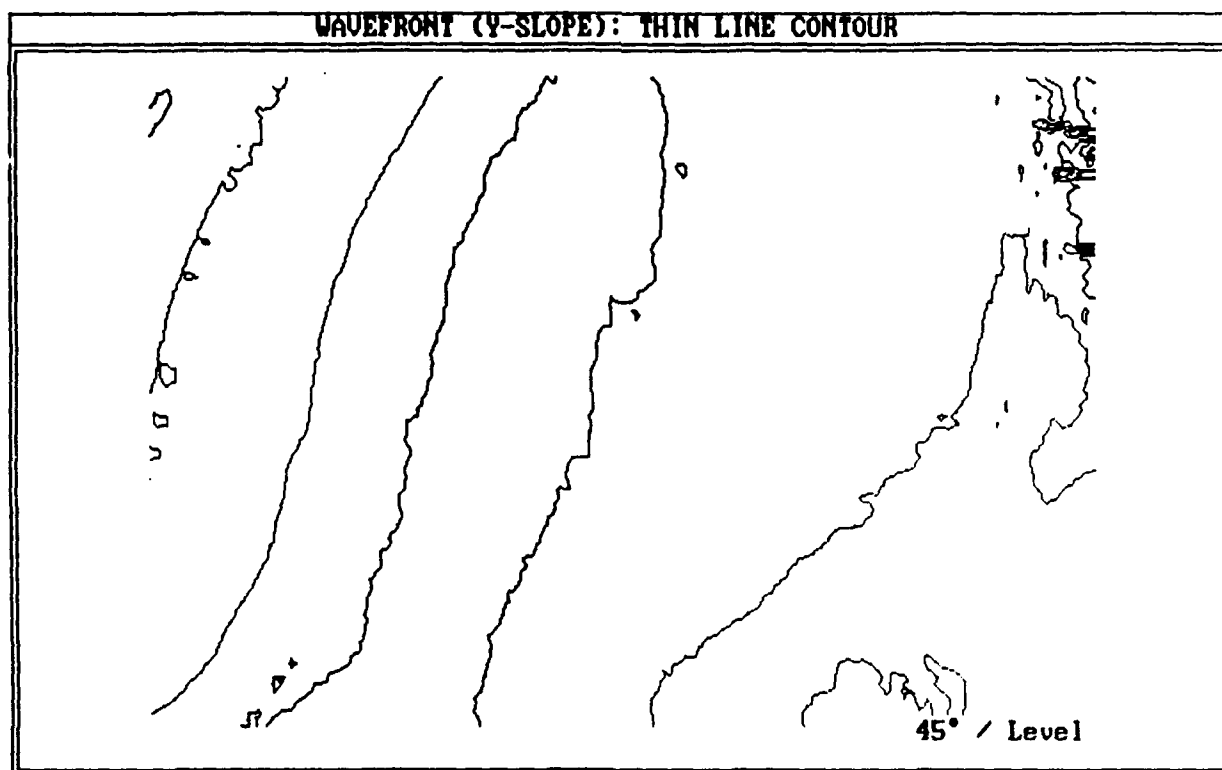
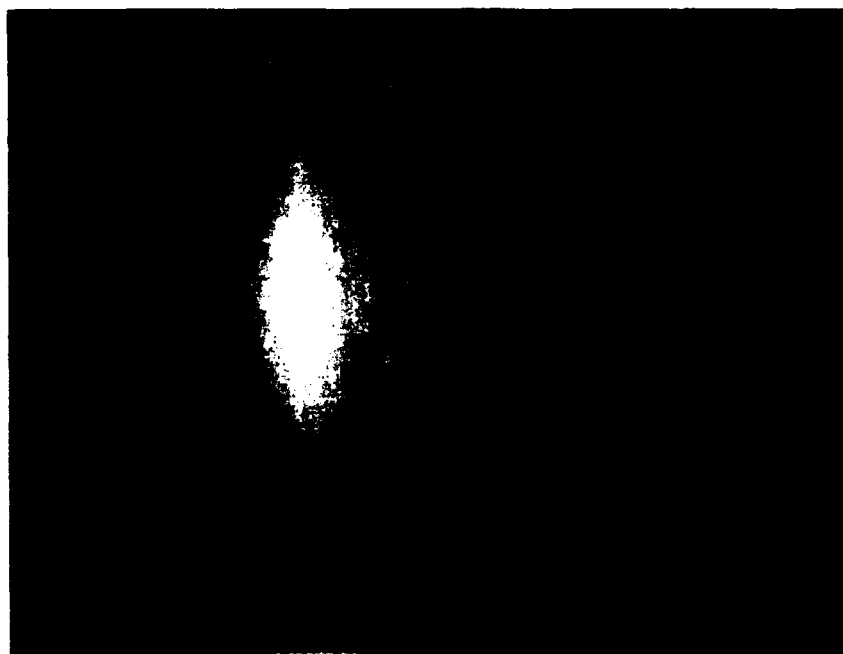


Figure 13: (e, f). Contour maps of wavefront slope, tilt removed (Y-shear, in focus, aligned)

(a)



(b)

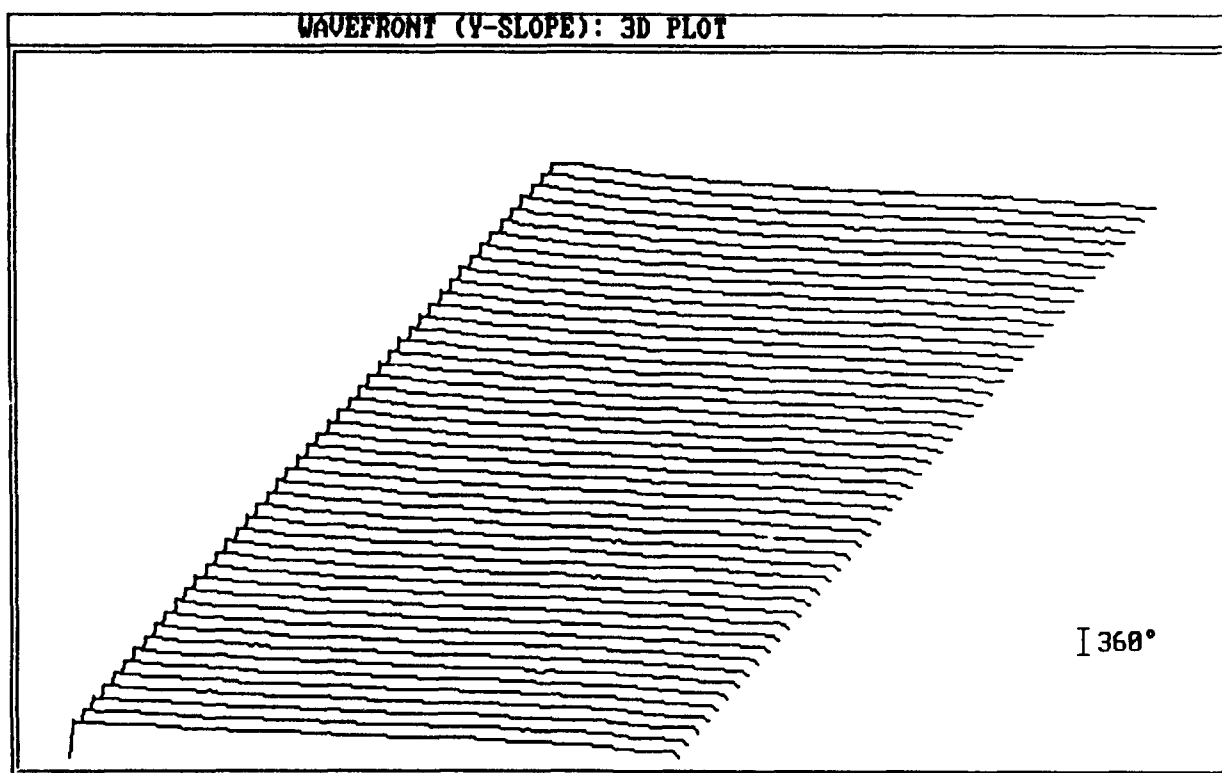
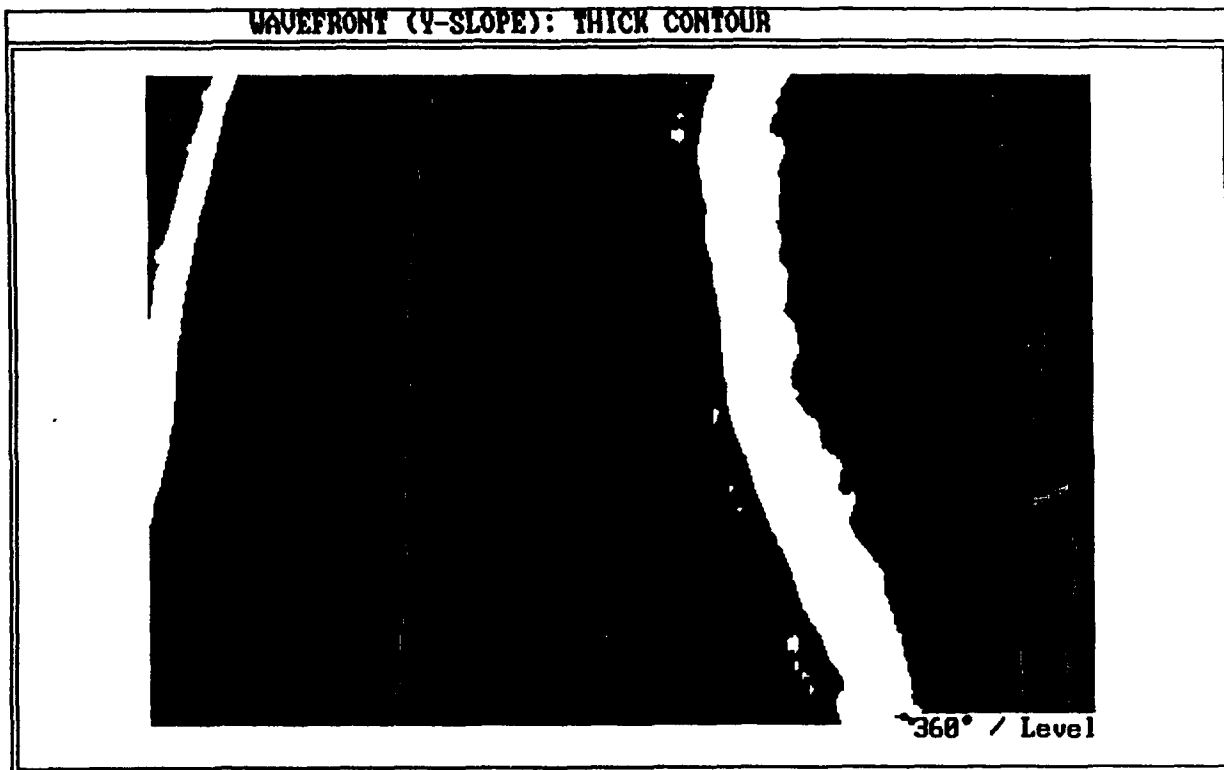


Figure 14: (a). Photograph of subaperture interferogram
(b). 3-D plot of wavefront slope
(Y-shear, in focus, small misalignment)

(c)



(d)

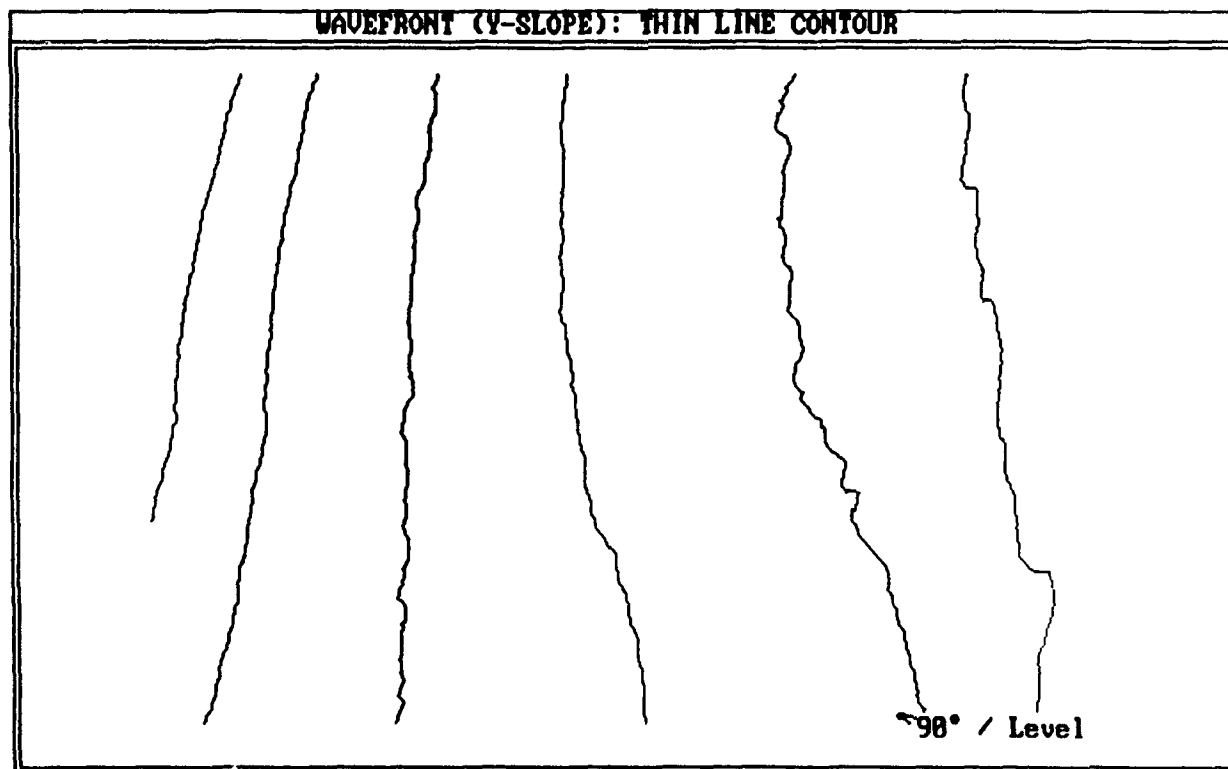
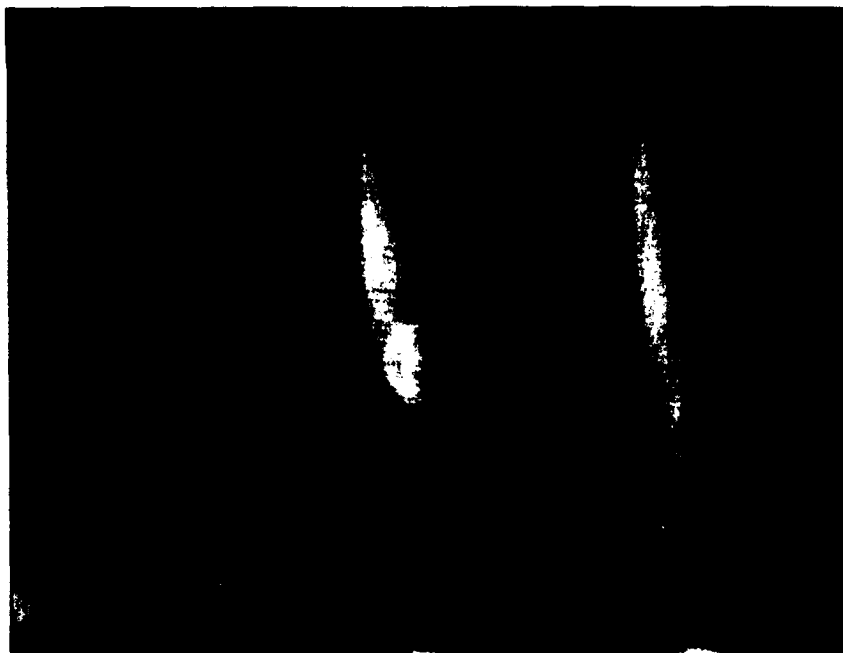


Figure 14: (c, d). Contour maps of wavefront slope
(Y-shear, in focus, small misalignment)

(a)



(b)

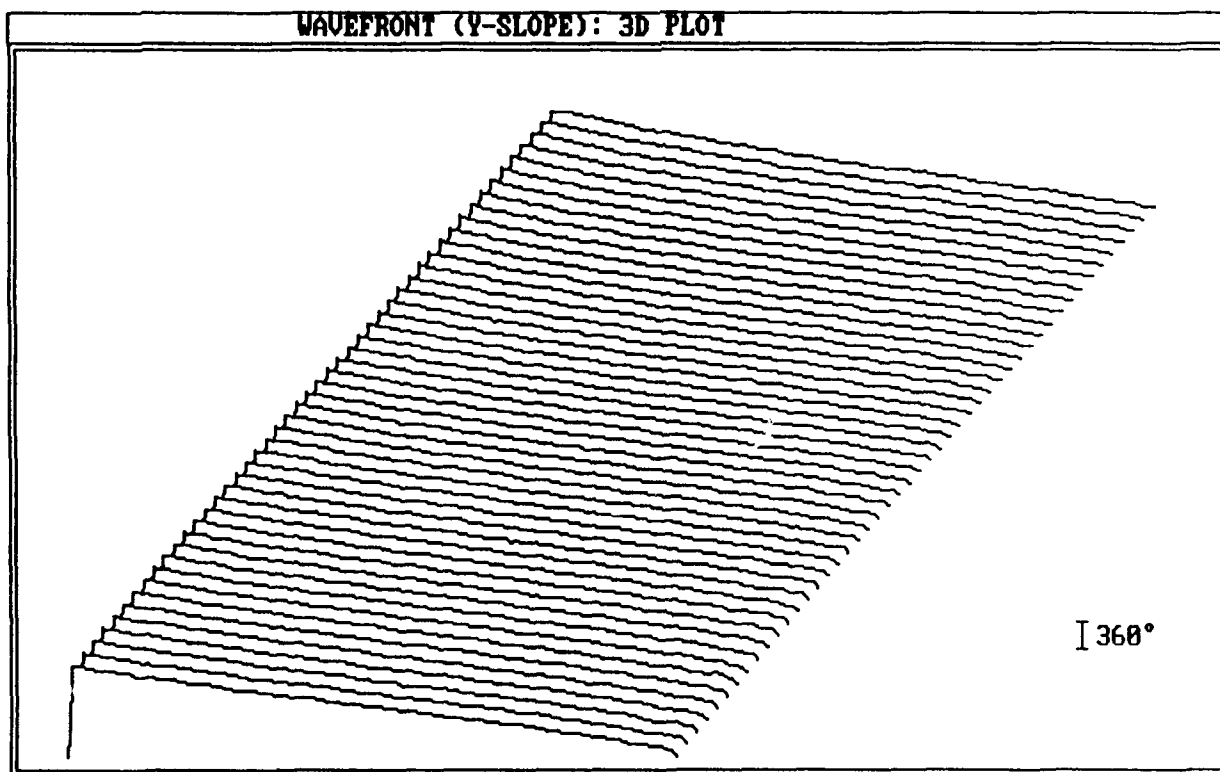
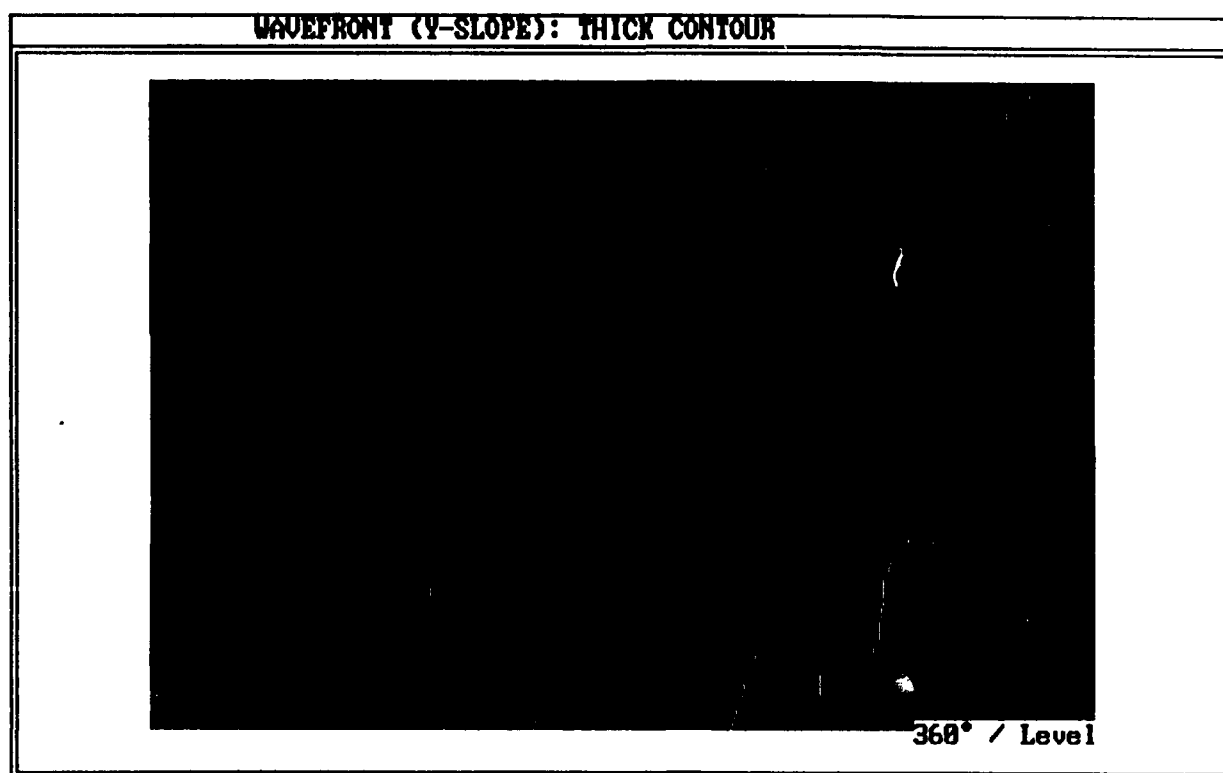


Figure 15: (a). Photograph of subaperture interferogram
(b). 3-D plot of wavefront slope
(Y-shear, in focus, medium misalignment)

(e)



(f)

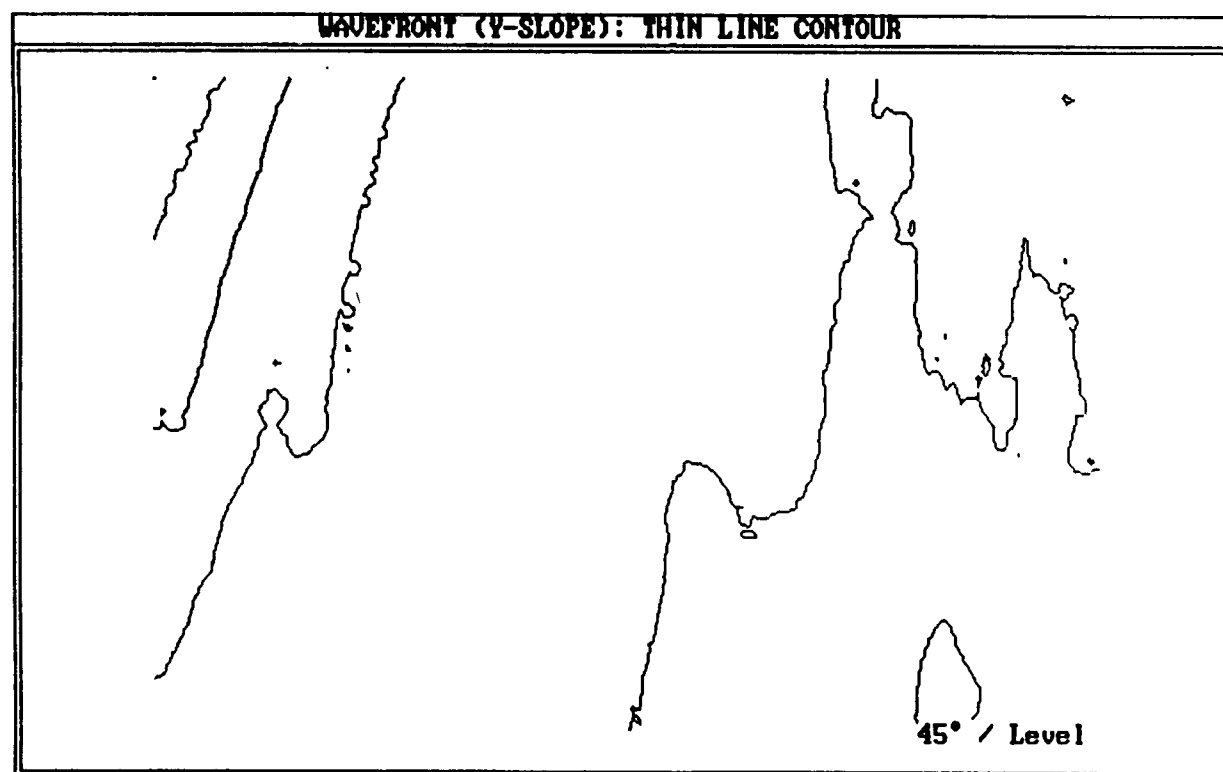


Figure 14: (e, f). Contour maps of wavefront slope, tilt removed (Y-shear, in focus, small misalignment)

(a)



(b)

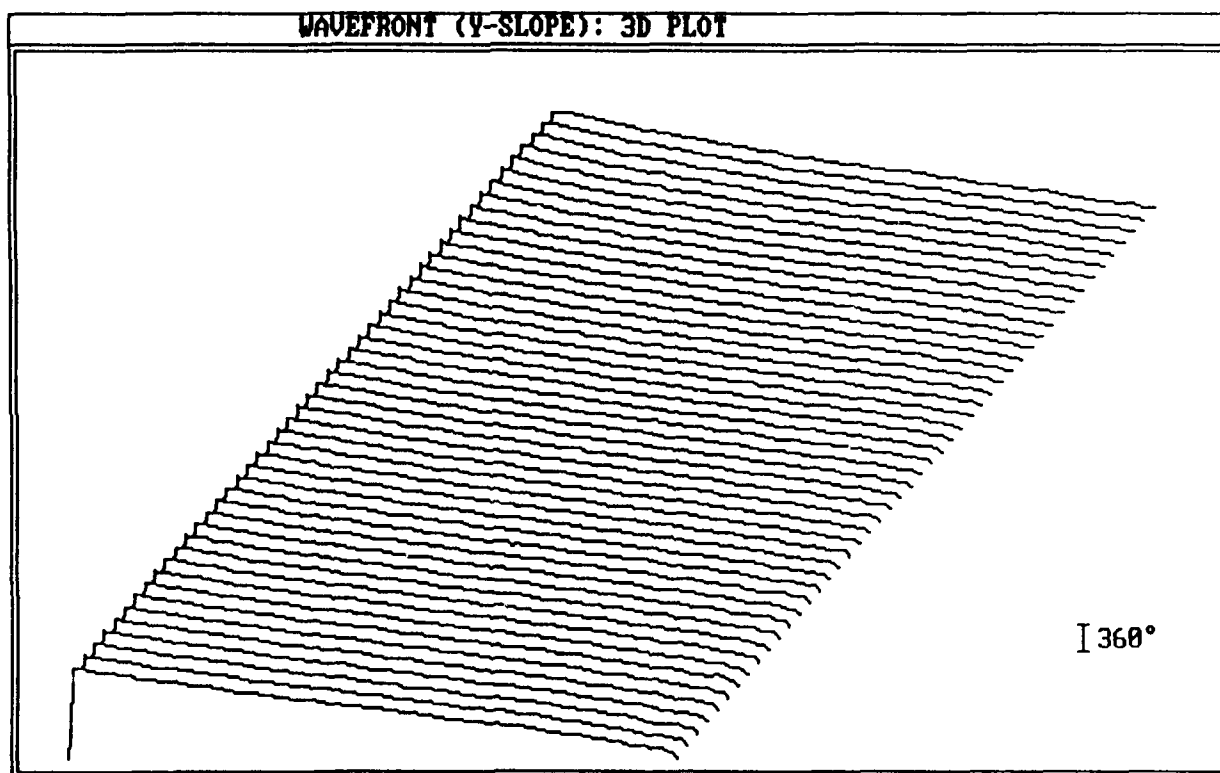
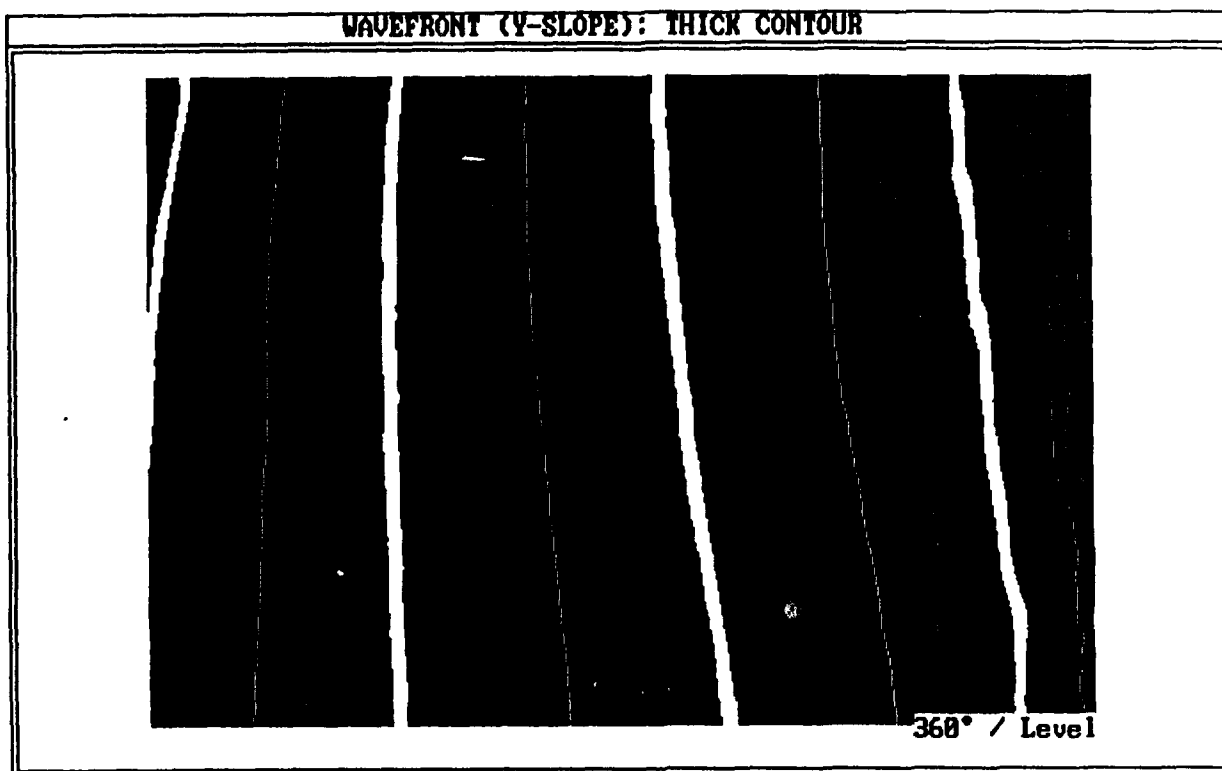


Figure 15: (a). Photograph of subaperture interferogram
(b). 3-D plot of wavefront slope
(Y-shear, in focus, medium misalignment)

(c)



(d)

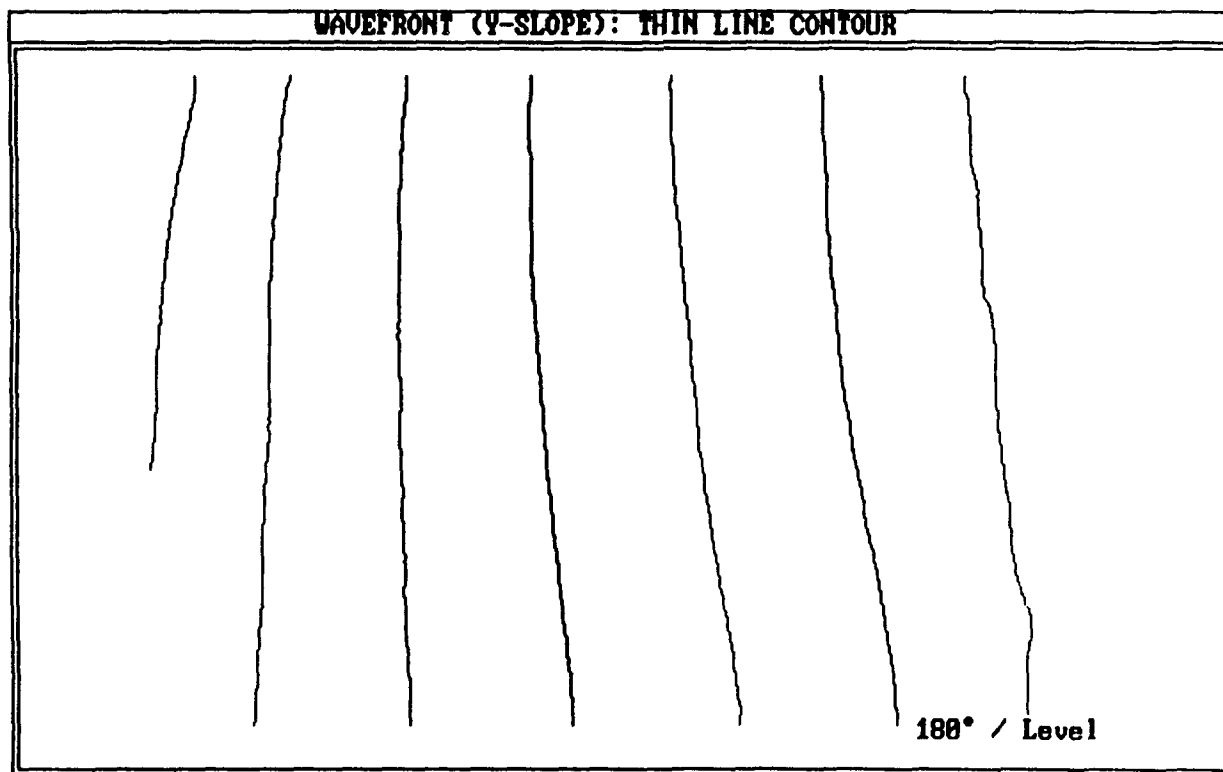
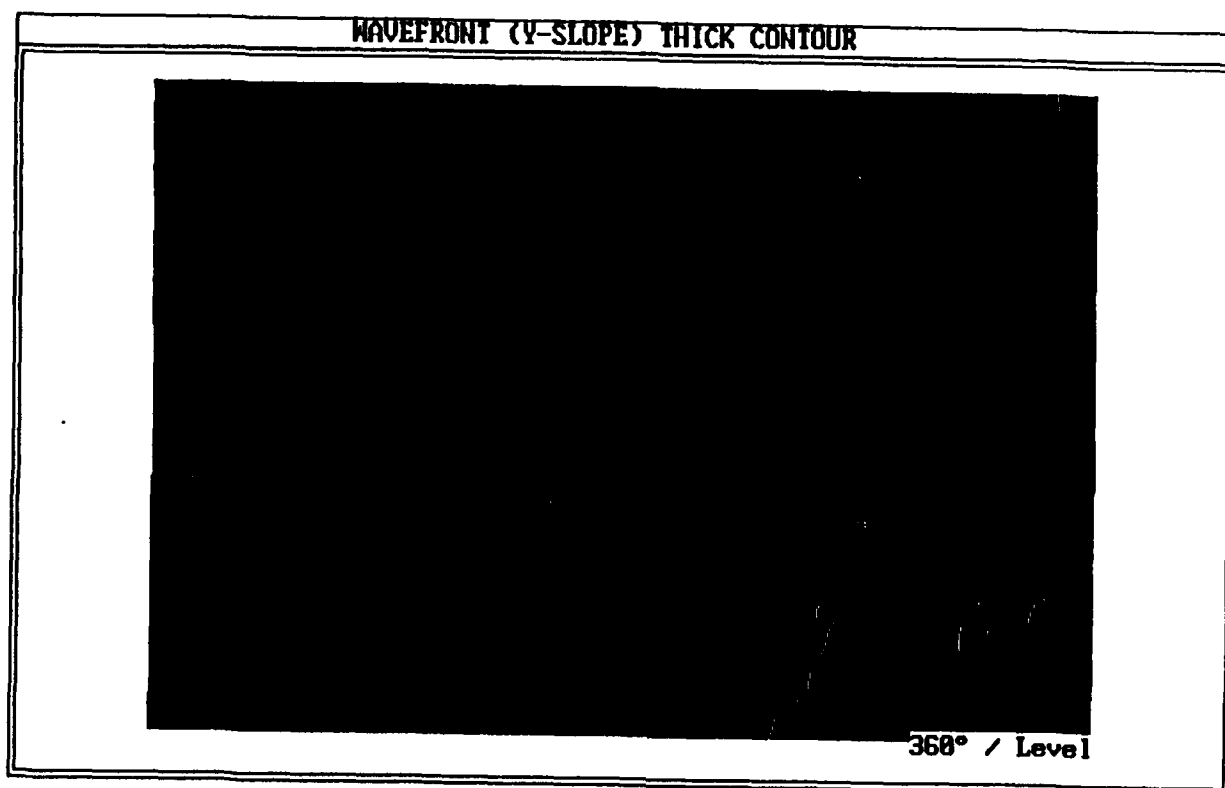


Figure 15: (c, d). Contour maps of wavefront slope
(Y-shear, in focus, medium misalignment)

(e)



(f)

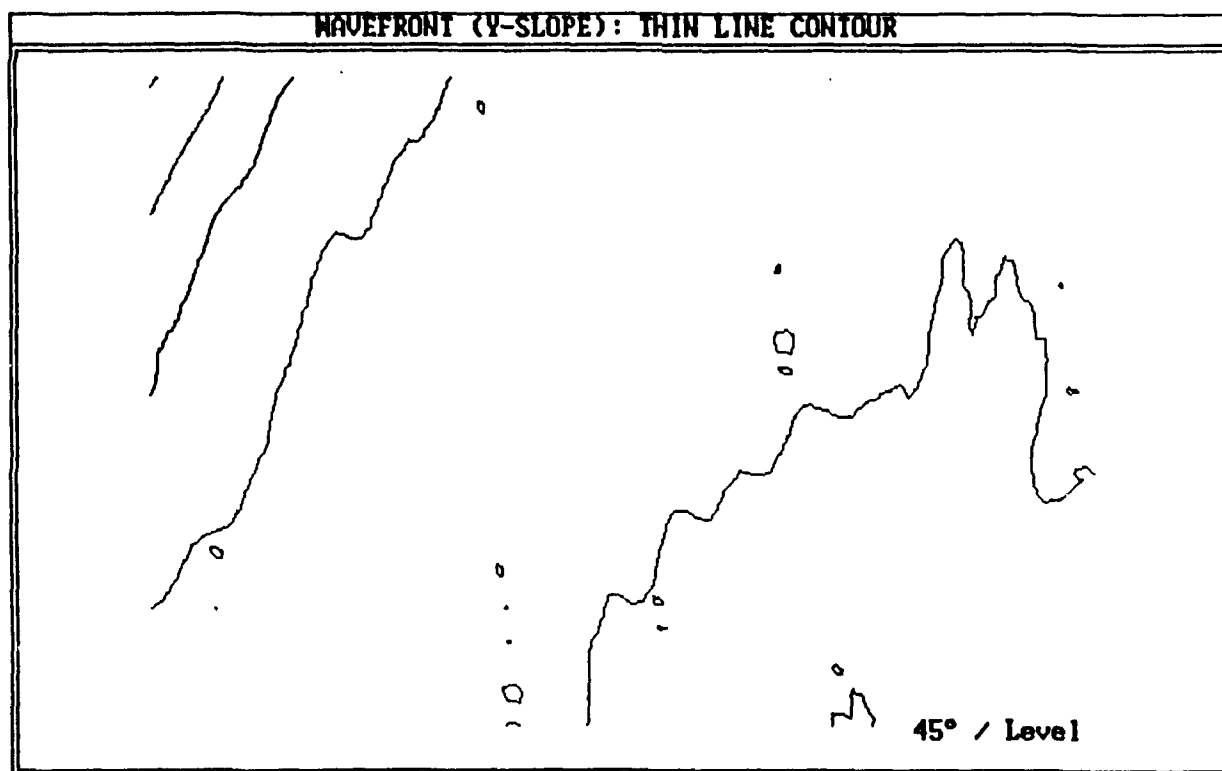
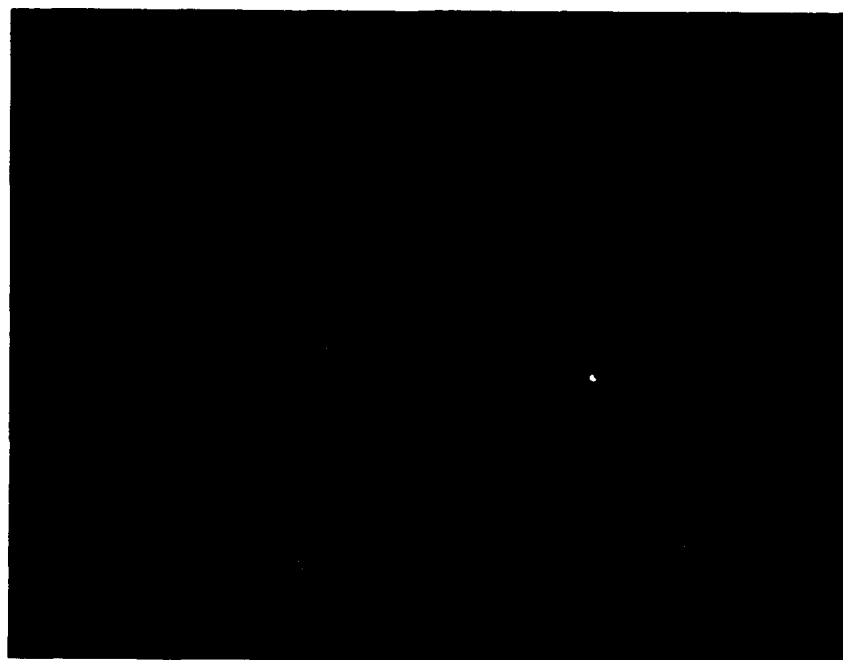


Figure 15: (e, f). Contour maps of wavefront slope, tilt removed (Y-shear, in focus, medium misalignment)

(a)



(b)

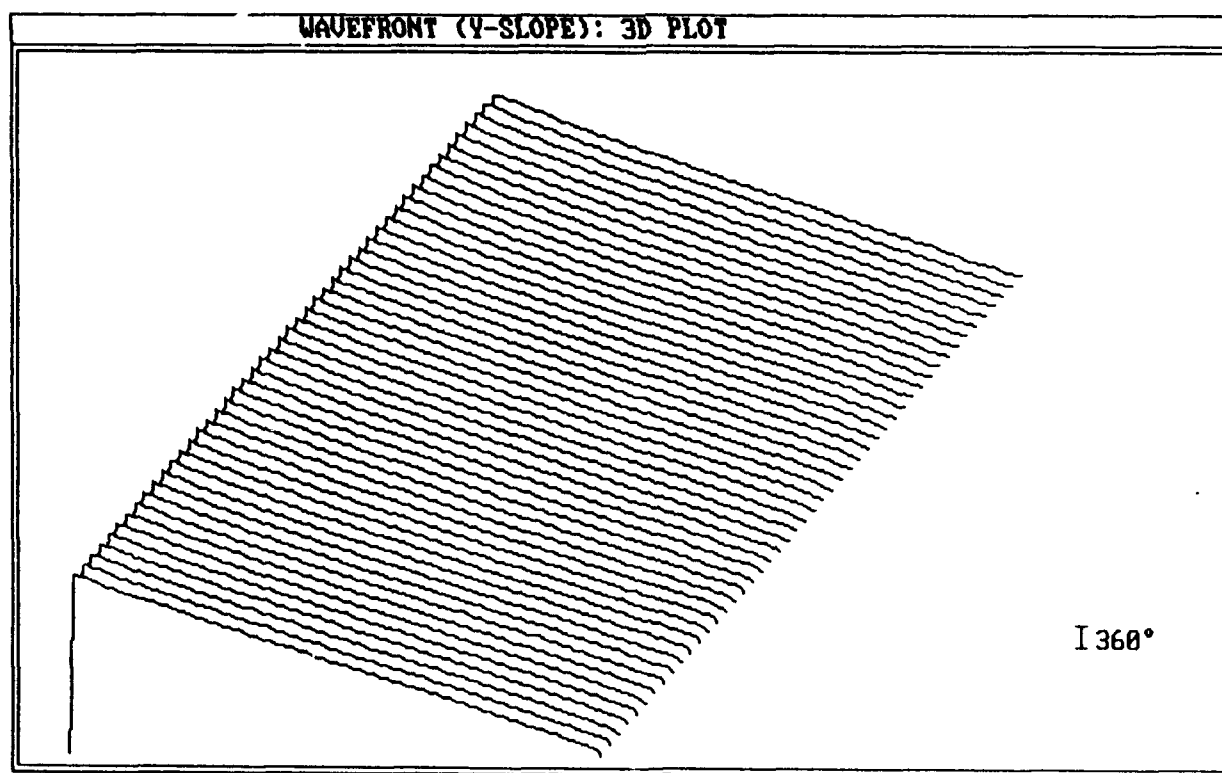
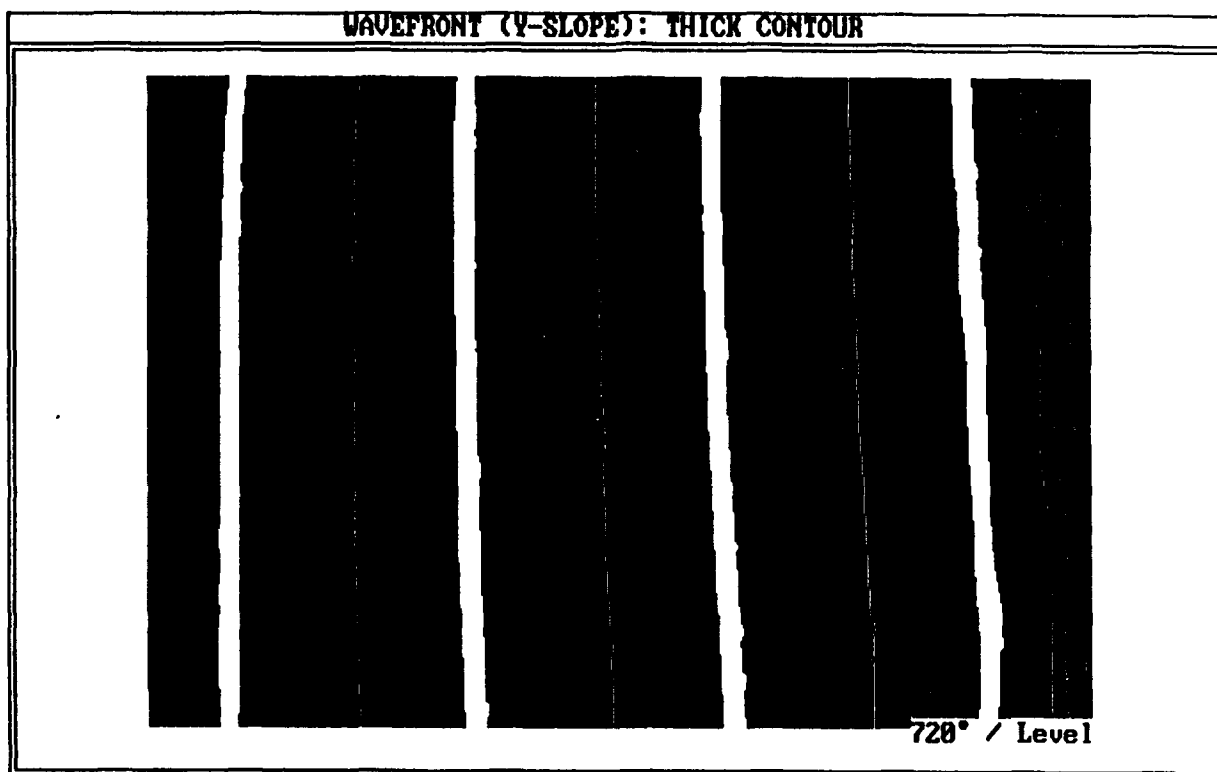


Figure 16: (a). Photograph of subaperture interferogram
(b). 3-D plot of wavefront slope
(Y-shear, in focus, large misalignment)

(c)



(d)

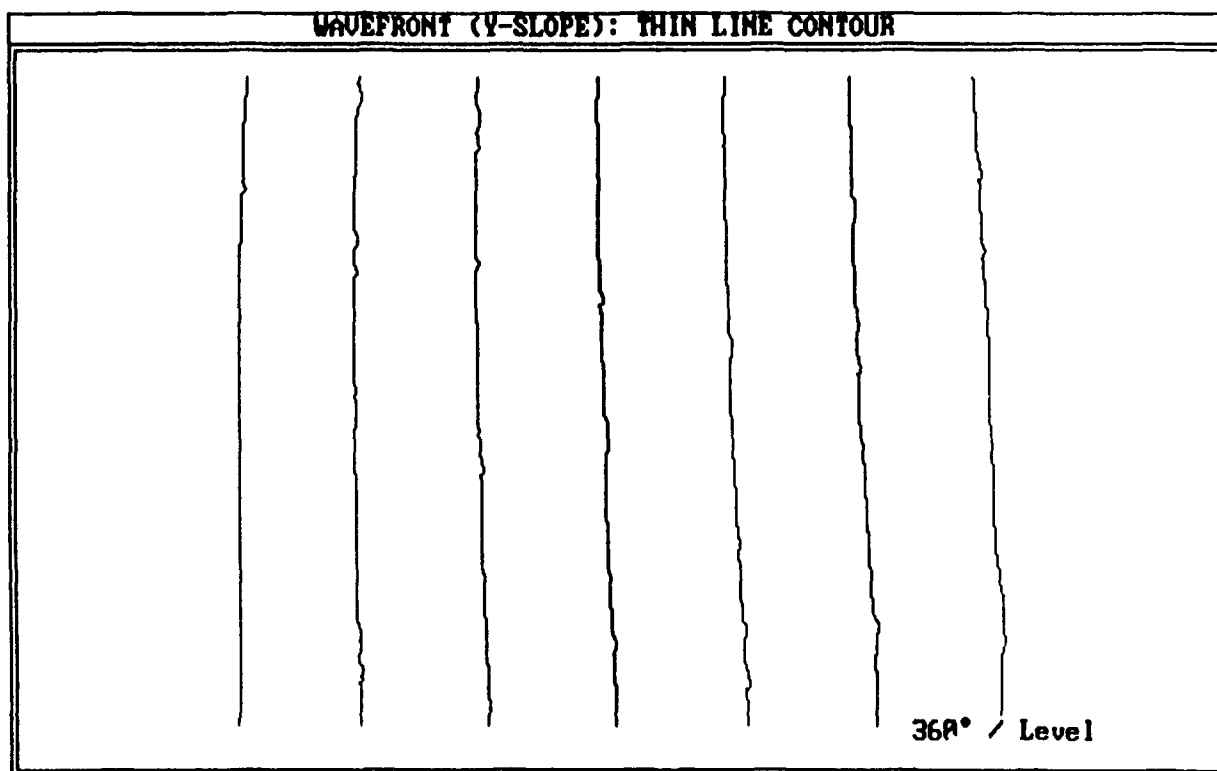
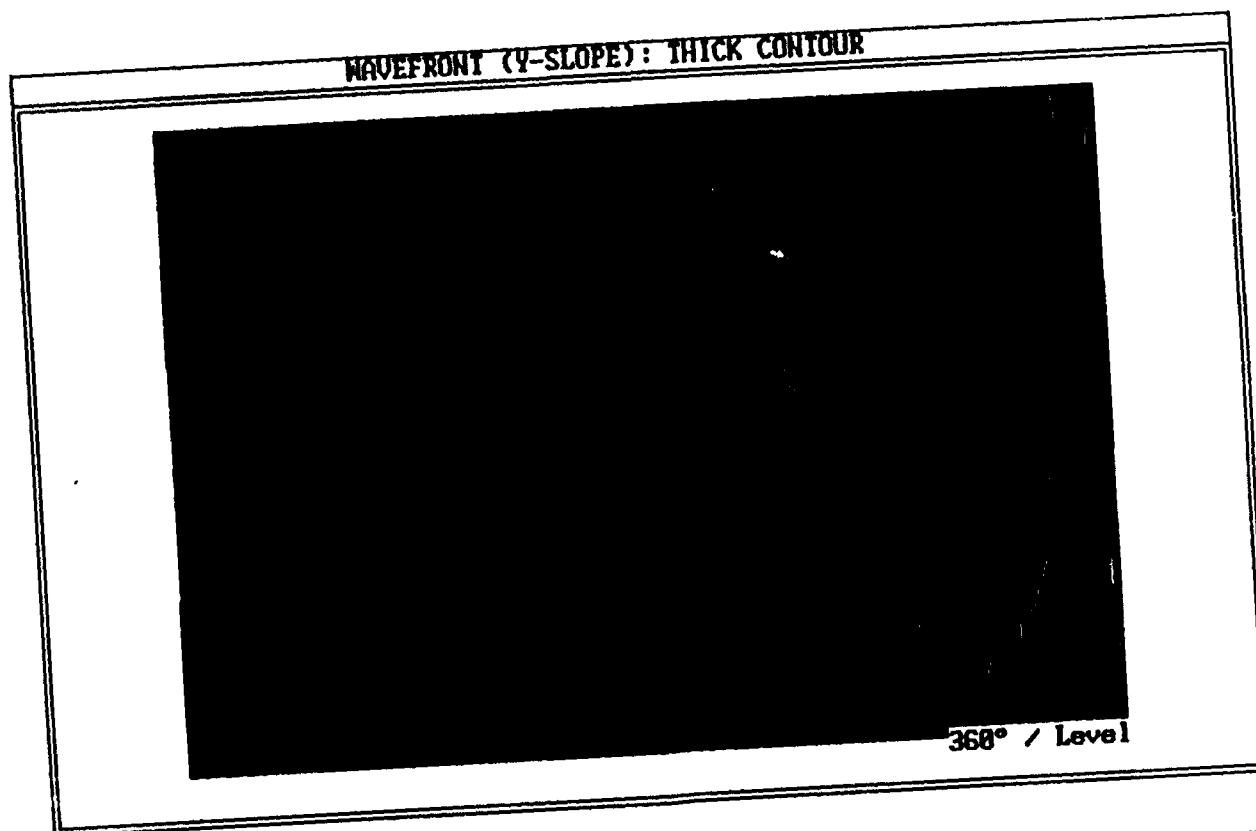


Figure 16: (c, d). Contour maps of wavefront slope
(Y-shear, in focus, large misalignment)

(e)



(f)

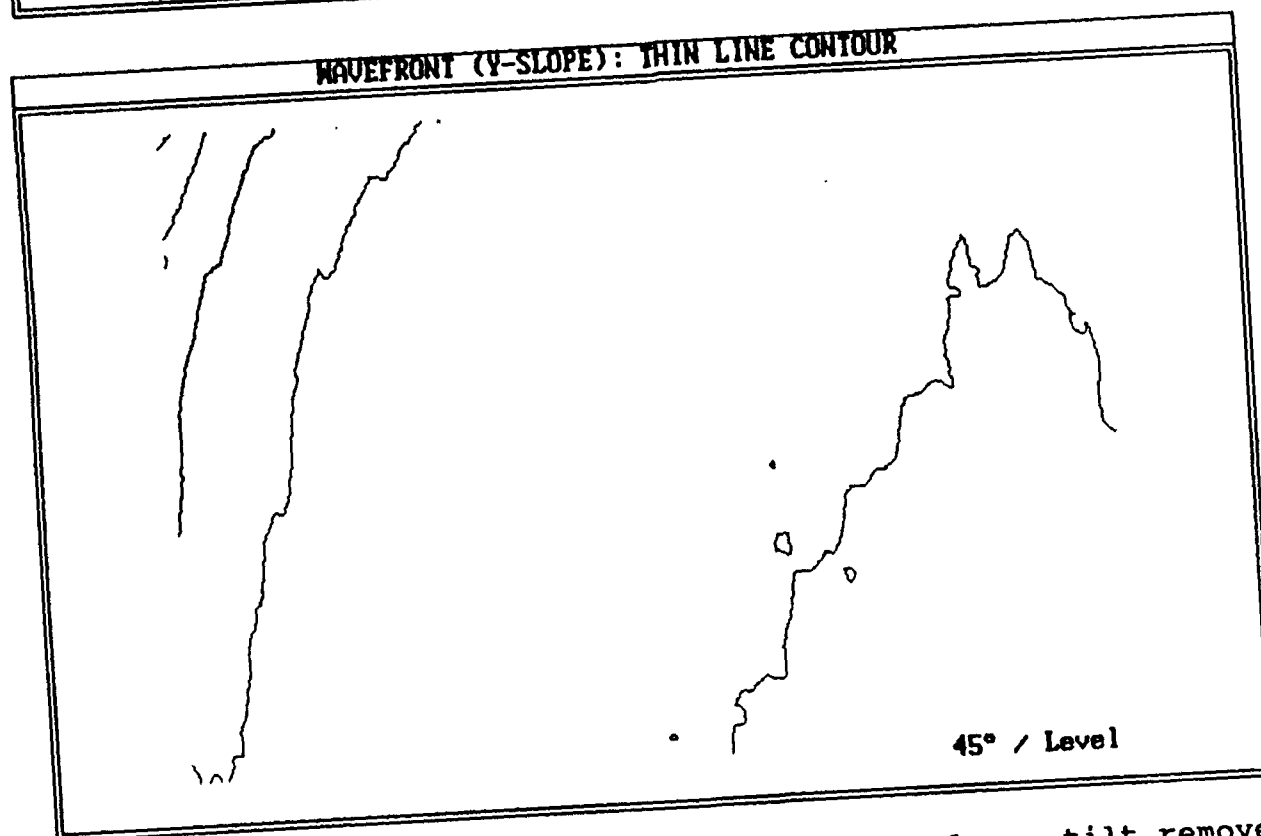
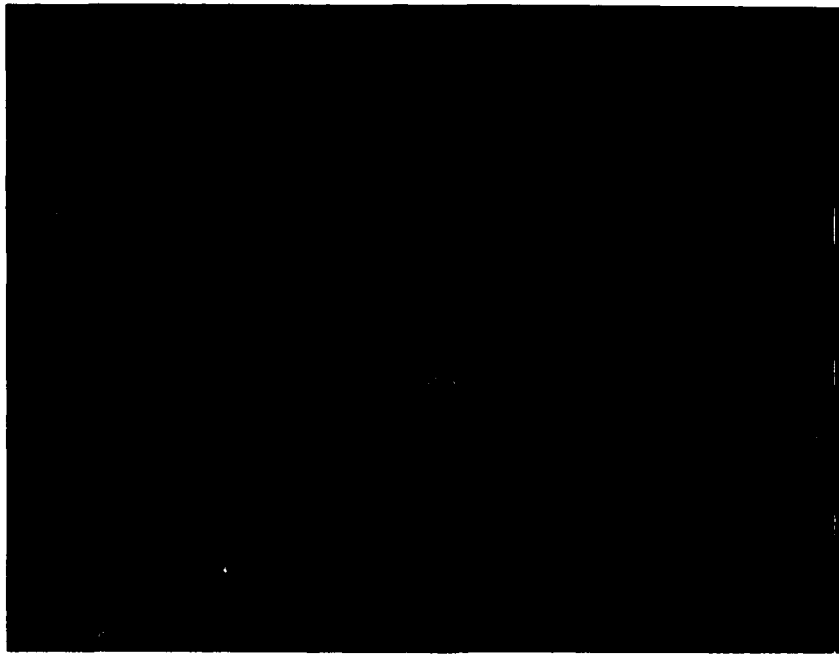


Figure 16: (e, f). Contour maps of wavefront slope, tilt removed (Y-shear, in focus, large misalignment)

(a)



(b)

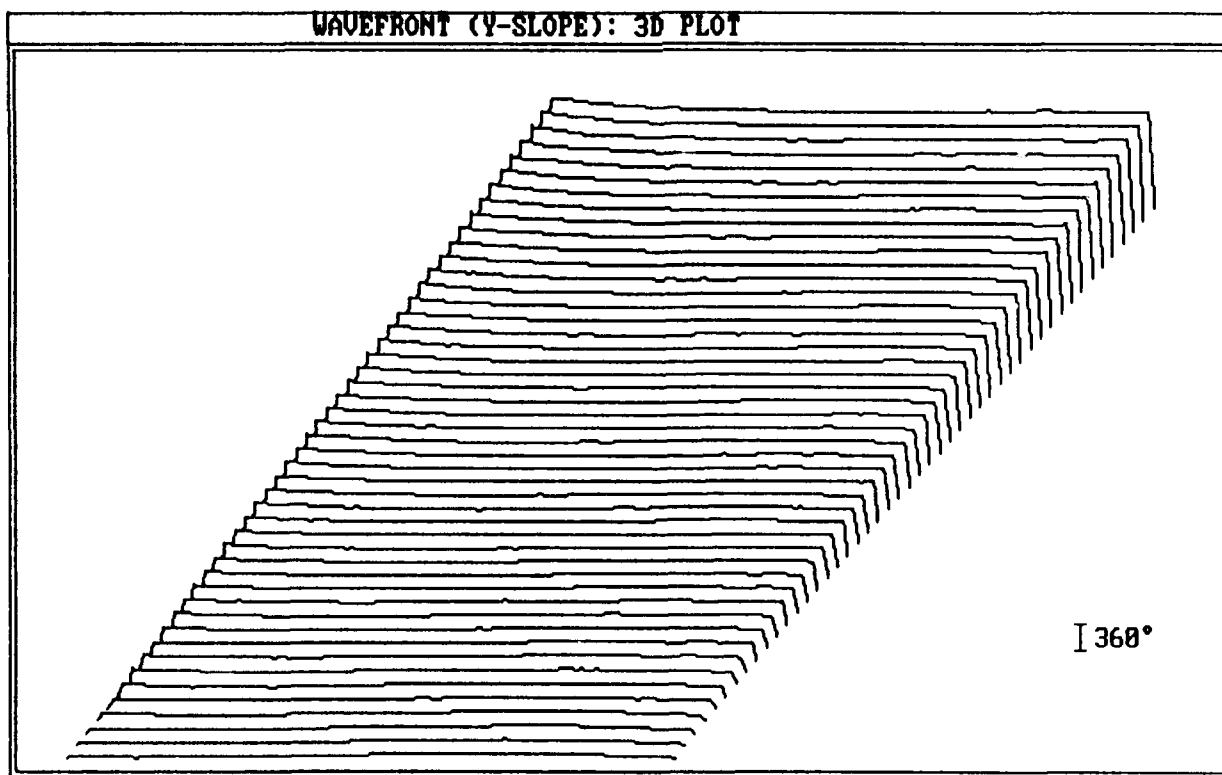
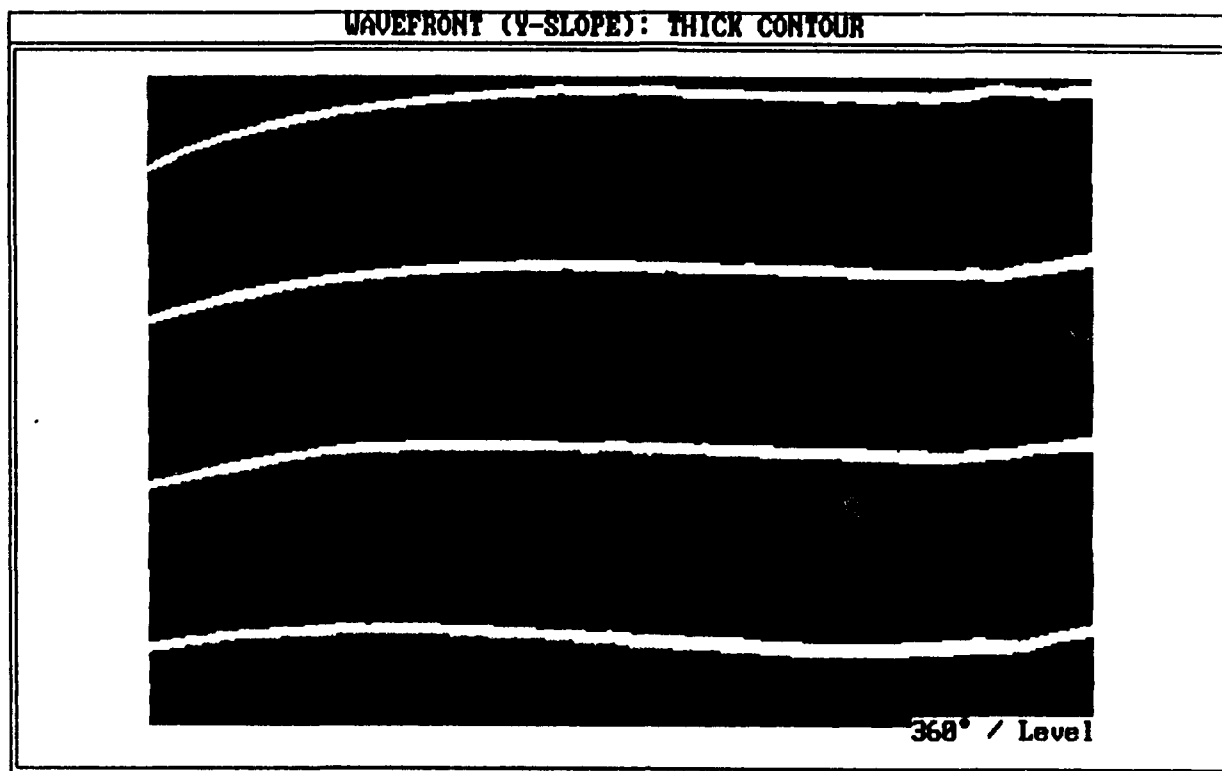
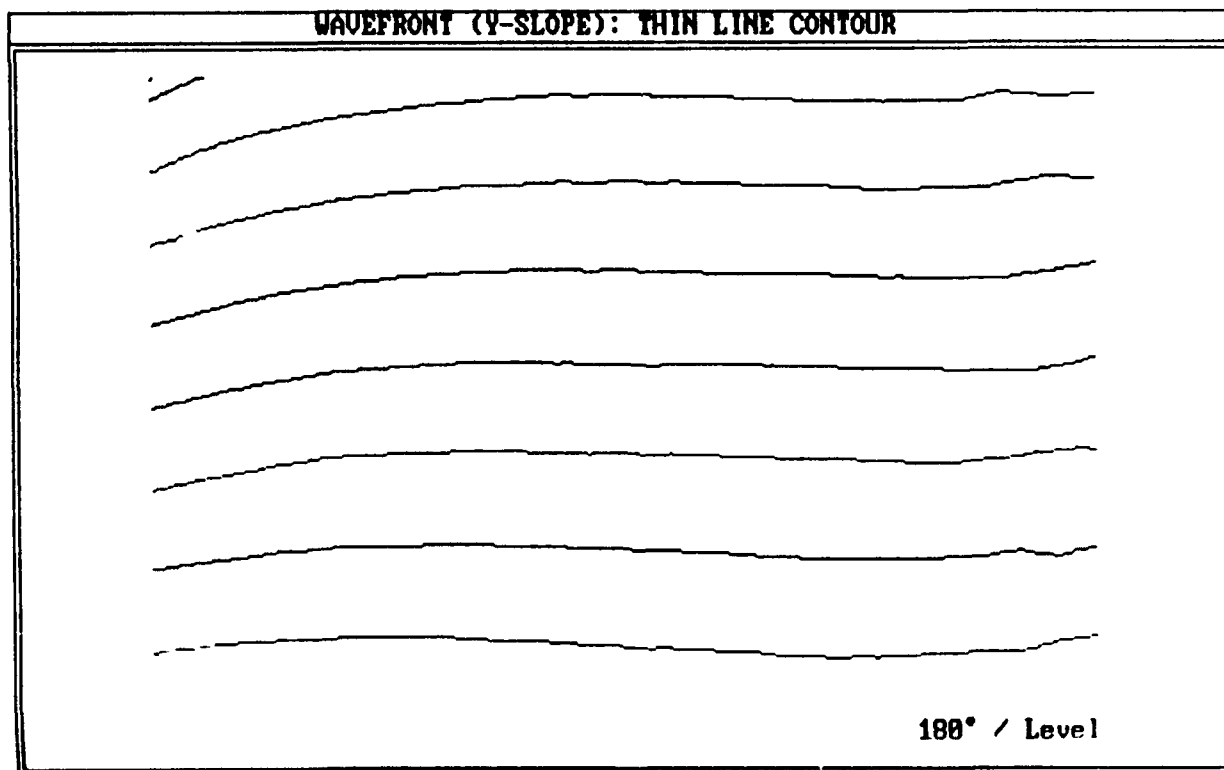


Figure 17: (a). Photograph of subaperture interferogram
(b). 3-D plot of wavefront slope
(Y-shear, off focus, aligned)

(c)

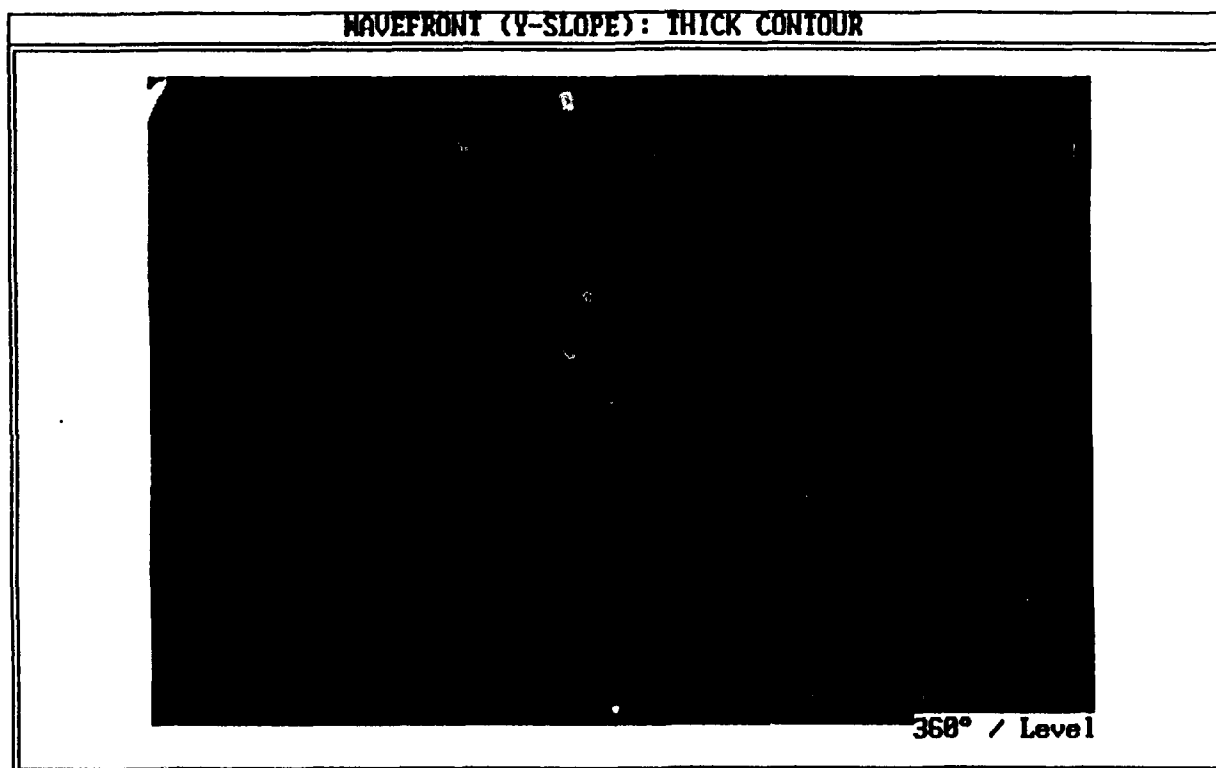


(d)



Copy available to DTIC does not permit full reproduction

(e)



(f)

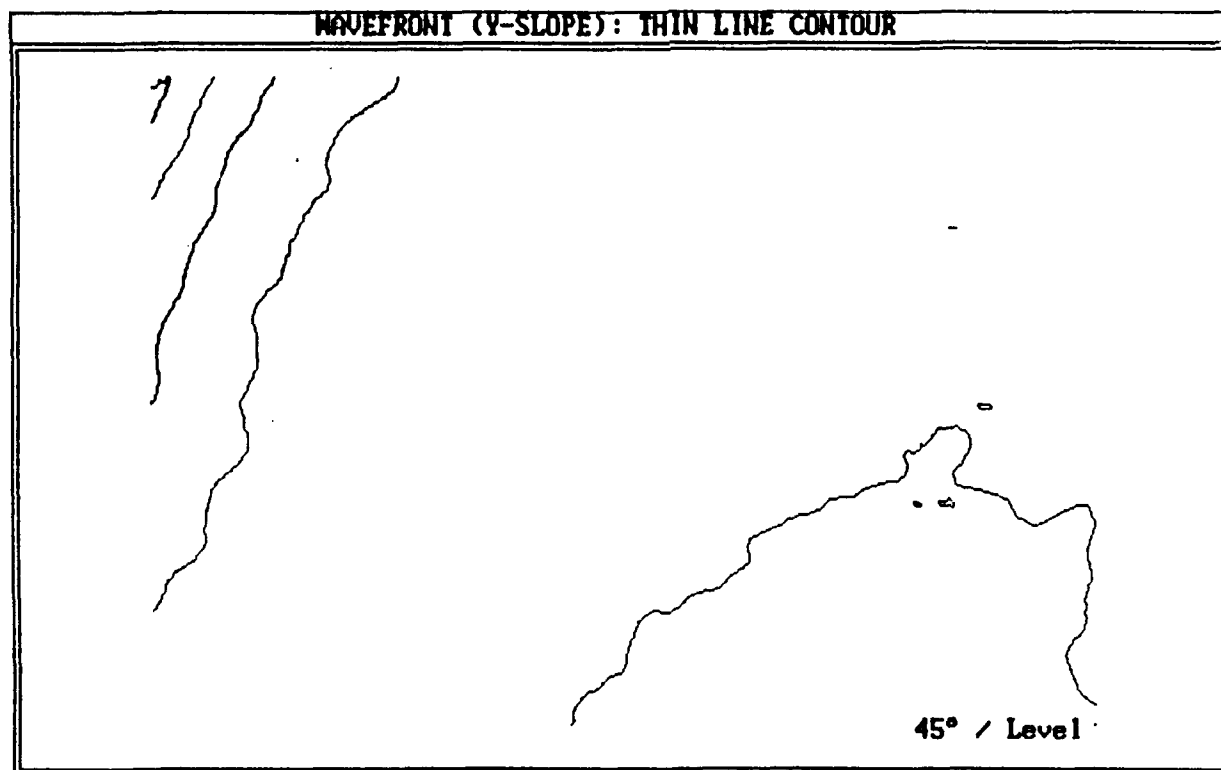


Figure 17: (e, f). Contour maps of wavefront slope, tilt removed (Y-shear, off focus, aligned)

(a)



(b)

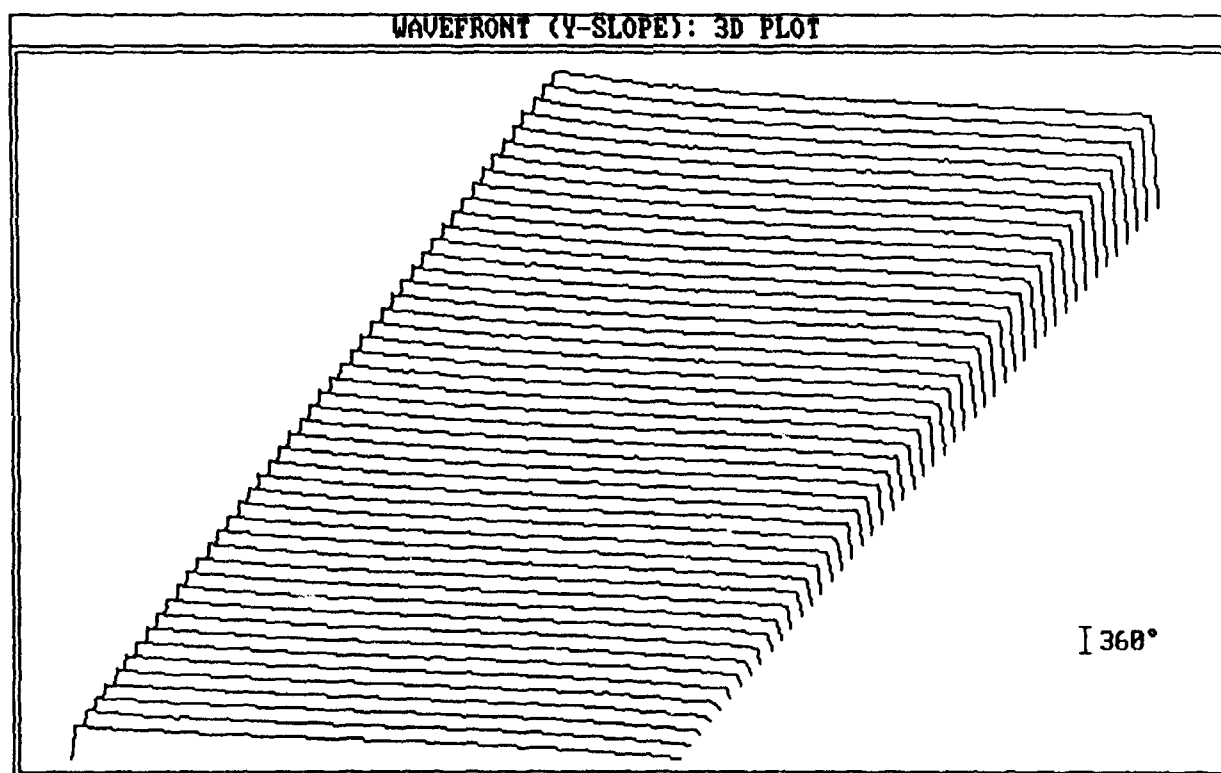
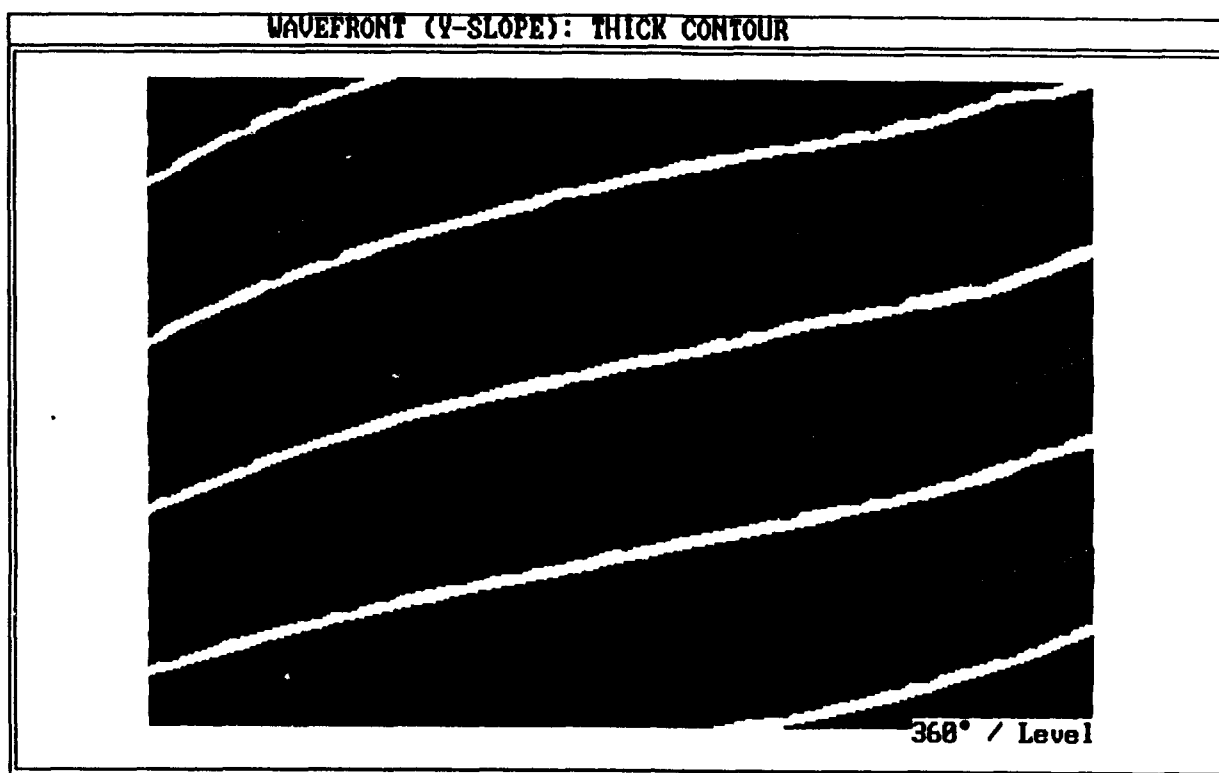


Figure 18: (a). Photograph of subaperture interferogram
(b). 3-D plot of wavefront slope
{Y-shear, off focus, small misalignment (positive)}

(c)



(d)

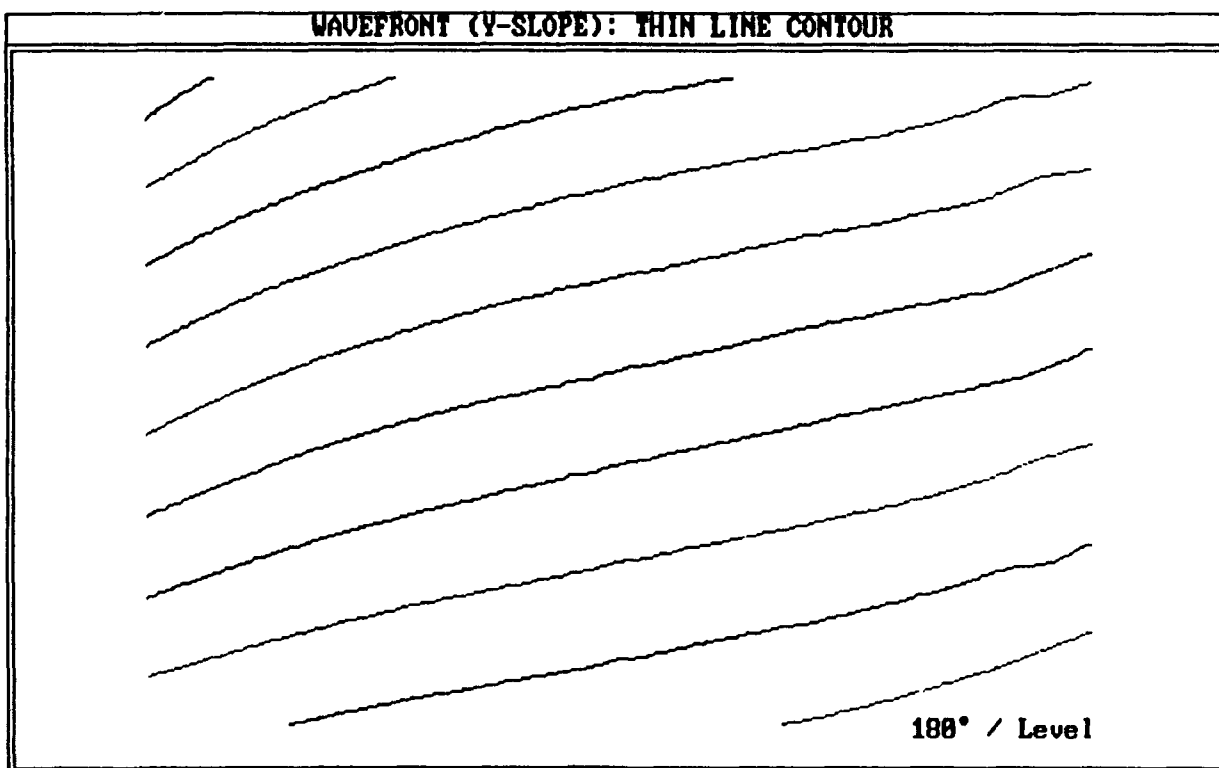
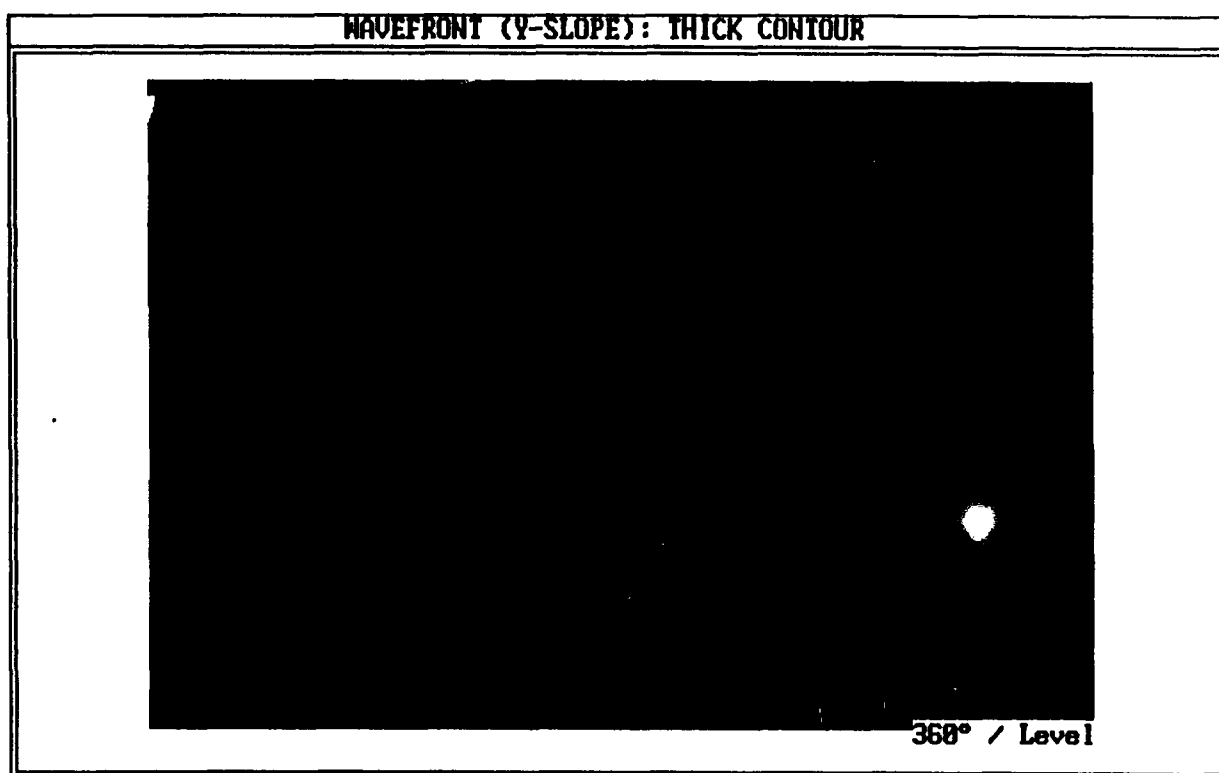


Figure 18: (c, d). Contour maps of wavefront slope
{Y-shear, off focus, small misalignment (positive)}

(e)



(f)

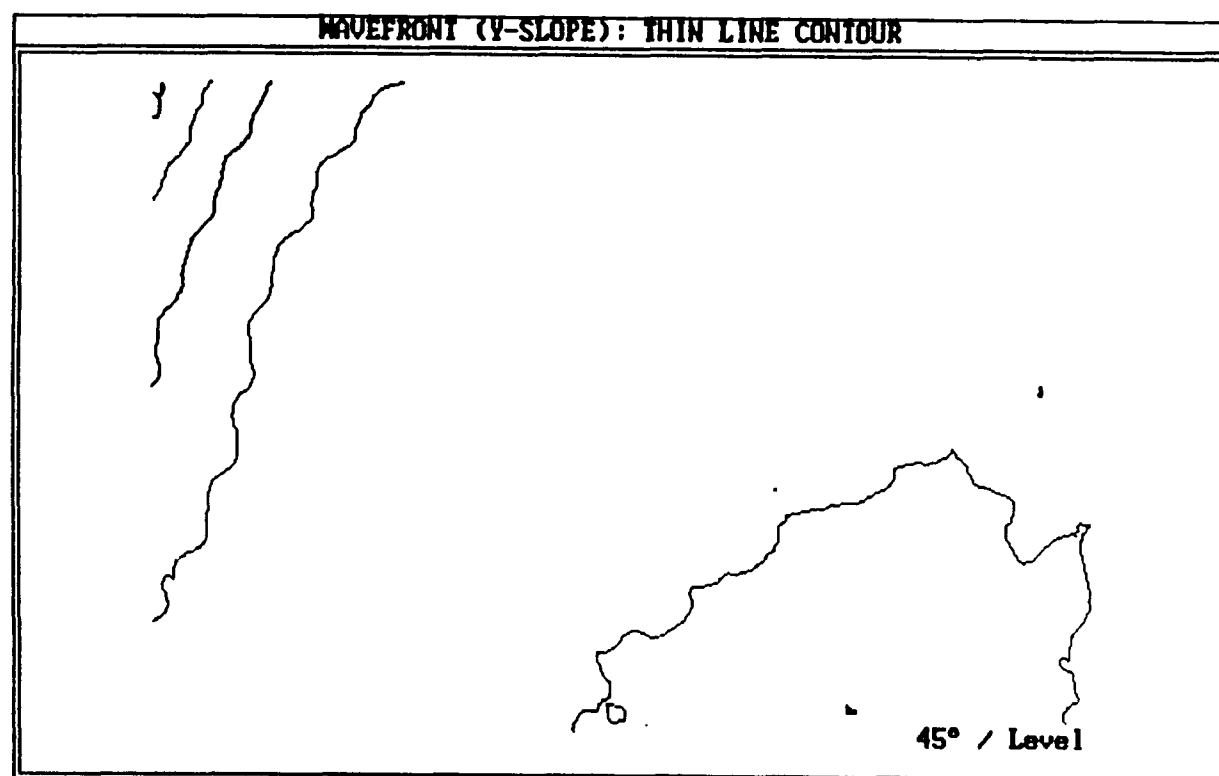


Figure 18: (e, f). Contour maps of wavefront slope, tilt removed
{Y-shear, off focus, small misalignment (positive)}

(a)



(b)

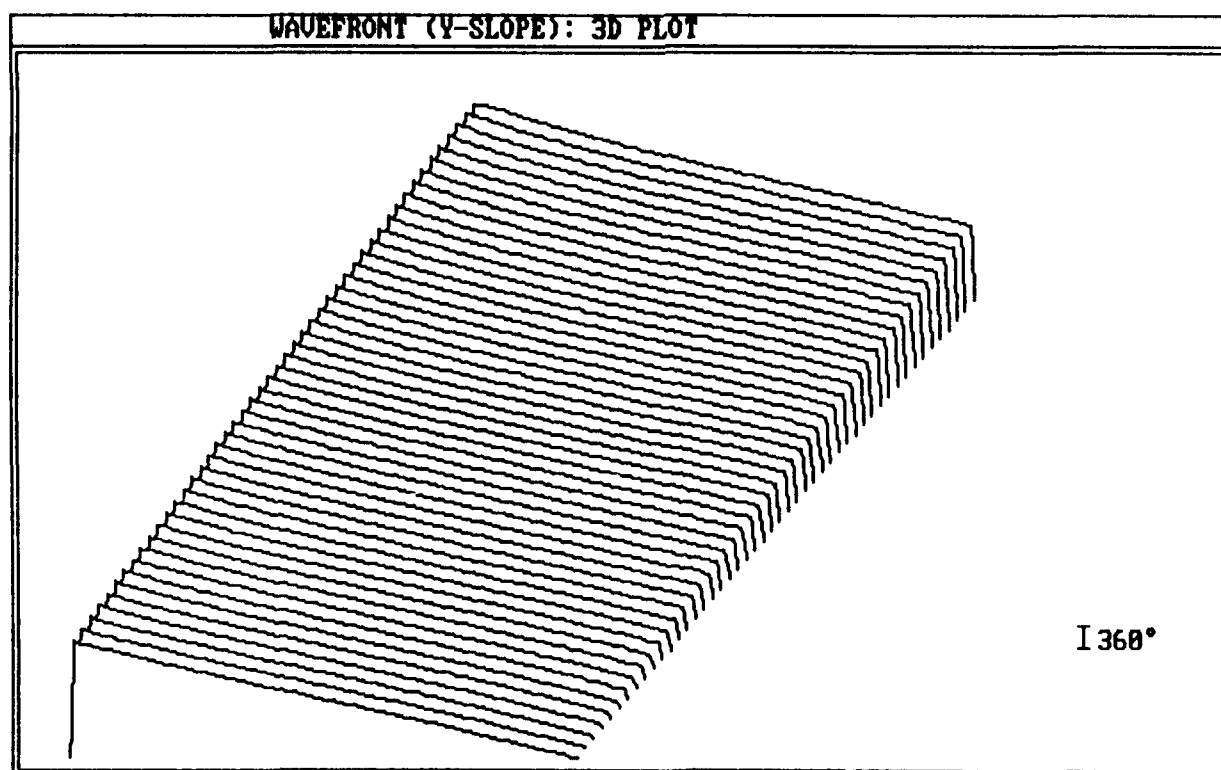
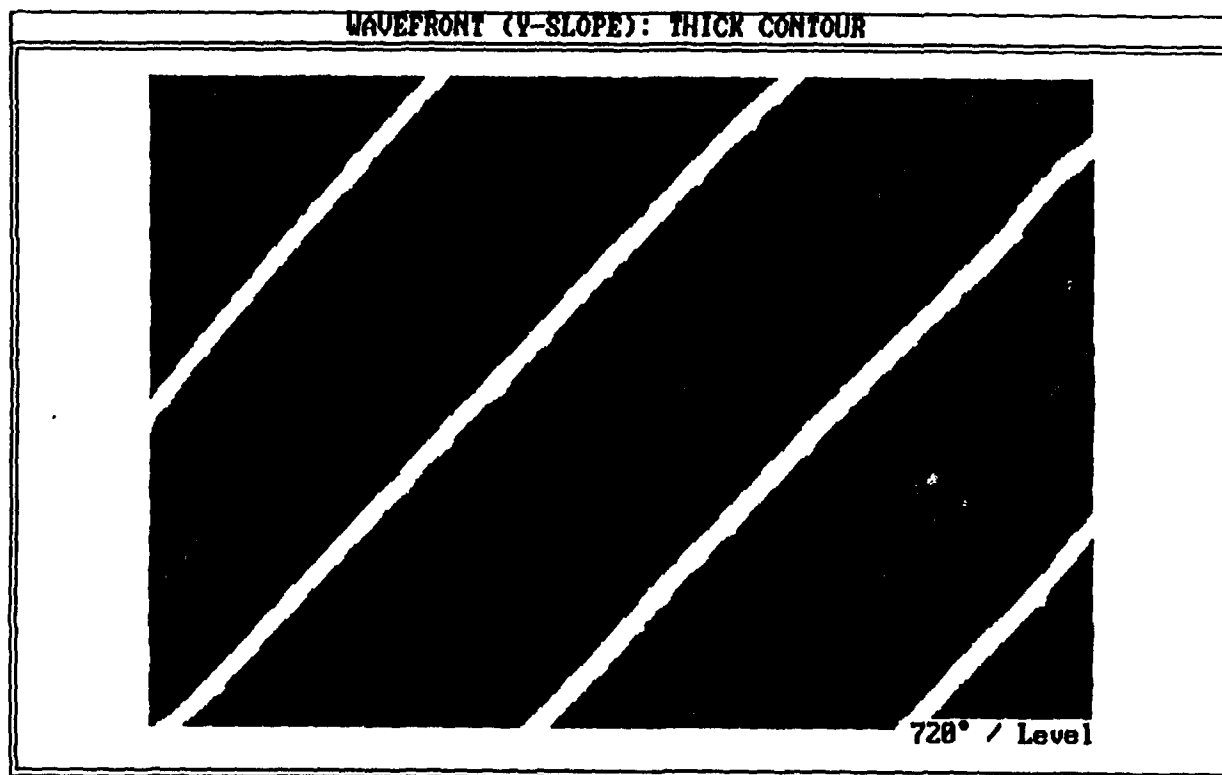


Figure 19: (a). Photograph of subaperture interferogram
(b). 3-D plot of wavefront slope
{Y-shear, off focus, large misalignment (positive)}

(c)



(d)

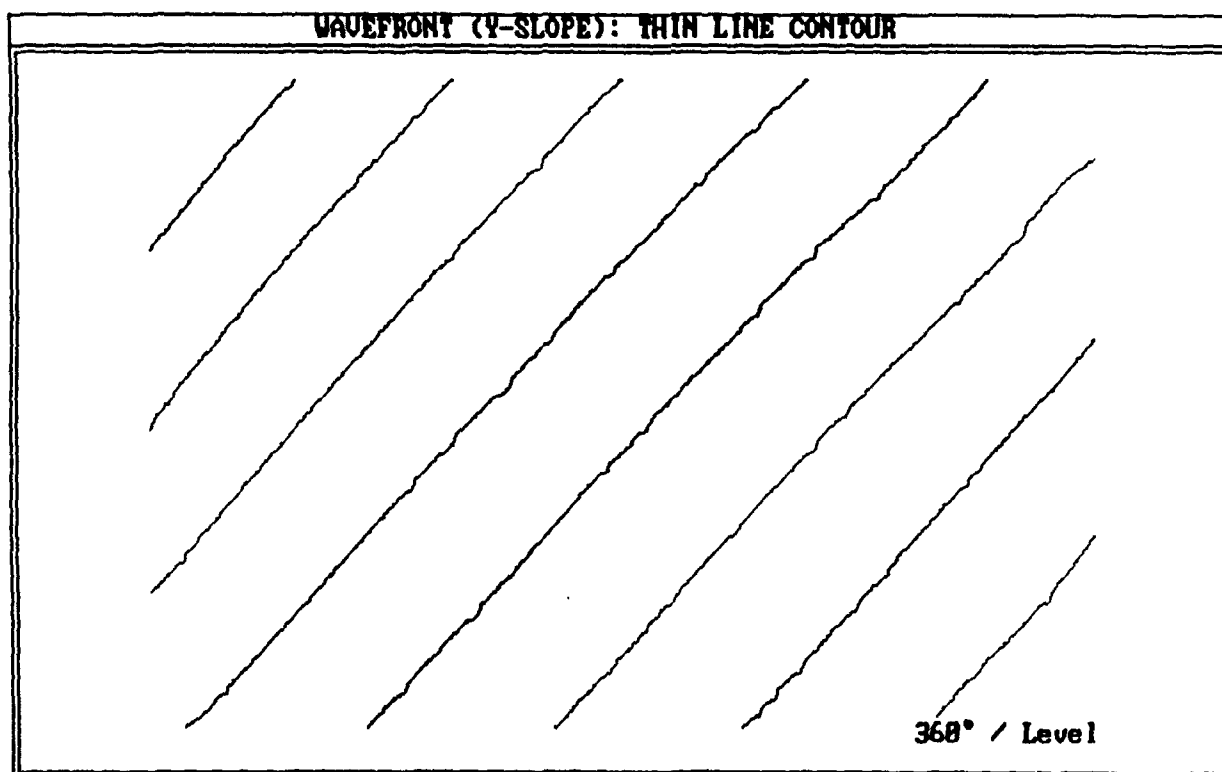
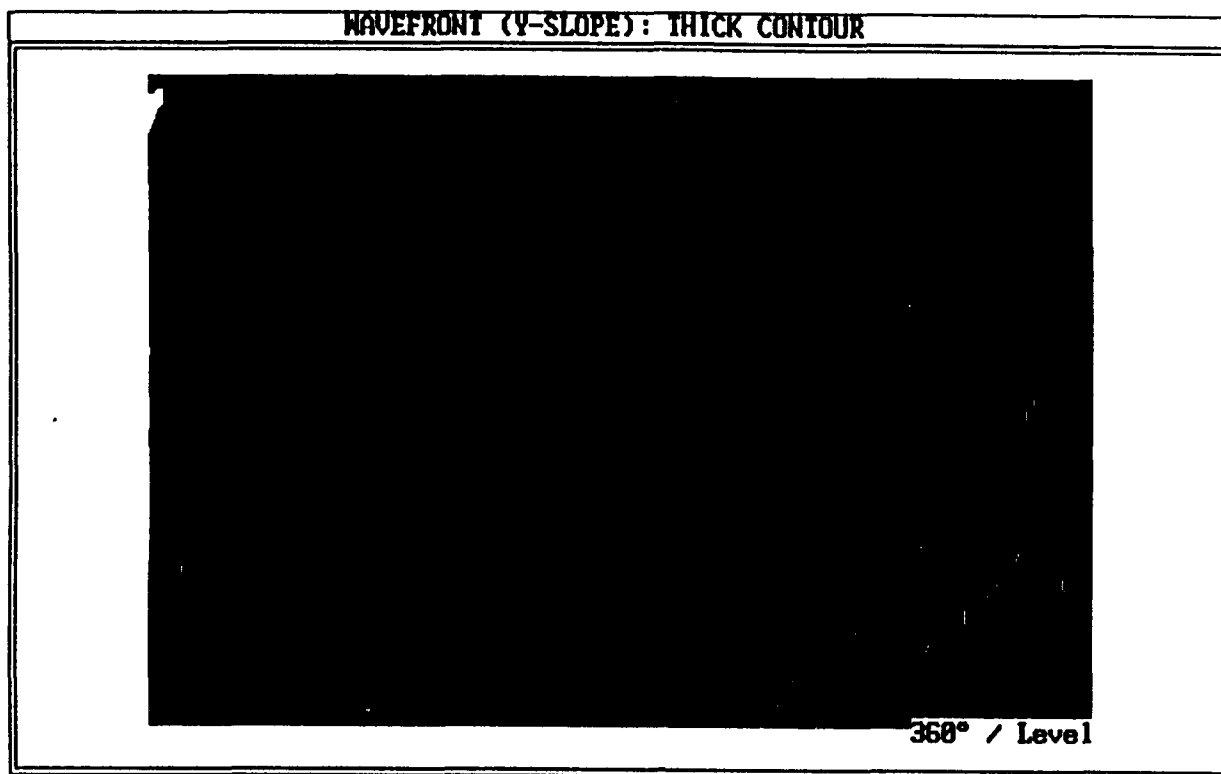


Figure 19: (c, d). Contour maps of wavefront slope
{Y-shear, off focus, large misalignment (positive)}

(e)



(f)

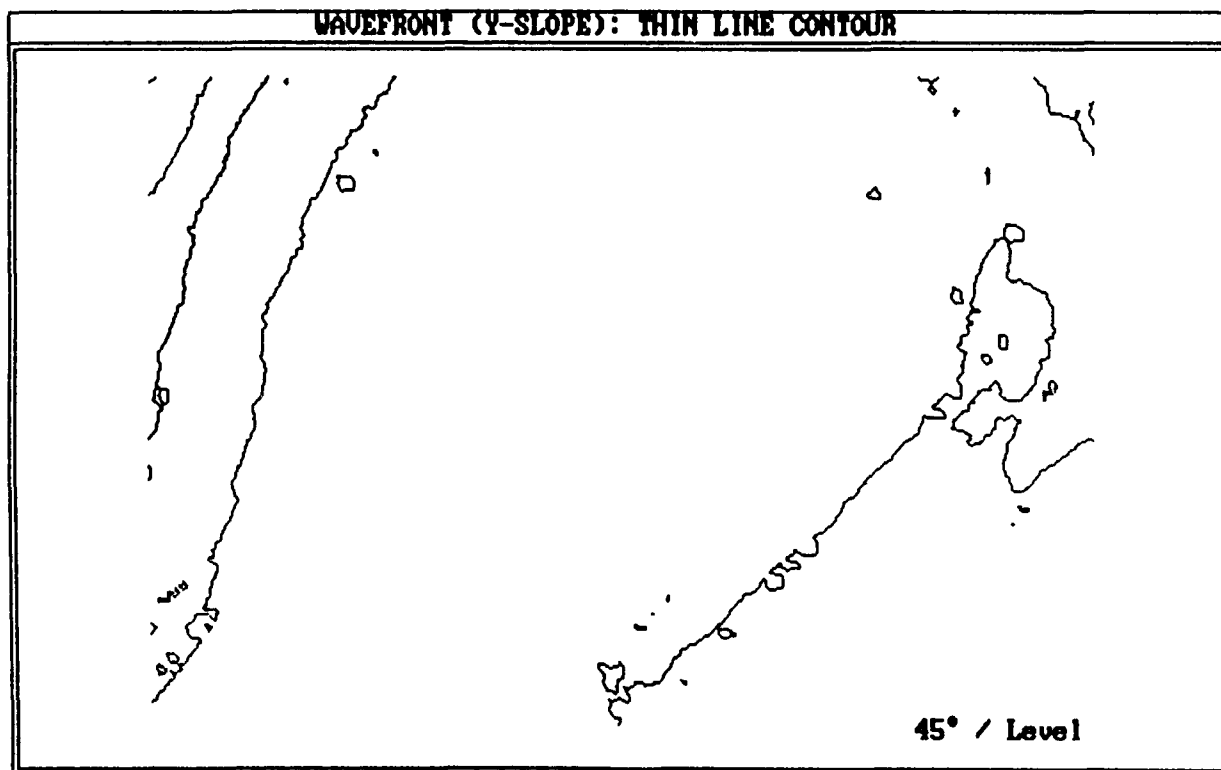


Figure 19: (e, f). Contour maps of wavefront slope, tilt removed
{Y-shear, off focus, large misalignment (positive)}

(a)



(b)

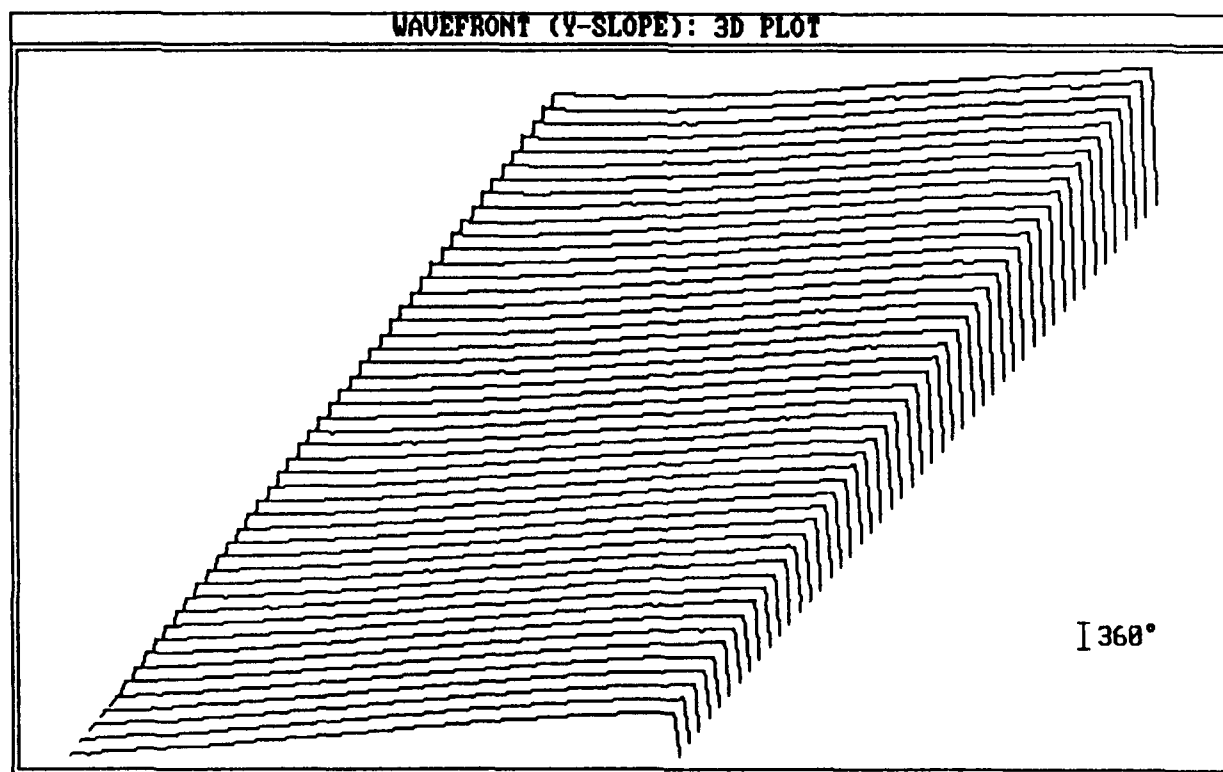
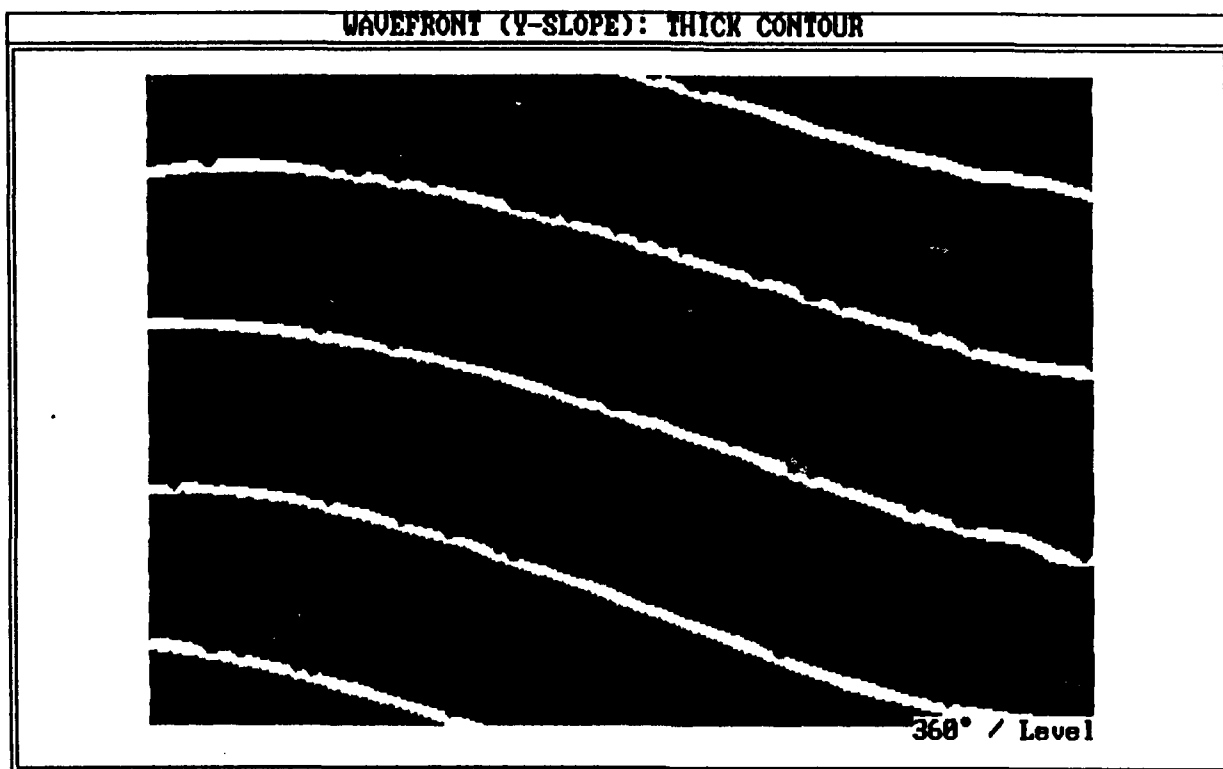


Figure 20: (a). Photograph of subaperture interferogram
(b). 3-D plot of wavefront slope
{Y-shear, off focus, small misalignment (negative)}

(c)



(d)

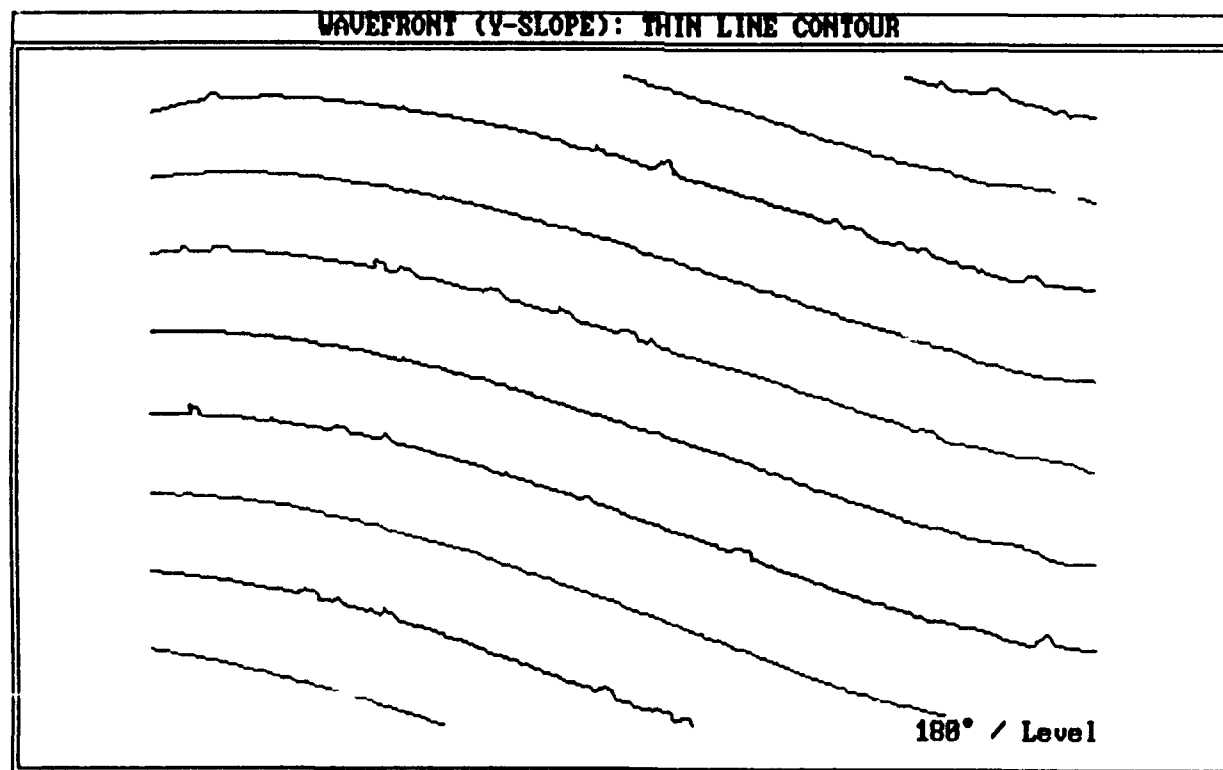
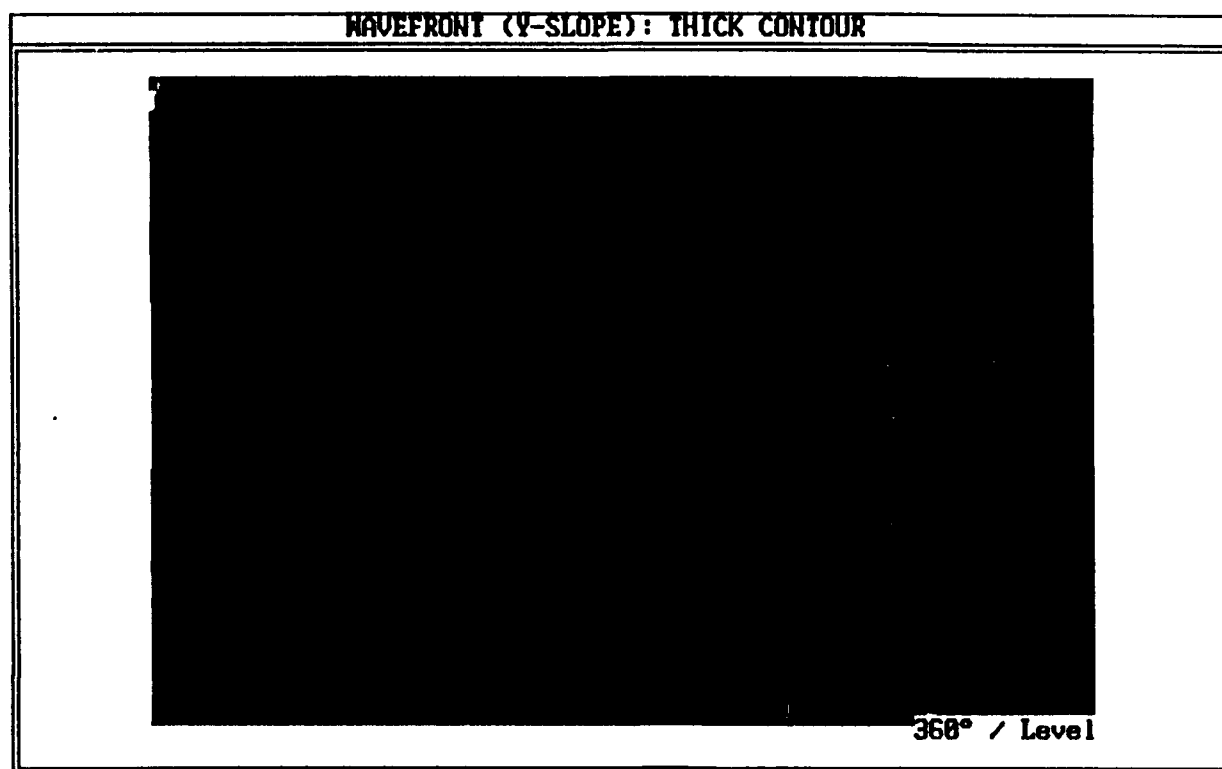


Figure 20: (c, d). Contour maps of wavefront slope
{Y-shear, off focus, small misalignment (negative)}

(e)



(f)

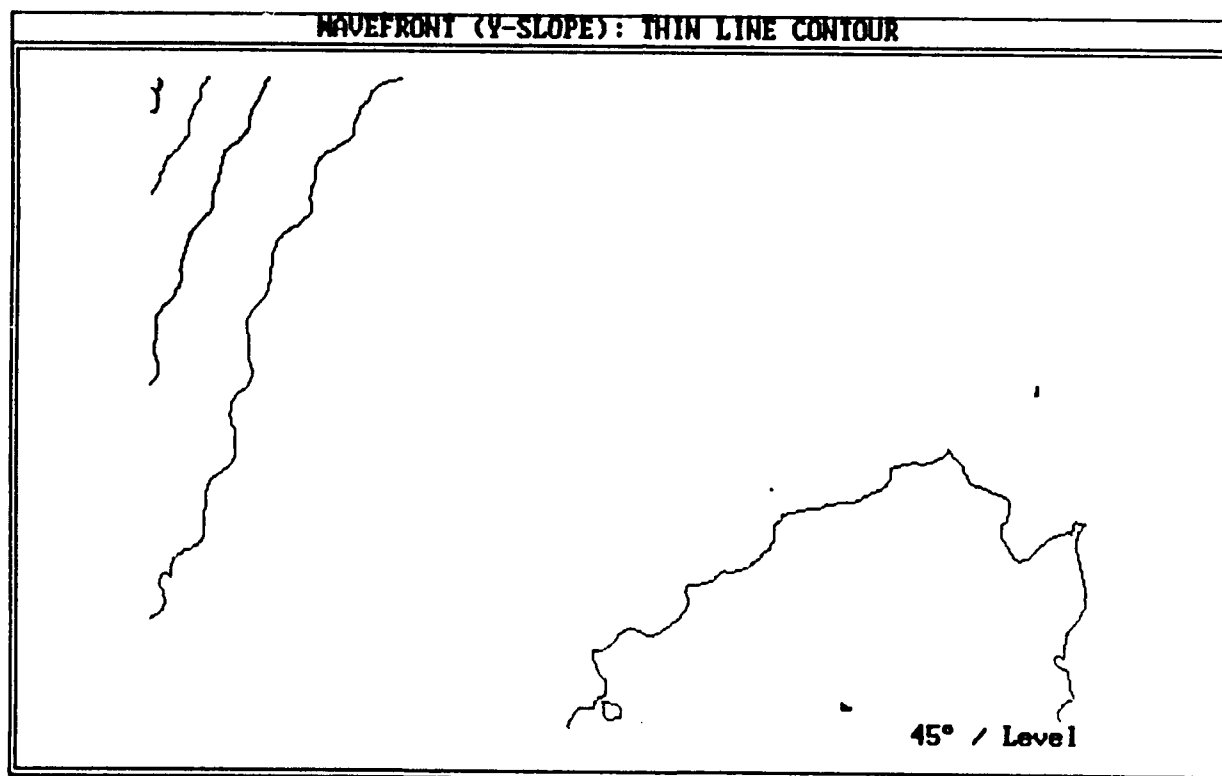


Figure 20: (e, f). Contour maps of wavefront slope, tilt removed
{Y-shear, off focus, small misalignment (negative)}

(a)



(b)

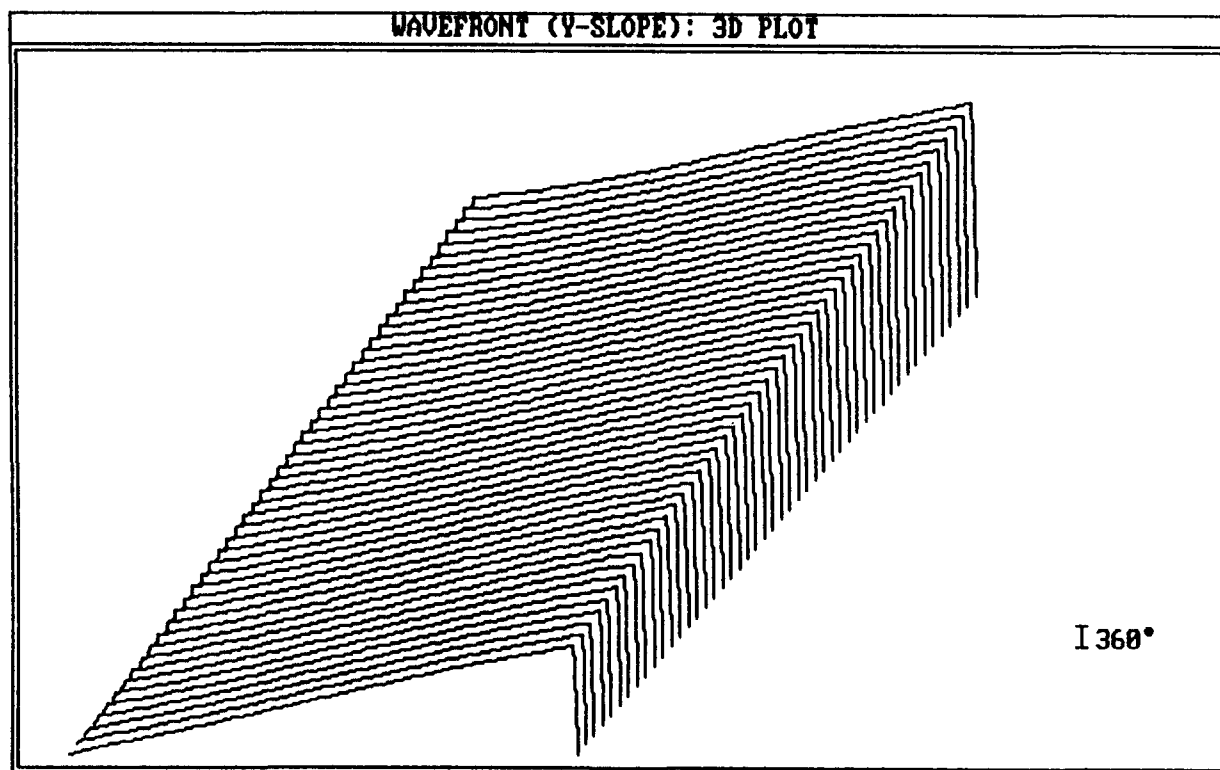
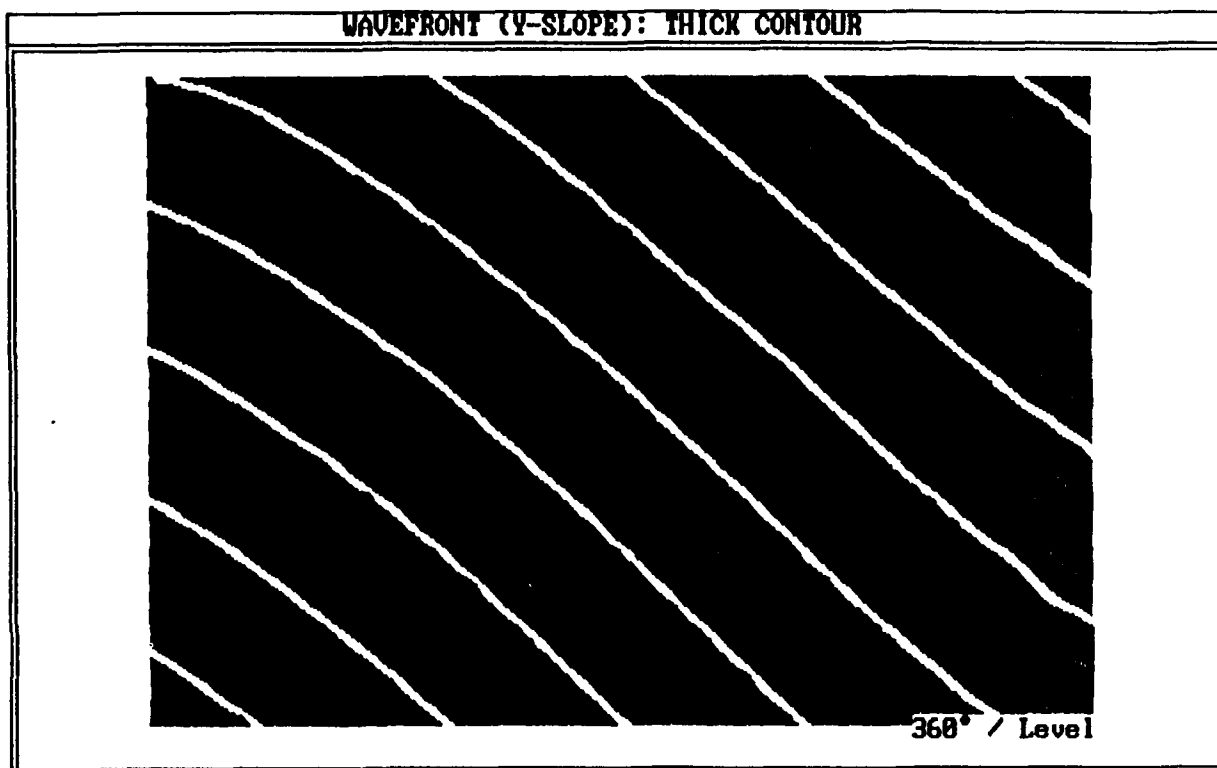


Figure 21: (a). Photograph of subaperture interferogram
(b). 3-D plot of wavefront slope
{Y-shear, off focus, large misalignment (negative)}

(c)



(d)

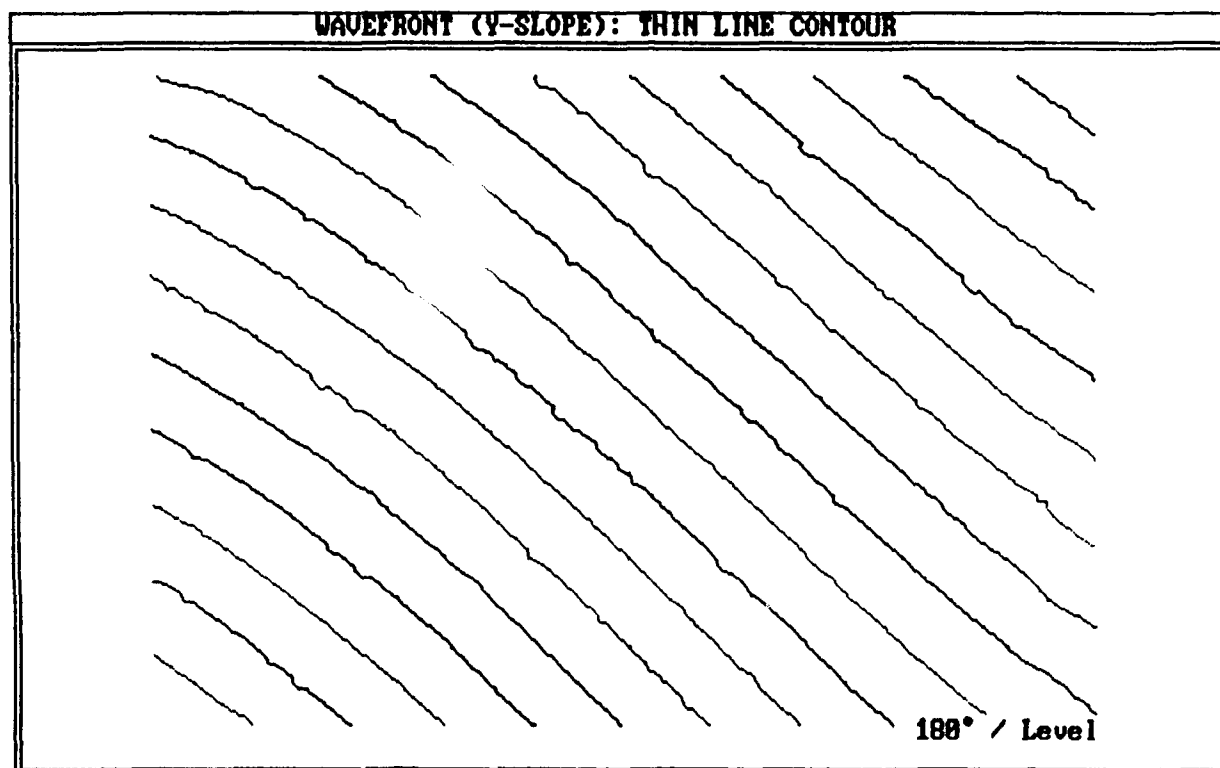
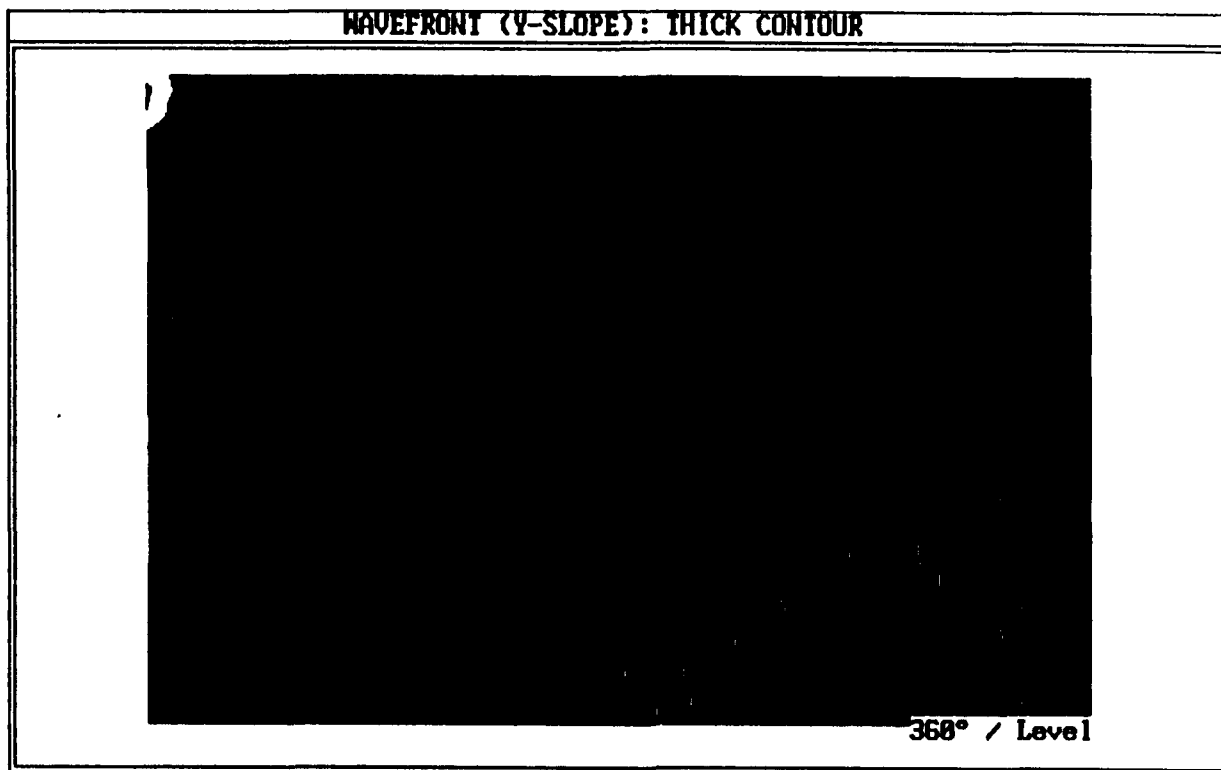


Figure 21: (c, d). Contour maps of wavefront slope
{Y-shear, off focus, large misalignment (negative)}

(e)



(f)

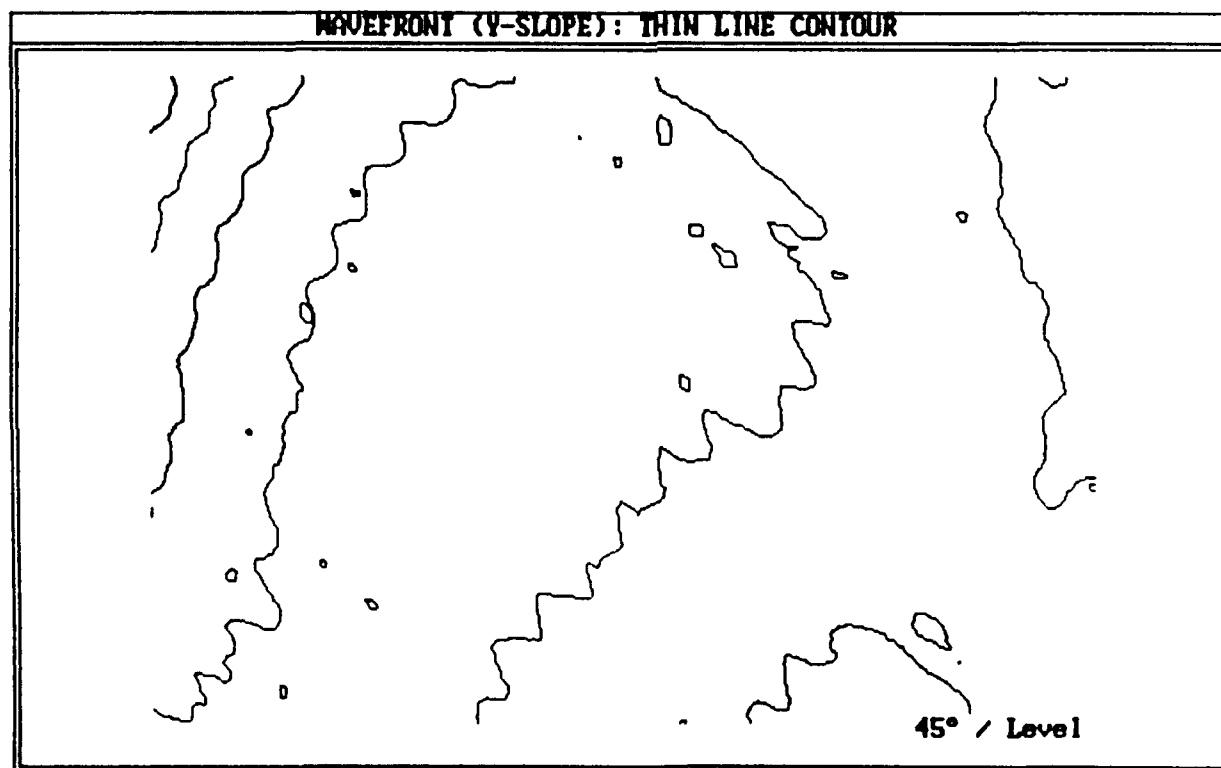


Figure 21: (e, f). Contour maps of wavefront slope, tilt removed
{Y-shear, off focus, large misalignment (negative)}